THE EFFECT OF HIGH PRESSURE ON SUBSTITUTION REACTIONS AND CHEMICAL EQUILIBRIA

by

Nafty Vanderhoek

B.Sc. (Hons.), University of Adelaide, 1969.

Thesis presented for the degree of

Doctor of Philosophy

Department of Physical and Inorganic Chemistry

UNIVERSITY OF ADELAIDE

August, 1973

THIS THESIS IS DEDICATED TO THE

MEMORY OF MY TWIN BROTHER

LEO

This thesis contains no material previously submitted for a degree or diploma in any University, and to the best of my knowledge and belief, contains no material previously published or written by another person, except where due reference is made in the text.

NAFTY VANDERHOEK

August, 1973

ACKNOWLEDGEMENTS

I wish to sincerely thank my supervisor, Professor D.R. Stranks, for his constant encouragement and inspired guidance throughout the course of this work. To Professor D.O. Jordan, Head of the Department of Physical and Inorganic Chemistry, University of Adelaide, I express my thanks for making laboratory facilities and equipment available to me within the Department.

I wish also to thank the other members of staff and research students for stimulating discussion throughout this project.

I express gratitude to Miss K. Whittall for typing this manuscript, and Miss M. Roberts for preparing the diagrams.

This project was sponsored by a research grant from the Australian Atomic Energy Commission. Grateful acknowledgment is made of this financial support.

Finally, my sincerest thanks goes to my wife Martha, and my family, for their encouragement, forbearance and understanding during the course of this work.

Summary

Several substitution reactions and chemical equilibria have been studied under high pressure, using spectrophotometric techniques to follow these processes.

The isomerisation of *trans*-Co $en_2(OH_2)_2^{3+}$ was investigated in aqueous solution in the range 1 to 1380 bar, 34.5 to 55°C and ionic strength 0.05 to 1.0 M. From the variation of the rate coefficient with pressure and temperature the activation parameters were determined to be $\Delta V^{\ddagger}$ = + 13.3 ± 0.7 $cm^3\ mol^{-1}$, $\Delta\beta^{\ddagger}$ = 1.0 ± 0.2 $cm^3\ mol^{-1}\ kbar^{-1}$, $\Delta H^{\ddagger}$ = 131.4 ± 1.2 kJ mol^{-1}, and $\Delta S^{\ddagger}$ = + 103 ± 5 J $K^{-1}\ mol^{-1}$ at 0.05 M ionic strength and $\Delta V^{\ddagger}$ = + 14.2 ± 0.2 $cm^3\ mol^{-1}$, $\Delta\beta^{\ddagger}$ = 10 ± 3 $cm^3\ mol^{-1}\ kbar^{-1}$, $\Delta H^{\ddagger}$ = 121.7 ± 1.0 kJ mol^{-1} and $\Delta S^{\ddagger}$ = 64 ± 4 J $K^{-1}\ mol^{-1}$ at 1.0 M ionic strength. The data were discussed in terms of a dissociative mechanism involving release of an aquo ligand to the bulk solvent. The changed activation parameters at higher ionic strengths were attributed to the effect of ion-pair formation.

The *trans* to *cis* interconversion of Co $en_2(OH_2)OSeO_2H^{2+}$ was studied in aqueous solution in the range 1 to 1360 bar and 21 to 35°C. The activation parameters for *trans*-Co $en_2(OH_2)OSeO_2H^{2+}$ at pH 3.3 and ionic strength 0.012 M were $\Delta H^{\ddagger}$ = 109.6 ± 1.3 kJ mol^{-1}, $\Delta S^{\ddagger}$ = + 53.1 ± 4.2 J $K^{-1}mol^{-1}$, $\Delta V^{\ddagger}_{t-c}$ = + 7.5 ± 0.2 $cm^3\ mol^{-1}$ and $\Delta V^{\ddagger}_{c-t}$ = + 12.7 ± 1.0 $cm^3\ mol^{-1}$. For *trans*-Co $en_2(OH_2)OSeO_2^{+}$ at pH

7.0 and ionic strength 0.5 M, $\Delta V^{\ddagger}_{t-c}$ = + 7.3 ± 0.2 cm^3 mol^{-1}. In both systems $\Delta V^{\ddagger}$ showed no measurable pressure dependence. The data were consistent with a dissociative interchange process. A subsidiary study of the effect of pressure on the *trans* $\rightleftarrows$ *cis* equilibrium for the Co $en_2(OH_2)OSeO_2H^{2+}$ complex revealed that the *cis* isomer was favoured with increasing pressure and ΔV = - 5.8 ± 0.4 cm^3 mol^{-1}.

The nucleophilic substitution of *cis*-Co $en_2(OH_2)_2{}^{3+}$ by $HC_2O_4{}^-$ to form Co $en_2C_2O_4{}^+$ was studied at 60°C and at pressures between 0 and 2 kbar. From the variation of the rate coefficients with pressure, the volume of activation for the anation process and molal volume change for ion-pair formation were found to exhibit respective values of + 4.8 ± 0.7 cm^3 mol^{-1} and + 2.3 ± 1.2 cm^3 mol^{-1}. Substitution by oxalate in the ion-pair was considered to involve a dissociative interchange process. A study was also made on the anation reaction at pressures between 1 and 1551 bar, 20 to 35°C, ionic strength 0.32 M and pH 7 where the principal species are Co $en_2(OH)OH_2{}^{2+}$ and $C_2O_4{}^{2-}$. The activation parameters were determined to be $\Delta H^{\ddagger}$ = 92.9 ± 1.7 kJ mol^{-1}, $\Delta S^{\ddagger}$ = + 9.6 ± 4.2 J K^{-1} mol^{-1} and $\Delta V^{\ddagger}$ = + 4.6 ± 0.4 cm^3 mol^{-1}; $\Delta H^{\ddagger}_{IP}$ = - 33.5 ± 16.7 kJ mol^{-1} and $|\Delta V| \leqslant 1.0$ cm^3 mol^{-1}. Again, the data for substitution of oxalate in the ion-pair are consistent with a dissociative interchange mechanism.

The rate of intramolecular reaction of Co $en_2(OH)C_2O_4{}^0$ was investigated at 50°C and pressures between 1 and 1379 bar. The volume of activation was measured to be + 2.6 ± 0.6 cm^3 mol^{-1}. From this study, an associative intramolecular concerted

mechanism has been proposed for the ring-closing reaction of $Co\ en_2(OH_2)C_2O_4^+$.

The effect of pressure on the first hydrolysis stage of the trivalent metal cations, Fe^{3+}_{aq}, Tl^{3+}_{aq} and $Co(NH_3)_5OH_2^{3+}$ were studied up to 1720 bar. The molal volume changes were $\Delta V_a(Fe^{3+}_{aq}) = -1.2 \pm 0.5$ $cm^3\ mol^{-1}$, $\Delta V_a(Tl^{3+}_{aq}) = -3.2 \pm 0.9\ cm^3\ mol^{-1}$ and $\Delta V_a(Co(NH_3)_5OH_2^{3+}) = -2.6 \pm 0.6\ cm^3\ mol^{-1}$. A comparison of the measured values with those predicted from electrostrictive considerations on symmetrical cations revealed poor agreement. An ion-pair model was suggested to explain the anomaly.

CONTENTS *Page*

Chapter 1. High Pressure Effects in Solution.

1.1 Introduction

Activation parameters are useful in understanding chemical reactions since they provide information about the nature of the activated complexes formed from the reactants. In the past many kinetic investigations have relied simply on enthalpies and entropies of activation, $\Delta H^{\ddagger}$ and $\Delta S^{\ddagger}$, for their interpretation and this information has often proved inadequate to unambiguously describe the intimate nature of the reaction process.

The volume of activation, $\Delta V^{\ddagger}$, which measures the difference in partial molal volume between the transition state and ground state, furnishes equally valuable mechanistic information, but is much less frequently reported. Its infrequent appearance in the literature is the result of experimental difficulties associated with its determination. In principle, the interpretation of a volume change involves a structural concept based on inferred changes in nuclear positions. This is intrinsically simpler to handle than the other activation parameters which depends on inferred changes in both nuclear positions and molecular energies.

As the rapid development of reaction kinetics has occurred at a time when pressure equipment was not readily available to workers in the field, pressure studies have largely played a confirmatory role with respect to major mechanistic discoveries.

However, with the development of specialised equipment in recent years, pressure effects on reactions have permitted a choice between mechanisms and further, have enabled refinement of mechanistic detail. This thesis will be concerned with the effect of high pressure on substitution reactions and chemical equilibria.

1.2 *Theory of Pressure Effects on Reaction Rates*

Several extensive reviews of kinetic pressure effects in solution have been published[1-8] during the last decade. For this reason only the more salient features of these effects on reaction rates and chemical equilibria will be presented in this and following sections.

In dilute solution, the variation in chemical potential of any species i with pressure is equal to the partial molar volume of that species:

$$(\partial \mu_i / \partial P)_T = \bar{V}_i \qquad 1.1$$

This fundamental relation may be applied, with the transition state theory, to the generalised reaction

$$aA + bB + \ldots \rightleftharpoons X^{\ddagger} \rightarrow \text{products}$$

or with the general equilibrium reaction

$$aA + bB + \ldots \rightleftharpoons cC + dD + \ldots$$

In the former case, the effect of pressure on the observed rate coefficient k is attributed to the pressure variation of the concentration quotient $K^{\ddagger}$ describing the assumed equilibrium between the activated complex $X^{\ddagger}$ in the transition state and the initial

reactant state. It then follows[9] that

$$-RT(\partial \ln k/\partial P)_T = \bar{V}_{X^{\ddagger}} - a\bar{V}_A - b\bar{V}_B - \ldots$$

$$= \Delta V^{\ddagger} \qquad 1.2$$

assuming that the transmission coefficient, κ, is independent of pressure. For the equilibrium

$$-RT(\partial \ln k/\partial P)_T = c\bar{V}^{\circ}_C + d\bar{V}^{\circ}_D + \ldots. -a\bar{V}^{\circ}_A - b\bar{V}^{\circ}_B - \ldots$$

$$= \Delta V^{\circ} \qquad 1.3$$

where $\Delta V^{\ddagger}$ represents the excess partial molar volume of the activated complex over those of the reactants and ΔV° is the excess partial molar volume of products over reactants. In reaction kinetics and for equilibrium measurements, the concentrations of the species in solution are normally expressed in terms of their molar concentrations. Equations 1.2 and 1.3 must then be corrected by a term including the compressibility of the solvent. At 25°C and 1 bar, this term is 1.1 $cm^3\ mol^{-1}$ for water.

1.3 Evaluation of Volumes and Compressibilities of Activation

Considerable controversy[8] exists in the literature as to the best analytical function describing the pressure dependence of the rate coefficient and, to date, several basic semiempirical functions have been employed.[10]

The simplest and most common method is to use a power series in pressure, for example, the expressions

$$\ln k_p = \ln k_o + bP \qquad 1.4$$

$$\ln k_p = \ln k_o + bP + cP^2 \qquad 1.5$$

Equation 1.4 essentially assumes that $\Delta V^{\ddagger}$ is pressure independent while the quadratic function takes into account the pressure variance of $\Delta V^{\ddagger}$. An alternative approach, proposed by Benson and Berson,[11] is based on the Tait equation of state.[12]

$$\ln(k_p/k_o)/P = A + BP^{0.523} \qquad 1.6$$

This relation implies that $\Delta V^{\ddagger}$ must always vary with pressure (as does equation 1.5), contrary to some experimental results. Whalley[4] favours the empirical expression

$$\ln(k_{n+1}/k_n)/(P_{n+1} - P_n) = A + B(P_{n+1} + P_n)/2 \qquad 1.7$$

which assumes that $\Delta V^{\ddagger}$ is independent of pressure over a small pressure range. Clearly, this method has only limited application. In a careful analysis of the functional pressure dependence of ln k, Hyne et. al.[10] has shown that equation 1.5 most accurately describes a variety of reactions. For this reason the power series will be assumed for subsequent discussion.

The fitting of experimental data to equation 1.5 requires a careful multiple regression analysis of the statistical significance of the coefficients b and c. In order to obtain reliable values for these coefficients a number of separate rate determinations is required at lower pressures (below 2 k bar). The mechanistic quantities of importance, the volume of activation at zero pressure, $\Delta V_o^{\ddagger}$, and the pressure variance of $\Delta V^{\ddagger}$, $(\partial \Delta V^{\ddagger}/\partial P)_T$, are then given from equation 1.5 as

$$\Delta V_o^{\ddagger} = - bRT \qquad 1.8$$

$$-(\partial \Delta V^{\ddagger}/\partial P)_T = \Delta\beta^{\ddagger} = 2RTc \qquad 1.9$$

where the term $\Delta\beta^{\ddagger}$ is defined[13] as the excess of the compressibility coefficient for the transition state over that of the combined initial reactants. If experimental data are analysed according to equation 1.4, it follows that

$$\Delta V_P^{\ddagger} = -bRT \qquad 1.10$$

which is analogous to equation 1.8.

The compressibility coefficient of activation, $\Delta\beta^{\ddagger}$, should be distinguished from the related compressibility of activation, $\Delta\kappa^{\ddagger}$, defined by

$$\Delta\kappa^{\ddagger} = -(\partial \Delta V^{\ddagger}/\partial P)_T/\Delta V^{\ddagger} = \Delta\beta^{\ddagger}/\Delta V^{\ddagger} \qquad 1.11$$

Values of $\Delta\kappa^{\ddagger}$ need be quoted when comparing different reactions but unlike $\Delta\beta^{\ddagger}$, the compressibility of activation cannot be separated into a linear combination of terms from the transition and initial states.

1.4 Interpretation of Volumes and Compressibilities of Activation.

It is convenient, as first suggested by Evans and Polanyi,[9] to regard $\Delta V^{\ddagger}$ as being composed of two terms

$$\Delta V^{\ddagger} = \Delta V_{int}^{\ddagger} + \Delta V_{el}^{\ddagger} \qquad 1.12$$

where $\Delta V_{int}^{\ddagger}$ represents the change in intrinsic volume of the molecules themselves in forming the transition state and $\Delta V_{el}^{\ddagger}$ the

volume change due to the rearrangement of solvent molecules accompanying the activation process.

1.4.1 The Term $\Delta V^{\ddagger}_{int}$

Intrinsic volume effects are important for reactions in which there is no change in formal charge on forming the transition state (as in solvent exchange or isomerisation reactions). However, before discussing this effect, it will be necessary first to consider the compressibility of complex ions.

An expression for estimating the compressibility, κ, of a complex may be derived from the potential function[14] in which a metal ion of charge, Ze, is visualized as surrounded by n dipoles of permanent dipole moment μ with a metal-ligand distance, d,

$$U(d,z) = -nZe\mu/d^2 + B/d^m \qquad 1.13$$

Then it follows for a crystal-field stabilized ion[13] that

$$\kappa = 6\pi d_o^4\, r[nZe\mu(m-2) + 3(m-6)C\,\Delta/d_o^4] \qquad 1.14$$

where d_o is the equilibrium metal-ligand bond distance, r the radius of the spherical complex ion, m the repulsive exponent calculable from known bond distances in different oxidation states, Δ the crystal-field splitting parameter and the quantity C is defined in terms of the number of electrons, $n(\varepsilon)$ of symmetry $d(\varepsilon)$ and $n(\gamma)$ of symmetry $d(\gamma)$ as

$$C = 4n(\varepsilon) - 6n(\gamma) \qquad 1.15$$

The change in radius of the complex ion with pressure is related to κ by

$$(\partial r/\partial P)_T = -\kappa r/3 \qquad 1.16$$

Using equations 1.14 and 1.16, Stranks[13] has estimated the probable volume change for the reaction

$$Ni(NH_3)_6^{2+} \rightarrow {}^{\ddagger}[Ni(NH_3)_5^{2+} + NH_3]$$

The reactant $Ni(NH_3)_6^{2+}$ cation with a calculated $\kappa = 2.2 \times 10^{-6}$ bar^{-1} has an intrinsic volume of 138 cm^3 mol^{-1}. The transition state species $Ni(NH_3)_5^{2+}$ with $\kappa = 1.8 \times 10^{-6}$ bar^{-1} has an estimated intrinsic volume of 137.9 cm^3 mol^{-1} based on a metal-ligand bond contraction of 0.0005 Å at 1 kbar pressure. This represents a negligible change in intrinsic volume between these two species. In general cases, for complex ions of charge 2+ and 3+ with metal-ligand distances ranging from 2.0 to 2.4 Å, analysis of equation 1.14 yield values for κ in the range 0.9×10^{-6} bar^{-1} to 2.8×10^{-6} bar^{-1}. These low values for κ imply that these complex ions may be reasonably treated as incompressible spheres in their reactions.

A consequence of the incompressibilities of complex ions for inorganic reactions is that reactant and transition state species may be assumed to occupy the same intrinsic volume in solution even if the transition state is five coordinate rather than six coordinate. Since contributions to $\Delta V^{\ddagger}_{int}$ arise entirely from bond making and/or bond breaking it may thus be concluded, for reactions where $\Delta V^{\ddagger}_{int}$ is alone important, that a positive value for $\Delta V^{\ddagger}_{0}$ is good evidence for a dissociative mechanism and a negative $\Delta V^{\ddagger}_{0}$ value strong support for an associative process.

1.4.2 The Term $\Delta V^{\ddagger}_{el}$

Electrostrictive volume effects will predominate in reactions

involving charged reactants (as for redox reactions) or the generation or removal of charge (as in substitution reactions with charged nucleophiles or leaving groups). In liquid systems, this effect arises from electrostatic factors which cause the surrounding dipolar solvent to contract or dilate around the activated complex.

An estimate for the degree of electrostriction of a solvent about an ion can be obtained by differentiating Born's equation[15] for the free energy of solvation of an ion with respect to pressure. This gives[1]

$$\Delta V_{el} = \frac{-Z^2 e^2}{Zr \varepsilon^2} \left(\frac{\partial \varepsilon}{\partial P}\right)_T \qquad 1.17$$

where ΔV_{el} is the contraction of a medium of dielectric constant ε around a sphere of radius r and charge Ze. Equation 1.17 assumes that the radius r is pressure invariant, as already justified. In solvent water, the dependence of ΔV_{el} on Z^2 involves contributions to $\Delta V_o^{\ddagger}$ ranging up to $\pm$ 20 $cm^3\ mol^{-1}$ for highly charged reactants.

1.5 *Volume Changes for Reactions of Complex Ions involving Coordinated Water.*

The introduction of a charged ion into a solvent causes a significant contraction of the system. A consequence of this electrostrictive effect is the formation of ordered solvation sheaths about these spheres. The electrostatic field of the ion

will cause a pressure in the solvent dielectric proportional to the second power of the electric field strength[16]

$$P = [(\varepsilon-1)/8\pi]\{Ze/\varepsilon r^2\}^2 \qquad 1.18$$

where all the symbols have been previously defined. For a complex ion of charge 3+ and radius 3 - 3.5Å, Stranks[13] has calculated that this pressure is about 32 k bar and 7.5 k bar respectively at the point where the first and second hydration spheres (or second and third coordination spheres) of the complex ion are located (Figure 1.1). Water in these hydration spheres will then exhibit properties characteristic of water at these pressures in which very little free volume remains. These quantities are listed in Table 1.1 for a 3+ complex ion together with corresponding properties for bulk solvent water. Pressure values for a 2+ complex ion will be less by the ratio (4/9).

Table 1.1

Estimated Properties of Solvent Water surrounding a 3+ Complex ion.

Hydration Sphere	V ($cm^3 mol^{-1}$)	$10^6 \kappa$ (bar^{-1})	β ($cm^3 mol^{-1}$ $kbar^{-1}$)
first	15.0	8.0	0.12
second	15.6	14.1	0.22
bulk	18.0	46.4	0.84

Thus, surrounding a complex ion of charge +3 are at least two layers of electrostricted water with molar volumes and compressibilities distinctly different to that of bulk solvent water.

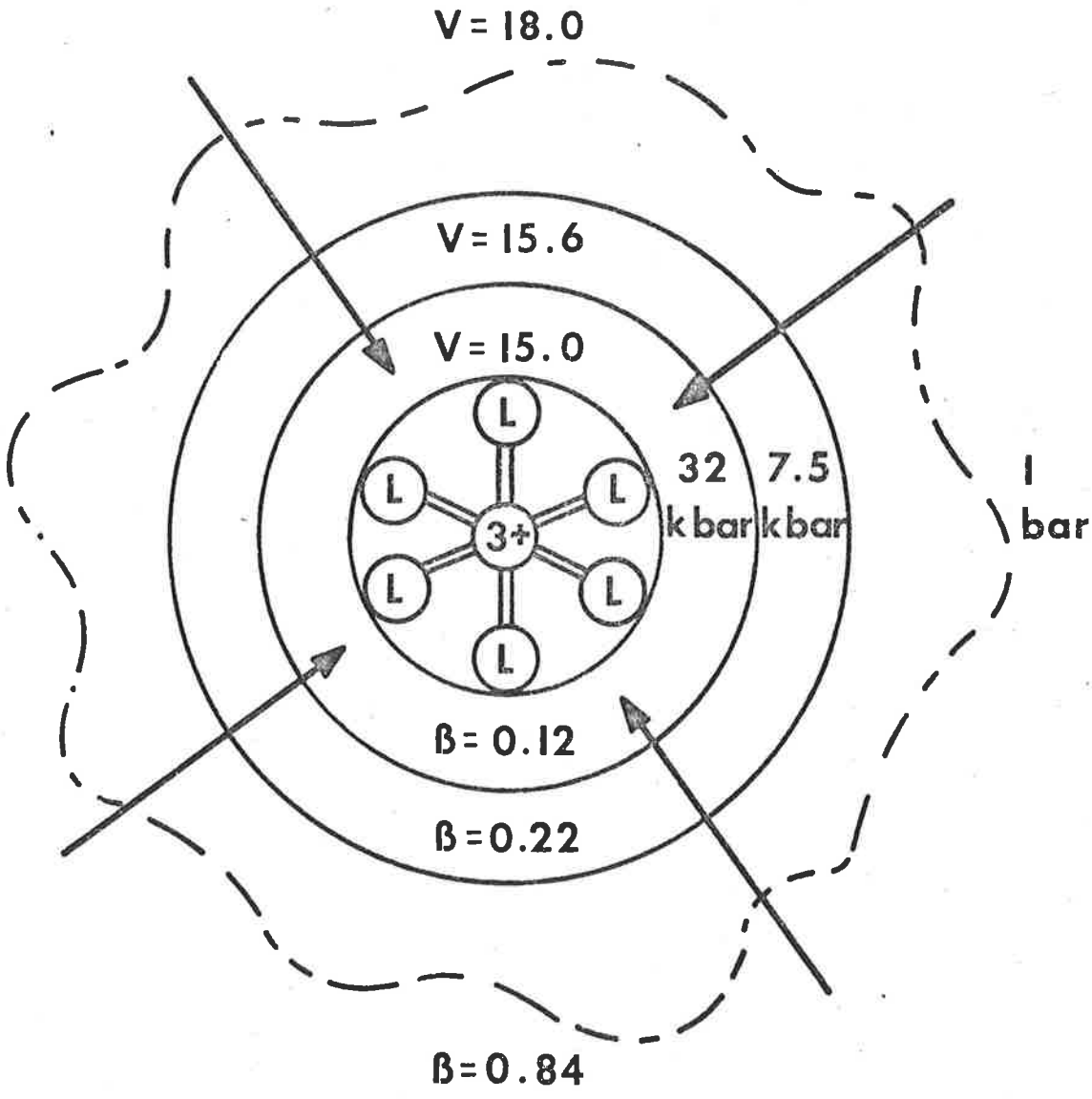

FIG. 1.1 Diagrammatic representation of estimated properties of solvent water surrounding a 3^+ complex ion.

The exchange of water in an activation step between bulk water and these hydration spheres should therefore contribute to $\Delta V_o^{\ddagger}$ and $\Delta\beta^{\ddagger}$.

1.6 Survey of High Pressure Data

In this section, a compilation has been made of reported $\Delta V^{\ddagger}$ values for inorganic reactions. For comparison, the corresponding values for $\Delta H^{\ddagger}$ and $\Delta S^{\ddagger}$ are also listed. Some important features of the data in Tables 1.2 to 1.4 will be briefly discussed.

Swaddle has extensively studied[18,19] the aquation of pentaammine-cobalt III and pentaamminechromium III ions in aqueous solution. For both the cobalt III and chromium III series, a good linear correlation of respective slope 0.98 and 0.59 was observed between $\Delta V^{\ddagger}$ and the overall volume change for the aquation reaction, ΔV°. It was concluded for the cobalt III systems that the transition state resembled closely the ionic products and a dissociative process was argued. On the other hand, the negative $\Delta V^{\ddagger}$ values in the chromium III series ~~was~~ were interpreted by an associative interchange mechanism.

In contrast to the behaviour observed for aquation reactions, there is a complete lack of correlation between $\Delta V^{\ddagger}$ and ΔV° (where a comparison is possible) in magnitude and sometimes sign for nucleophilic substitution reactions (Table 1.2 (B)). In each metal series, however, $\Delta V^{\ddagger}$ is virtually constant regardless of the nucleophile which implies that the common process is dissociative release of an aquo ligand.

The base hydrolysis of ammine-metal complex ions are usually interpreted in terms of a conjugate-base mechanism:

$$Co(NH_3)_5X^{(3-n)+} + OH^- \rightleftharpoons Co(NH_3)_4NH_2X^{(2-n)+} + H_2O \qquad \Delta V^0_{CB}$$

$$Co(NH_3)_4NH_2X^{(2-n)+} + H_2O \rightarrow Co(NH_3)_5OH^{2+} + X^{n-} \qquad \Delta V_2^{\ddagger}$$

such that $\Delta V_o^{\ddagger} = \Delta V^0_{CB} + \Delta V_2^{\ddagger}$. There is evidence[66] for assigning $\Delta V^0_{CB} \simeq 18$ cm^3 mol^{-1}. Consequently from the data in Table 1.2(C), $\Delta V_2^{\ddagger} = -10$ cm^3 mol^{-1}, -0.9 cm^3 mol^{-1} and 1.5 cm^3 mol^{-1} when X = Br^-, OSO_3^{2-} and OPO_3^{3-} respectively. This suggests a dissociative interchange mechanism for the base hydrolysis of $Co(NH_3)_5Br^{2+}$. However the near zero values of $\Delta V_2^{\ddagger}$ for the o-bonded sulphato and phosphato complexes, imply little dissociative release of these ligands in the transition state. The measured activation parameters for the base hydrolysis of the selenitopentaamminecobalt III ion are markedly different to those of the other systems. An associative mechanism involving hydroxide attack at the selenium centre has been suggested[29] for this reaction.

Table 1.2

Activation Parameters for Substitution Reactions

A: Aquation $ML_5X^{n+} + H_2O \rightarrow ML_5H_2O^{(n-m)+} + X^{m-}$

ML_5	X	$\Delta H^{\ddagger}$ (k J mol^{-1})	$\Delta S^{\ddagger}$ (J $K^{-1}mol^{-1}$)
$Co(NH_3)_5^{3+}$	NO_3^-	106	+25
	Br^-	98	-13
	Cl^-	96	-38
	SO_4^{2-}	78	-100
	N_3^-	140	+59
	NCS^-	112	-33
$Cr(NH_3)_5^{3+}$	Cl^-	98	+35
	Br^-	100	+46
	I^-	87	+28
	NCS^-	103	-8
$Cr(NCS)_5^{2-}$	NCS^-	-	-
$Cr(NCS)_3(NH_3)_2^{\circ}$	NCS^-	110	+12
$Pt(NH_3)Cl_2^{\circ}$	Cl^-	79	-96
$PtCl_3^-$	Cl^-	88	-33

$\Delta V^{\ddagger}$ ($cm^3\ mol^{-1}$)	$\Delta V°$ ($cm^3\ mol^{-1}$)	Ref.
-5.9 ± 0.4	-7.2	37,17,18
-8.7 ± 0.2	-10.8	38,39,17,18
-9.9 ± 0.5	-11.6	38,17,18
-7.5 ± 1.0		36
-17.0 ± 0.6	-19.2	40,17,18
+16.0 ± 0.4	-	41,18
-4.0 ± 1.0	-	42,18
-10.6 ± 0.3	-8.4	43,44,19
-9.9 ± 0.3	-7.2	43,44,19
-9.2 ± 0.2	-6.0	43,19
-8.6 ± 1.0	-	42,36
+16 ± 2	-	20
-2.4 ± 0.8	-	45,20
-14 ± 2	-	46,21
-17 ± 2	-	46,47,21

B: Anation $ML_6^{m+} + Y^{n-} \rightarrow ML_{6-n}Y^{(m-n)+} + nL$

ML_6	Y^-	$\Delta H^{\ddagger}$ (kJ mol^{-1})
Fe_{aq}^{3+}	SCN^-	54
Co_{aq}^{2+}	pada[a]	43
	NH_3	25
	$NH_2CH_2CO_2^-$	-
Ni_{aq}^{2+}	pada[a]	57
	NH_3	42
	$NH_2CH_2CO_2^-$	-
Cu_{aq}^{2+}	$NH_2CH_2CO_2^-$	-
Zn_{aq}^{2+}	$NH_2CH_2CO_2^-$	-
Cr_{aq}^{3+}	ox[b]	-
$Cr(ox)(OH_2)_4^+$	ox[b]	-
$Cr(ox)_2(OH_2)_2^-$	ox[b]	-
trans-$Pt(P(C_2H_5)_3)_2Cl^+$	Br^-	-

a: pada is the propriety term for the nitrogen base pyridine-2-azodimethylaniline.

b: the symbol ox indicates free oxalate in the form $H_2C_2O_4$, $HC_2O_4^-$, $C_2O_4^{2-}$.

$\Delta S^{\ddagger}$ ($J\ K^{-1}mol^{-1}$)	$\Delta V^{\ddagger}$ (cm^3mol^{-1})	$\Delta V°$ (cm^3mol^{-1})	ref.
-21	+5.5 ± 0.5	+17.5	48,22
-8	+7.2 ± 0.2	+5.8 ± 0.4	49,23,24
-63	+4.8 ± 0.7	-8.6 ± 1.6	50,23,24
-	+8 ± 2	+7.3 ± 1.8	25
+4	+7.7 ± 0.3	+0.9 ± 0.7	49,23,24
-25	+6.0 ± 0.3	-2.3 ± 0.7	50,23,24
-	+10 ± 1	+2.1 ± 0.6	25
-	+12 ± 1	+13.4 ± 0.4	25
-	+7 ± 1	+5.2 ± 0.8	25
-	-2.2 ± 1	-	26
-	-8.2 ± 0.5	-	26
-	-10.0 ± 0.5	-	26
-	-28 ± 3	-	27

C: Base Hydrolysis

$ML_5X^{(3-n)+} + OH^- \rightarrow ML_5OH^{2+} + X^{n-}$

ML_5X	$\Delta H^{\ddagger}$ (kJ mol^{-1})	$\Delta S^{\ddagger}$ (J $K^{-1}mol^{-1}$)	$\Delta V^{\ddagger}$ (cm^3mol^{-1})	ref.
$Co(NH_3)_5Br^{2+}$	115	167	+8.5	39,51,28
$Co(NH_3)_5OSO_3^{+}$	110	100	+19.5 ± 1.1	52,29
$Co(NH_3)_5OSeO_2^{+}$	48	-121	-17.1 ± 1.0	52,53,29
$Co(NH_3)_5OPO_3^{0}$	146	137	+22 ± 2	54,29

The potential usefulness of volumes of activation is well illustrated from the $\Delta V^{\ddagger}$ values for the exchange of $^{18}OH_2$ solvent with aquo metal complexes (Table 1.3). For the last three systems, the systematic uncertainties in $\Delta S^{\ddagger}$ ($\pm$ 4.2 J K^{-1} mol^{-1}) do not permit a satisfactory conclusion as to the mechanistic role of water for these reactions. However the negative values of $\Delta V^{\ddagger}$ clearly establish the associative nature of these water exchanges and the slightly dissociative character in the first system. In the associative reactions, there are significant differences in the extent to which the water nucleophile is associated in the transition state.

Table 1.3

Activation Parameters for Water Exchange Reactions

$$ML_5OH_2^{3+} + {}^{18}OH_2 \rightarrow ML_5{}^{18}OH_2^{3+} + OH_2$$

ML_5	$\Delta H^{\ddagger}$ (kJ mol^{-1})	$\Delta S^{\ddagger}$ (J $K^{-1}mol^{-1}$)	$\Delta V^{\ddagger}$ (cm^3mol^{-1})	ref.
$Co(NH_3)_5$	111	+28	+1.2 ± 0.2	30
trans-$Cr(C_2O_4)_2OH_2$[a]	76	-62	-16 ± 1	65
$Rh(NH_3)_5$	103	+3	-4.1 ± 0.4	31,55
$Cr(NH_3)_5$	97	0	-5.8 ± 0.2	31,56
$Cr(OH_2)_5$	110	+1	-9.3 ± 0.3	32,57

a - studied via the *trans* → *cis* isomerization.

Jolley has investigated[34] the volume change for several outer-sphere electron exchange reactions. The volume of activation, $\Delta V^{\ddagger}$, for these reactions may be separated as follows:

$$\Delta V_0^{\ddagger} = \Delta V_{coul}^{\ddagger} + \Delta V_{SR}^{\ddagger} + \Delta V_{IR}^{\ddagger} + \Delta V_{DH}^{\ddagger} \qquad 1.19$$

where these separate terms represent in turn the volume change for coulombic work in bringing charged reactions to the transition state ($\Delta V_{coul}^{\ddagger}$), the solvent rearrangement on formation of the charged transition state ($\Delta V_{SR}^{\ddagger}$), the internal rearrangement of the metal-ligand bonds to an intermediate configuration ($\Delta V_{IR}^{\ddagger}$) and the change in activity due to interionic interactions in a reaction medium of finite ionic strength ($\Delta V_{DH}^{\ddagger}$). Values for $\Delta V_0^{\ddagger}$ may be estimated from equation 1.19 using the Marcus-Hush theory for outer-sphere electron transfer reactions in solution. Good agreement was found between the measured and predicted values (Table 1.4(A)). It was concluded that the major contributions to the volume of activation stem from electrostatic repulsions and electrostrictive processes outside the primary coordination sphere.

Candlin and Halpern have studied[35] a series of electron transfer reactions between cobalt III complexes and Fe_{aq}^{2+} (Table 1.4(B)). The aim of this study was to provide a means for distinguishing between inner-sphere and outer-sphere mechanisms. According to the authors, the liberation of a water molecule from the first coordination sphere to the bulk solvent, in the case of an inner-sphere mechanism, should lead to a significant difference in the

$\Delta V^{\ddagger}$ for each mechanism. For all the reactions studied, positive values for $\Delta V_o^{\ddagger}$ were observed and an inner-sphere mechanism was argued in each case.

Table 1.4

Activation Parameters for Electron Transfer Reactions

A: $M^{a+} + {}^{*}N^{b+} \rightarrow {}^{*}M^{a+} + N^{b+}$

M	N	$\Delta H^{\ddagger}$ (kJ mol^{-1})	$\Delta S^{\ddagger}$ (J $K^{-1}mol^{-1}$)	$\Delta V_o^{\ddagger}$ (cm^3mol^{-1})	$\Delta V^{\ddagger}_{calc.}$ (cm^3mol^{-1})	ref.
Tl^{3+}_{aq}	Tl^{+}_{aq}	73	-88	-13.2 ± 1	-13.7	58,33
$Co(EDTA)^{2-}$	$Co(EDTA)^{-}$	92	-69	-4.5 ± 0.5	-7.2	59,60,34
$Co\ en_3^{3+}$	$Co\ en_3^{2+}$	56	-134	-21.1 ± 1.5	-14.2	61,34
Fe^{3+}_{aq}	Fe^{2+}_{aq}	39	-105	-12.2 ± 1.5	-16.0	62,34

B: Redox Reactions

Reaction	$\Delta H^{\ddagger}$ (kJ mol^{-1})	$\Delta S^{\ddagger}$ (J $K^{-1}mol^{-1}$)	$\Delta V^{\ddagger}$ (cm^3mol^{-1})	ref.
Fe^{2+}_{aq} + $Co(NH_3)_5F^{2+}$	57	-96	+11 ± 1	63,35
Fe^{2+}_{aq} + $Co(NH_3)_5Cl^{2+}$	52	-126	+8 ± 1	63,35
Fe^{2+}_{aq} + $Co(NH_3)_5Br^{2+}$	56	-117	+8 ± 1	63,35
Fe^{2+}_{aq} + $Co(NH_3)_5N_3^{2+}$	-	-	+14 ± 1	35
Fe^{2+}_{aq} + *cis*-$Co(NH_3)_4(N_3)_2^{+}$	-	-	+14 ± 1	35
Fe^{2+}_{aq} + $Co(HEDTA)Cl^{-}$	47	-92	+3 ± 1	64,35
Fe^{2+}_{aq} + *trans*-$Co(NH_3)_4(N_3)_2^{+}$	-	-	+2.2 ± 1	35

1.7 Present Study

It is clear that the volume of activation and compressibility of activation provide mechanistic insight into the structure of the reactants in the transition state and the participation of the solvent in the activation process. It is obviously highly desirable to have a bank of measured $\Delta V^{\ddagger}$'s for reactions from all classes of inorganic reactions in solution for it might then be possible to impute certain mechanistic features to a given reaction from a consideration of its measured $\Delta V^{\ddagger}$. However, very little data is available for inorganic systems and a systematic analysis is possible in only a few cases. One of the reasons for the present studies is to offset this dearth in information.

The volumes of activation for the following systems are examined:

$$\textit{trans}\text{-Co en}_2(OH_2)_2^{3+} \rightleftarrows \textit{cis}\text{-Co en}_2(OH_2)_2^{3+}$$

$$\textit{trans}\text{-Co en}_2(OH_2)OSeO_2H^{2+} \rightleftarrows \textit{cis}\text{-Co en}_2(OH_2)OSeO_2H^{2+}$$

$$\textit{cis}\text{-Co en}_2(OH_2)_2^{3+} + HC_2O_4^- \rightarrow \text{Co en}_2C_2O_4^+ + H^+_{aq}$$

The first of these reactions is believed to proceed by a dissociative mechanism. The second reaction has not been previously investigated. An ion-pair mechanism has been suggested for the third system.

Often the mechanism for inorganic reactions involves several successive steps. An example of this is the ion-pair mechanism which involves two stages, a rapid pre-equilibrium and a rate

determining interchange step. In order to fully interpret the reaction process, a knowledge of the volume change for both steps is required. However, pressure effects on equilibrium reactions have received little attention. A second aim of the present studies is to provide data for the hydrolysis equilibria of aqueous metal ions.

The volume changes for the following equilibria are examined:

$$Fe^{3+}_{aq} \rightleftarrows FeOH^{2+} + H^{+}_{aq}$$

$$Tl^{3+}_{aq} \rightleftarrows TlOH^{2+} + H^{+}_{aq}$$

$$Co(NH_3)_5OH_2^{3+} \rightleftarrows Co(NH_3)_5OH^{2+} + H^{+}_{aq}$$

References to Chapter 1.

1. S.D. Hamann, *"Physico-Chemical Effects of Pressure"*, *Academic Press Inc., New York*, 1957.
2. S.D. Hamann, in *"High Pressure Physics and Chemistry"*, *Academic Press Inc., New York*, 1963, 2, Ed. R.S. Bradley.
3. S.D. Hamaan, *Ann. Rev. Phys. Chem.*, 1964, 15, 349.
4. E. Whalley, *Advan. Phys. Org. Chem.*, 1963, 2, 93.
5. E. Whalley, *Ann. Rev. Phys. Chem.*, 1967, 18, 205.
6. W.J. le Noble, *Prog. Phys. Org. Chem.*, 1967, 5, 207.
7. G. Kohnstram, *Prog. React. Kinetics*, 1970, 5, 335.
8. C.A. Eckert, *Ann. Rev. Phys. Chem.*, 1972, 23, 239.
9. M.G. Evans and M. Polanyi, *Trans. Faraday Soc.*, 1935, 31, 875.
10. H.S. Golinkin, W.G. Laidlaw and J.B. Hyne, *Canad. J. Chem.*, 1966, 44, 2193.
11. S.W. Benson and J.A. Berson, *J. Amer. Chem. Soc.*, 1962, 84, 152.
12. H.S. Harned and B.B. Owen, *"The Physical Chemistry of Electrolyte Solutions"*, 3rd edn., *Reinhold Publ. Corp., New York*, 1958.
13. D.R. Stranks, *Plenary Lecture to the 15th International Conference on Coordination Chemistry, Moscow*, June 1973.
14. N.S. Hush, *Discuss. Faraday Soc.*, 1958, 26, 154.
15. M. Born, *Z. Physik.*, 1920, 1, 45.
16. E. Whalley, *J. Chem. Phys.*, 1968, 38, 1400.
17. W.E. Jones and T.W. Swaddle, *Chem. Comn.*, 1969, 998.

18. W.E. Jones, L.R. Carey and T.W. Swaddle, *Canad. J. Chem.*, 1972, 50, 2739.

19. G. Guastalla and T.W. Swaddle, *Canad. J. Chem.*, 1973, 51, 821.

20. D.L. Gay and R. Nalepa, *Canad. J. Chem.*, 1971, 49, 1644.

21. H.E. Brower, L. Hathaway and K.R. Brower, *Inorg. Chem.*, 1966, 5, 1899.

22. K.R. Brower, *J. Amer. Chem. Soc.*, 1968, 90, 5401.

23. E.F. Caldin, M.W. Grant and B.B. Hasinoff, *Chem. Comm*, 1971, 1351.

24. E.F. Caldin, M.W. Grant and B.B. Hasinoff, *J. Chem. Soc. Faraday I*, 1972, 68, 2247.

25. M.W. Grant, *J. Chem. Soc., Faraday I*, 1973, 69, 560.

26. C. Schlenk and H. Kelm, *J. Coord. Chem.*, 1972, 2, 71.

27. T. Taylor and L.R. Hathaway, *Inorg. Chem.*, 1969, 8, 2135.

28. C.T. Burris and K.J. Laidler, *Trans. Faraday Soc.*, 1955, 51, 1497.

29. J.V. Dubrawski, J.M. Lucie and D.R. Stranks, *unpublished results, quoted in reference 13.*

30. H.R. Hunt and H. Taube, *J. Amer. Chem. Soc.*, 1958, 80, 2642.

31. T.W. Swaddle and D.R. Stranks, *J. Amer. Chem. Soc.*, 1972, 94, 8357.

32. D.R. Stranks and T.W. Swaddle, *J. Amer. Chem. Soc.*, 1971, 93, 2783.

33. M.G. Adamson and D.R. Stranks, *Chem. Comm.*, 1967, 684.

34. W.H. Jolley, *Ph.D. Thesis, University of Adelaide*, 1970.

35. J.P. Candlin and J. Halpern, *Inorg. Chem.*, 1965, 4, 1086.

36. D.L. Gay and R. Nalepa, *Canad. J. Chem.*, 1970, 48, 910.

37. J.N. Bronsted, Z. *Phys. Chem.*, 1926, 122, 383.

38. A.W. Adamson and F. Basolo, *Acta Chem. Scand.*, 1955, 9, 1261.

39. J.N. Bronsted and R.J. Livingston, *J. Amer. Chem. Soc.*, 1927, 49, 435.

40. B. Adell, *Z. Anorg. Chem.*, 1942, 249, 251.

41. G.C. Lalor and E.A. Moelwyn-Hughes, *J. Chem. Soc.*, 1963, 1560.

42. D.L. Gay and G.C. Lalor, *J. Chem. Soc.*, 1966A, 1179.

43. W.A. Levine, T.P. Jones, W.E. Harris and W.J. Wallace, *J. Amer. Chem. Soc.*, 1961, 83, 2453.

44. A. Ogard and H. Taube, *J. Amer. Chem. Soc.*, 1958, 80, 1084.

45. A.W. Adamson, *J. Amer. Chem. Soc.*, 1958, 80, 3183.

46. U. Belluco, R. Ettore, F. Basolo, R.G. Pearson and A. Turco, *Inorg. Chem.*, 1966, 5, 591.

47. L.F. Grantham, T.S. Elleman and D.S. Martin, *J. Amer. Chem. Soc.*, 1955, 77, 2965.

48. J.F. Bellow, R.E. Connick and C.P. Cappell, *J. Amer. Chem. Soc.*, 1958, 80, 2961.

49. M.A. Cobb and D.N. Hague, *J. Chem. Soc., Faraday I*, 1972, 68, 1.

50. D.B. Rorabacker, *Inorg. Chem.*, 1966, 5, 1891.

51. C.T. Burris and K.J. Laidler, *Trans. Faraday Soc.*, 1955, 51, 1497.

52. J.V. Dubrawski, *Honours Report, University of Adelaide*, 1972.

53. N. Vanderhoek, *Honours Report, University of Adelaide*, 1969.

54. S.F. Lincoln and D.R. Stranks, *Aust. J. Chem.*, 1968, 21, 1733.

55. H.L. Bott, A.J. Poe and K. Shaw, *J. Chem. Soc. A.*, 1970, 1745.

56. N.V. Duffy and J.E. Earley, *J. Amer. Chem. Soc.*, 1967, 89, 272.

57. J.P. Hunt and R.A. Plane, *J. Amer. Chem. Soc.*, 1954, 76, 5960.

58. E. Roig and R.W. Dodson, *J. Phys. Chem.*, 1961, 65, 2175.

59. A.W. Adamson and K.S. Vorres, *J. Inorg. Nucl. Chem.*, 1956, 3, 206.

60. Y.A. Im and D.H. Bush, *J. Amer. Chem. Soc.*, 1961, 83, 3357.

61. F.P. Dwyer and A.M. Sargeson, *J. Phys. Chem.*, 1961, 65, 1892.

62. J. Silverman and R.W. Dodson, *J. Phys. Chem.*, 1952, 56, 846.

63. J.H. Espenson, *Inorg. Chem.*, 1965, 4, 121.

64. A. Pidcock and W.C.E. Higginson, *J. Chem. Soc.*, 1963, 2798.

65. E.G. Conze, H. Stieger and H. Kelm, *Chem. Ber.*, 1972, 105, 2334.

66. T.G. Spiro, A. Revesz and J. Lee, *J. Amer. Chem. Soc.*, 1968, 90, 4000.

Chapter 2 The Effect of Pressure on the trans to cis Isomerisation of the diaquobis(ethylenediamine)-cobalt III cation.

2.1 Introduction

The behaviour of the cation Co $en_2(H_2O)_2^{3+}$ in relation to the rates of isomerisation, water exchange and the position of the *cis/trans* equilibrium as a function of pH, has been previously investigated.[1]

Three hydroxylic species Co $en_2(H_2O)_2^{3+}$, Co $en_2(OH)OH_2^{2+}$ and Co $en_2(OH)_2^{+}$ have been reported[1] and both *cis* and *trans* isomers have been identified for each species. At 25°C and in a 1 M $NaNO_3$ aqueous medium the following overall equilibrium scheme exists:[1]

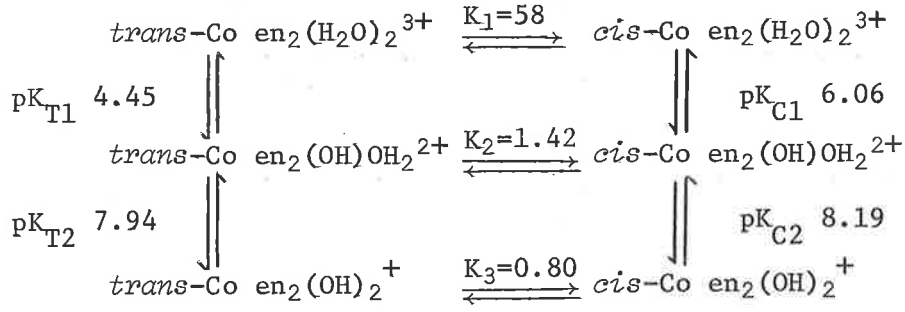

where K_n is the equilibrium constant for the *cis/trans* isomers and pK_{an}, the acidity constants. The equilibrium K_2 is established far more rapidly than both K_1 and K_3. Whereas K_1 strongly favours the *cis* isomer, with increasing acidity, K_2 and K_3 are the predominant equilibria and the *trans* isomer is increasingly favoured. When

$NaClO_4$ is used as the supporting electrolyte,[2,3] the *cis/trans* ratios are similar, but not identical to those found by Bjerrum and Rasmussen.[1] The *cis/trans* ratio is invariant of temperature at all pH[2,4].

Tong and Yankwich[5] have measured the rates of isomerisation for the diaquo and dihydroxo ions. The rate coefficient for the isomerisation of Co $en_2(H_2O)_2^{3+}$ in 1 M perchloric acid was found at 24.8°C to be 4.2×10^{-4} $mins^{-1}$. At 35°C, 0.01 M hydroxide concentration and total ionic strength of 1.0 M, the rate constant for the *trans* to *cis* conversion of the dihydroxo species was determined to be 2.6×10^{-3} $mins^{-1}$. The aquo hydroxo ions isomerise[6] at 25°C much more rapidly than their diaquo and dihydroxo analogues.

In a detailed study, Kruse and Taube[4] have attempted to correlate the rates of isomerisation of the various hydroxylic species with the rates of water exchange of these species. The activation parameters for the various rate processes are summarised in Table 2.1.

Table 2.1

Activation Parameters for the isomerisation reaction of Co en_2X_2 at 25°C.

R ≡ Co en_2 ; X = H_2O or OH

Reaction Type	10^6 k (sec^{-1})	$\Delta H^{\ddagger}$ (k J mol^{-1})	$\Delta S^{\ddagger}$ (J K^{-1} mol^{-1})
cis $R(H_2O)_2^{3+}$ exchange	7.5	120.5	63
cis $R(OH)_2^{+}$ exchange	30.0	114.6	54
trans $R(H_2O)_2^{3+}$ exchange	11.3	128.0	88
trans $R(OH)_2^{+}$ exchange	2.3	127.2	84
trans $R(H_2O)_2^{3+} \rightarrow$ *cis*	6.8	107.1	17
cis $R(H_2O)_2^{3+} \rightarrow$ *trans*	0.12[a]	-	-
trans $R(OH)_2^{+} \rightarrow$ *cis*	3.2	117.1	-
cis $R(OH)_2^{+} \rightarrow$ *trans*	3.7	117.1	-

a: from reference 7.

For *cis* and *trans* Co $en_2(OH_2)_2^{3+}$, one molecule of water is brought into exchange with the solvent for each act of isomeric change. The kinetic data did not allow an unambiguous designation of the intermediate involved in the reaction, but a dissociative process was favoured. The data could not be explained by a single intermediate

since this requires the water exchange of *cis*-Co $en_2(OH_2)_2^{3+}$ to be equal to or less than its rate of isomerisation, in contrast to that observed. A reaction profile was suggested in which two intermediates, of tetragonal pyramidal structure, formed from the *trans* and *cis* complexes respectively by the loss of a coordinated water molecule. These intermediates either returned to the initial substrates to allow water exchange without rearrangement or are further distorted (to a trigonal bipyramidal arrangement) to permit isomerisation.

The present study was undertaken for the following reasons; 1) the isomerisation in aqueous acidic medium is slow enough to permit a study by high pressure techniques and 2) a pressure dependence study should provide further insight as to the mechanism of the reaction.

2.2 *Experimental*

2.2.1 *Materials*

trans-$[Co\ en_2(H_2O)(OH)](ClO_4)_2$ was prepared by the method of Kruse and Taube.[4] The product was purified by recrystallisation and obtained in 50% yield.

$HClO_4$

Perchloric acid of the desired molarity was prepared from concentrated Analar perchloric acid by dilution with doubly distilled water and standardised against A.R. mercuric oxide and potassium iodide to a methyl red end point.

$NaClO_4$

Sodium perchlorate, supplied by G.F. Smith Company, was recrystallised twice from water and dried overnight at 120°C.

2.2.2 *Apparatus*

Pressure Vessels

Both the high pressure sampling vessel and optical vessel used in these studies are described elsewhere (Appendix I).

Spectrophotometers

Accurate absorbance measurements were made using a manually-operated Shimadzu spectrophotometer, Model QR-50. Measurements on duplicate samples were reproducible to ± 0.001 optical absorbance units. Matched 1 cm silica cells were used.

For complete spectra in the U.V. and visible regions,

the Unicam S.P. 800 recording spectrophotometer (± 0.01 absorbance units) was used.

Temperature Control

The high pressure sampling vessel was maintained at the desired temperature by immersion in an oil bath (Ondina 33) maintained to within ± 0.01 degree of the required temperature by a solid state proportional control heater, regulated by a thermistor probe.

With the optical vessel, the cell temperature was kept at the desired value by the rapid circulation of constant temperature water through the water jackets of the cell holders. Temperature control (± 0.1°C) of the water bath was achieved as above.

2.2.3 Procedure for Kinetic Runs

Sampling Procedure

A weighed quantity of the *trans* hydroxo salt was dissolved in a known volume of perchloric acid and brought to the reaction temperature. Aliquot samples were withdrawn at regular time intervals, quenched in ice-chilled tubes and analysed spectrophotometrically at 492 nm where the respective molar extinction coefficients for *cis* and *trans* Co $en_2(OH_2)_2^{3+}$ are 19.2 M^{-1} cm^{-1} and 80.9 M^{-1} cm^{-1}.[1]

A similar procedure was followed for the pressure runs. The reactant solution was prepared, as before, and transferred to the Perspex reaction vessel. The Teflon plunger was placed in position, the apparatus lowered into the pressure vessel and the pressure

raised to the desired value. After thermal equilibrium had been attained (30 minutes) aliquot samples were withdrawn and analysed as above.

Procedure with the Optical Vessel

The sample cuvette, filled with the reactant solution and sealed by a teflon cap, was transferred to the optical vessel mounted inside the cell compartment of the Unicam SP 800 spectrophotometer. The pressure was raised to the desired value and the reactant solution left at this pressure for at least 30 minutes to attain thermal equilibrium. Each run was followed by recording, on a Riken Denshi Speedex Model SP-G3 slave recorder, the change with time in optical absorbance at 492 nm, using the Scale Expansion Accessory with the spectrophotometer.

2.3 Results

2.3.1 Evaluation of Kinetic Data

Sampling Technique

Values of $\log \frac{OD_\infty - OD_o}{OD_\infty - OD_t}$ were plotted against time, where OD_∞, OD_o and OD_t represents the infinite, zero and time t optical absorbance readings. The observed first order isomerisation rate coefficients, k_{isom}, were obtained from the slope of such plots. This observation is in agreement with previous workers who reported first order kinetics.

All reactions were followed over one or two half lives and the final absorbance measurements taken after at least six half lives.

Direct monitoring technique

For convenience, the Guggenheim method of analysis was employed. Plots of $\log (OD_t - OD_{t+\Delta})$ against time, where OD_t and $OD_{t+\Delta}$ denote the optical absorbance and time t and $t+\Delta$, and Δ is fixed time increment of at least two reaction half times, were linear. The slope of such plots is equal to $-k_{isom}/2.303$.

2.3.2 The Effect of Temperature on the Isomerisation Rate Constant.

The values of k_{isom} obtained from first order plots are, in fact, equal to $k_{t-c} + k_{c-t}$ where k_{t-c} represents the change of *trans* isomer to *cis* product and k_{c-t} governs the change for the reverse

process. In strongly acidic solution the *cis* to *trans* ratio at equilibrium has a reported[1] value of 58. It follows then that k_{c-t} contributes only 2% to k_{isom}. Any change in k_{isom} with temperature (and pressure) may, therefore, to a good approximation, be ascribed as arising from variations in k_{t-c}. Furthermore, this assumption is valid at least from 34.5°C to 55°C since within experimental uncertainty there is no observed change in the infinite absorbance readings.

The temperature dependence on the *trans* to *cis* isomerisation rate process was studied between 34.5°C and 55°C at total ionic strengths of 0.05M and 1.0 M. The data are listed in Tables 2.2 and 2.3, where k_{isom} represents the mean value of at least three determinations at each temperature and ionic strength; the standard deviation in k_{isom} being close to 3% in all cases.

In Figures 2.1 and 2.2, log k_{isom} have been plotted against 1/T. The straight lines drawn through these data are the lines of best fit, calculated using a least squares method. The derived activation parameters are;

$$\Delta H^{\ddagger}(1M\ HClO_4) = 121.7 \pm 1.0 \quad kJ\ mol^{-1}$$

$$\Delta S^{\ddagger}(1M\ HClO_4) = 64 \pm 4 \quad JK^{-1}mol^{-1}$$

$$\Delta H^{\ddagger}(0.05M\ HClO_4) = 131.4 \pm 1.2 \quad kJ\ mol^{-1}$$

$$\Delta S^{\ddagger}(0.05M\ HClO_4) = 103 \pm 5 \quad JK^{-1}mol^{-1}$$

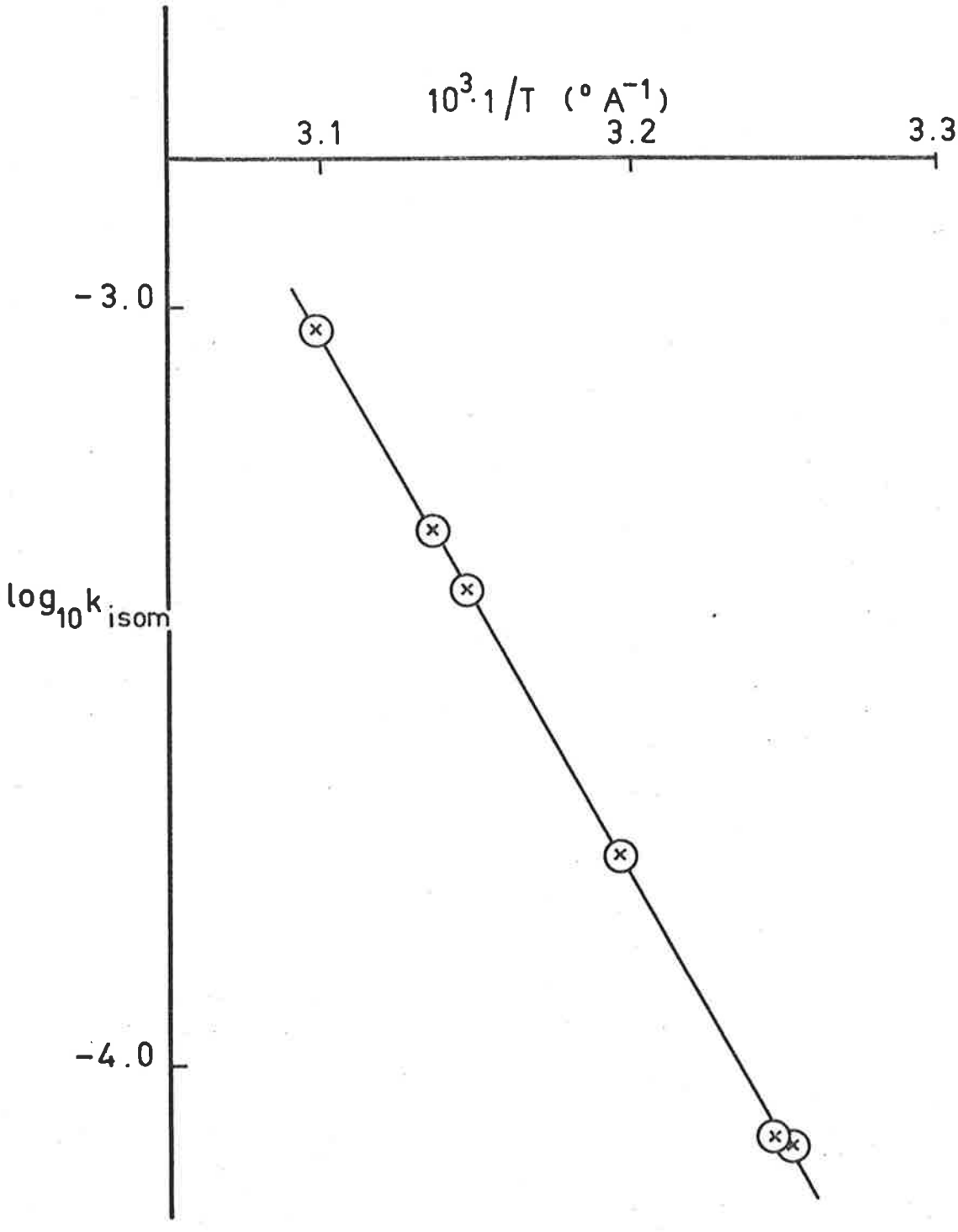

FIG. 2.1 The effect of temperature on k_{isom} in 0.05 M $HClO_4$.

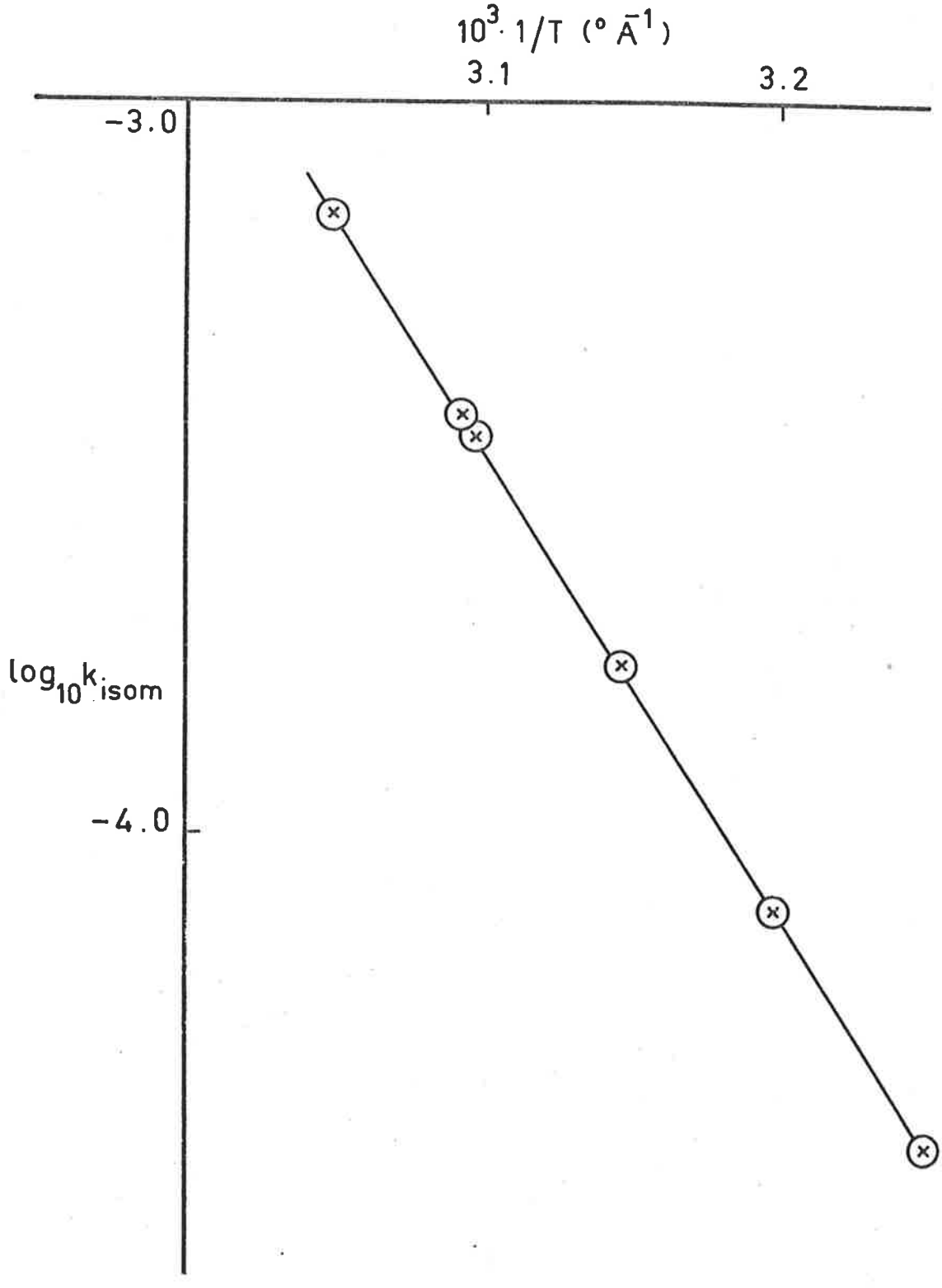

FIG. 2.2 Variation of k_{isom} with temperature in 1 M $HClO_4$.

Table 2.2

Effect of Temperature on the Rate of Isomerisation of trans-Co $en_2(H_2O)_2^{3+}$ in 0.05 M $HClO_4$

Temp (°C)	$10^5 . k_{isom}$ (sec^{-1})	no. of runs
34.5	7.85 ± 0.10	6
35.0	8.18 ± 0.12	3
40.0	19.1 ± 0.25	4
45.0	42.8 ± 0.28	3
46.0	51.3 ± 0.52	4
50.0	95.1 ± 1.10	3

Table 2.3

Effect of Temperature on the Rate of Isomerisation of trans-Co $en_2(H_2O)_2^{3+}$ in 1.0 M $HClO_4$

Temp (°C)	$10^5 . k_{isom}$ (sec^{-1})	no. of runs
35.0	3.63 ± 0.05	3
40.0	7.76 ± 0.08	4
45.0	16.8 ± 0.15	6
50.0	34.4 ± 0.28	5
50.5	37.0 ± 0.51	5
55.0	69.3 ± 0.80	3

2.3.3 Pressure Dependence of k_{isom}

The rate of isomerisation of *trans*-Co $en_2(OH_2)_2^{3+}$ was studied at pressures between 0 and 2 kbar and acid concentrations between 0.05 M and 1.0 M using a reactant concentration of 0.01 M for the aquo species. The results are listed in Tables 2.4 to 2.7.

At the same reaction temperature, there was no detectable difference in the rates observed with glass and perspex vessels. At identical reaction conditions, there was good agreement in observed rates when using the two different reactors and kinetic procedures. A number of runs at each pressure revealed that the standard deviation of each mean value for k_{isom} was close to ± 2%.

The variation of the rate coefficient with pressure at three reaction conditions is shown in Figure 2.3 where log k_p/k is plotted against pressure. At ionic strengths greater than 0.50 M the pressure dependence is seen to be clearly non-linear. The volume of activation, $\Delta V^{\ddagger}$, must then be estimated from the slope of the tangent to the curve of log k and P as $P \rightarrow 0$. A curve was fitted to the experimental data by using a non-linear least squares multiple regression computer program. This program calculates, for a set of data, the curve of best fit in the form of a polynomial up to degree four. To obtain a more accurate value for the derivative $(\partial \log k_{isom}/\partial P)_T$, several values of log k_{isom} were found at the lower pressures. Based on the statistical "t" best for 95% confidence levels, it was found that the data in Tables 2.4 to 2.7 could be best represented by a polynomial of the form

$$\log k_p = \log k_o + bp + cp^2$$

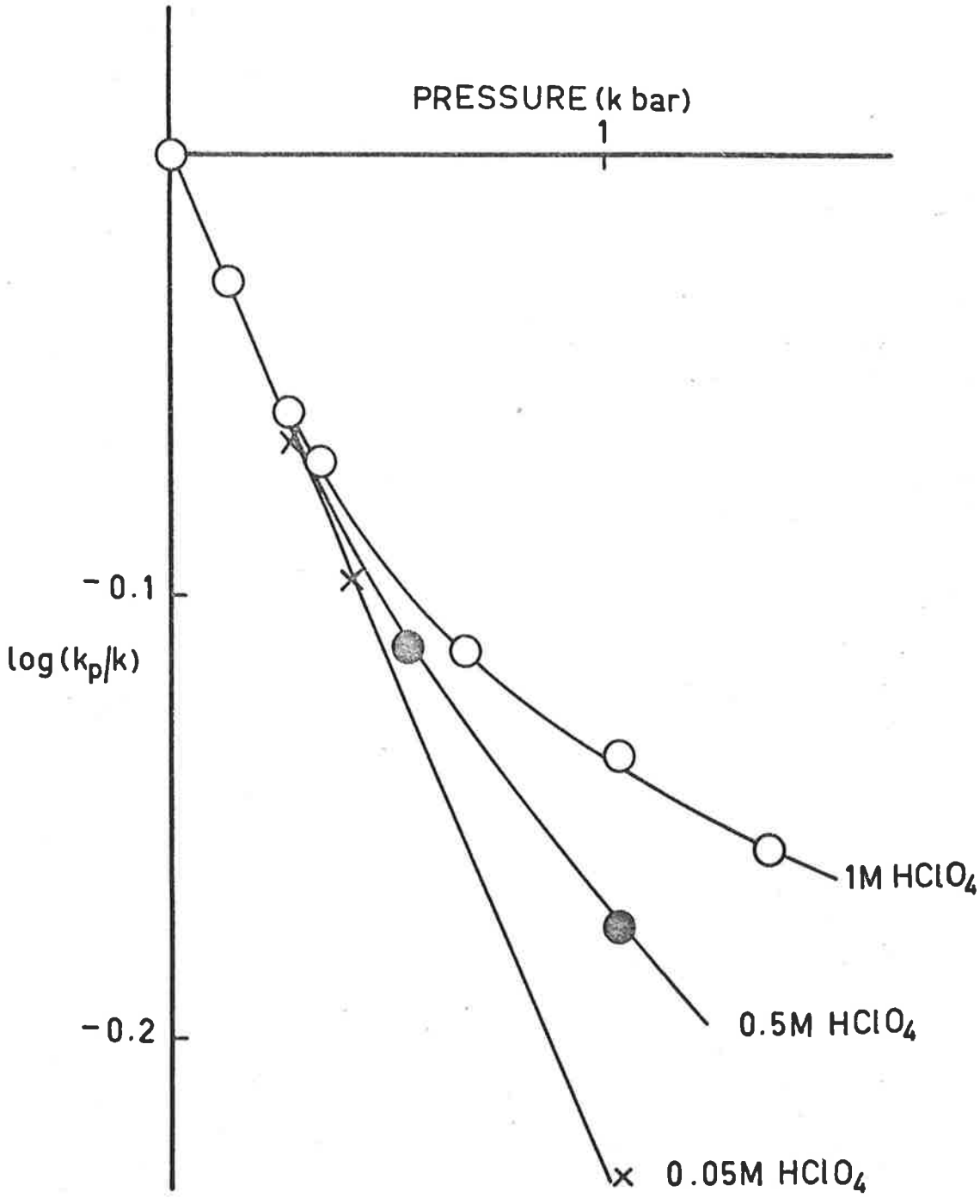

FIG. 2.3 Variation of k_{isom} with pressure.

Table 2.4

Effect of Pressure on the Rate of Isomerisation of *trans*-Co $en_2(H_2O)_2^{3+}$ in 1 M $HClO_4$

Temp; 45.0 ± 0.1°C — Sampling Vessel

Pressure (bar)	$10^4.k_{isom}$ (sec^{-1})	No. of runs	Reaction Vessel
0[a]	1.30	-	glass
0	$1.68 \pm 0.02_0$	6	glass
0	$1.67 \pm 0.01_5$	4	perspex
139	$1.57 \pm 0.01_0$	6	perspex
278	$1.47 \pm 0.01_8$	6	perspex
345	$1.43 \pm 0.02_5$	6	perspex
690	$1.30 \pm 0.02_0$	6	perspex
1035	$1.23 \pm 0.01_5$	6	perspex
1380	$1.17 \pm 0.01_0$	6	perspex

a - computed from the activation parameters of Kruse and Taube.[4]

Temp; 50.5 ± 0.1°C — Optical Vessel

0	$3.62 \pm 0.02_6$	4	perspex[b]
0	3.70 ± 0.03	5	glass
172	3.37 ± 0.03	4	glass
344	$3.16 \pm 0.03_5$	4	glass
516	$3.00 \pm 0.02_5$	4	glass
1020	2.70 ± 0.03	5	glass

b - obtained using the sampling vessel.

Table 2.5

Effect of Pressure on the Rate of Isomerisation of *trans*-Co $en_2(H_2O)_2^{3+}$ in 1 M $NaClO_4$

Temp; 45.0 ± 0.1°C Sampling Vessel

Pressure (bar)	$10^4 k_{isom}$ (sec^{-1})	No. of runs	Reaction Vessel
0	2.82 ± 0.05	4	perspex
136	2.62 ± 0.03	5	perspex
272	2.47 ± 0.03	5	perspex
544	2.27 ± 0.02	5	perspex
1020	2.08 ± 0.03	6	perspex

Table 2.6

Effect of Pressure on the Rate of Isomerisation of *trans*-Co $en_2(H_2O)_2^{3+}$ in 0.5 M $HClO_4$

Temp; 48.0 ± 0.1°C Sampling Vessel

Pressure (bar)	$10^4 k_{isom}$ (sec^{-1})	No. of runs	Reaction Vessel
0	$2.38 \pm 0.04_5$	4	perspex
136	$2.21 \pm 0.03_5$	5	perspex
272	2.09 ± 0.04	5	perspex
544	1.85 ± 0.04	5	perspex
1020	1.60 ± 0.03	5	perspex

Table 2.7

Effect of Pressure on the Rate of Isomerisation of *trans*-Co $en_2(H_2O)_2^{3+}$ in 0.05 M $HClO_4$

Pressure (bar)	$10^5 k_{isom}$ (sec^{-1})	No. of runs	Reaction Vessel
Temp; 34.5 ± 0.1°C			Sampling Vessel
0	7.85 ± 0.10	6	perspex
136	7.31 ± 0.08	6	perspex
272	6.74 ± 0.08	6	perspex
408	6.29 ± 0.05	6	perspex
1020	4.60 ± 0.08	6	perspex
Temp; 46.0 ± 0.1°C			Optical Vessel
0	51.3 ± 0.8	4	glass
172	46.7 ± 0.8	4	glass
344	42.6 ± 0.5	4	glass
516	38.7 ± 0.6	5	glass
860	32.0 ± 0.3	5	glass

The determined values for $\Delta V^{\ddagger}$ and $\Delta\beta^{\ddagger}$, together with their standard deviations, are summarised in Table 2.8. In this there is only a slight decrease in $\Delta V_o^{\ddagger}$ when the ionic strength is increased from 0.05 M to 1.0 M. However, $\Delta\beta^{\ddagger}$ increased by a factor close to 10 for the same range in ionic strength.

Table 2.8

Volumes of Activation, and their Pressure Dependence for the Reaction:

trans → *cis* Co $en_2(OH_2)_2^{3+}$

Reaction Vessel	Electrolyte Concentration	Temp (°C)	$\Delta V^{\ddagger}$ ($cm^3\ mol^{-1}$)	$\Delta\beta^{\ddagger}$ ($cm^3 mol^{-1} kbar^{-1}$)
Sampling	1 M $HClO_4$	45.0	12.6 ± 0.8	10 ± 3
Optical	1 M $HClO_4$	50.5	13.7 ± 0.7	10 ± 2
Sampling	1 M $NaClO_4$	45.0	13.7 ± 0.5	11 ± 3
Sampling	0.5 M $HClO_4$	48.0	14.2 ± 0.5	8 ± 2
Sampling	0.05 M $HClO_4$	34.5	14.3 ± 0.2	0.9 ± 0.2
Optical	0.05 M $HClO_4$	46.0	14.2 ± 0.2	1.0 ± 0.2

2.4 *Discussion*

2.4.1 *Effect of Pressure on the Rate of Isomerisation*

As a first approximation, experimentally determined volumes of activation, $\Delta V^{\ddagger}_{exp}$, are considered to arise from two contributions. The first, $\Delta V^{\ddagger}_{int}$, represents the change in intrinsic volume of the reacting molecules when they form the transition state and the second, $\Delta V^{\ddagger}_{el}$, corresponds to the change in solvation during this process. In the present system this second effect (electrostriction) can be ignored since there is no change in formal charge in forming the transition state nor is it likely that the effective ionic radius of the complex changes. Hence, the values of $\Delta V^{\ddagger}$ observed can be largely ascribed to the seat of the reaction.

Expected values of $\Delta V^{\ddagger}$ may be estimated by assuming certain mechanistic models. Suppose the isomerisation reaction proceeds via a limiting dissociative process, D, involving the synchronous expulsion of an aquo ligand from the primary coordination sphere and release of electrostricted water to the bulk solvent. If it is assumed that a 5-coordinate species occupies the same intrinsic volume as a 6-coordinate species, for a 3+ complex ion this would be expected to lead to a molal volume change approaching the molal volume of a water molecule in solvent water namely 18.0 cm^3mol^{-1}. Additionally, for one water molecule released to the bulk, $\Delta\beta^{\ddagger}$ should equal 0.72 $cm^3mol^{-1}kbar^{-1}$. Likewise, $\Delta V^{\ddagger}_{o}$ and $\Delta\beta^{\ddagger}$ for a a limiting associative mechanism, A, should approach the values

$-18\ cm^3\ mol^{-1}$ and $-0.72\ cm^3\ mol^{-1}\ kbar^{-1}$.

The dissociative interchange mechanism, I_d, entails only the release of an aquo ligand to the first hydration (second coordination) sphere. Correspondingly, the associative interchange process, I_a, involves the entry of a secondary water to the primary coordination sphere. The I_d and I_a mechanisms should involve limiting $\Delta V_o^{\ddagger}$ values of $+ 15\ cm^3\ mol^{-1}$ and $-15\ cm^3\ mol^{-1}$ respectively and $\Delta\beta^{\ddagger}$ should be close to zero in both cases (see chapter 1).

Clearly, the large positive value $\Delta V^{\ddagger} = + 13.7 \pm 0.6\ cm^3\ mol^{-1}$ found over a substantial change in electrolyte concentration and a moderate range in temperature, directly establishes the dissociative nature of the isomerisation process. An immediate finding of these studies, therefore, is that an edge-displacement associative mechanism, suggested by Kruse and Taube[4] as one possibility to explain the isomerisation process, may be eliminated. This hypothesis would require the rate-determining entry of a water molecule along an octahedral edge of the diaquo complex to form an intermediate of increased coordination. On this basis a large and negative value for $\Delta V^{\ddagger}$ would be expected.

An increase in volume in forming the transition state might be explained in terms of decreased electrostriction as a result of one-ended opening of an ethylenediamine ring in Co $en_2(OH_2)_2^{3+}$. However, at 35°C and pH1, the rate of exchange[8] of amine protons in the related species *trans*-Co $en_2(SO_3)H_2O^{+}$ with D_2O (k_{ex} = $2.0 \times 10^{-10}\ sec^{-1}$) is some 10^5 times slower than the rate of

isomerisation at the same reaction conditions. Likewise, at 25°C and pH1, the analogous exchange process[15] with Co en_3^{3+} (k_{ex} = 7.3 x 10^{-8} sec^{-1}) is about 100 times slower than *trans* to *cis* interconversion of Co $en_2(OH_2)_2^{3+}$ and this mechanism, therefore, seems unlikely. The more likely explanation for the observed volume increase is from cobalt-aquo bond rupture. In terms of the reaction profile of Kruse and Taube it is assumed that this volume increase arises only from the formation of the first intermediate (square pyramidal structure). The subsequent hypothesis is considered equally applicable.

Some correlation of $\Delta V^{\ddagger}$ with $\Delta S^{\ddagger}$ might be expected since the release of an aquo ligand from *trans* Co $en_2(H_2O)_2^{3+}$ can be regarded as an increase in the degree of freedom of the solvent. For this system, $\Delta S^{\ddagger}$(μ = 0.05 M) = + 103 ± 5 J K^{-1} mol^{-1} and $\Delta S^{\ddagger}$(μ = 1.0 M) = +64 ± 4.5 J K^{-1} mol^{-1}, compatible with a positive $\Delta V_o^{\ddagger}$.

Another interesting observation in the present studies is that experimental ln k_p vs P plots are distinctively curved. This curvature becomes more pronounced at higher ionic strengths. At 0.05 M ionic strength, the mean value of $\Delta\beta^{\ddagger}$ (1.0 ± 0.2 cm^3 $mol^{-1}kbar^{-1}$) suggests that one water molecule is released to the bulk solvent and a D mechanism is strongly suggested. At 0.5 M and 1.0 M ionic strengths, $\Delta\beta^{\ddagger}$ = 9 ± 3 cm^3 mol^{-1} $kbar^{-1}$. Since the release of one mole of water from an electrostricted zone to the bulk solvent involves a change in β of 0.72 cm^3 mol^{-1} $kbar^{-1}$, this value of $\Delta\beta^{\ddagger}$ implies that at least eight solvent molecules are released into the bulk. It has

been argued (Chapter 1) that the change in molar volume when a water molecule moves from the first hydration sphere to the bulk is approximately (18.0 - 15.6) = 2.4 $cm^3\ mol^{-1}$. The measured $\Delta V_o^{\ddagger}$ values, 14.2 $cm^3\ mol^{-1}$ at μ = 0.5 M and 13.7 $cm^3\ mol^{-1}$ at μ = 1.0 M, suggests that (for example 14.2/2.4) about six water molecules are released. When all the approximations are recognized the agreement is quite reasonable. This analysis confirms the recent expectations of El'yanov and Gonikberg[9] that there should be a correlation between $\Delta V_o^{\ddagger}$ and $\Delta\beta^{\ddagger}$. It appears from the analysis above that the work done in forming the transition state is primarily involved in detaching water molecules from the outer electrostricted zone.

The changed mechanistic details at higher ionic strengths, when the rate of isomerization is reduced, is possibly due to the formation of Co $en_2(OH_2)_2^{3+}$. ClO_4^- ion pairs. The water structure in these ion pairs could be so heavily ordered that in order to create a defect in the structure to allow release of an aquo ligand, the whole hydrated ion pair aggregate must be broken before an aquo ligand can emerge from the primary coordination sphere and isomerization proceed. There are corresponding changes in $\Delta H^{\ddagger}$ and $\Delta S^{\ddagger}$ when the ionic strength is increased. Whereas at 0.05 M ionic strength $\Delta H^{\ddagger}$ = 131.4 ± 1.2 kJ mol^{-1} and $\Delta S^{\ddagger}$ = 103 ± 5 J $K^{-1}\ mol^{-1}$ at ionic strength 1.0 M $\Delta H^{\ddagger}$ = 121.7 ± 1.0 kJ mol^{-1} and $\Delta S^{\ddagger}$ = 64 ± 4 J $K^{-1}\ mol^{-1}$. This lowering in $\Delta H^{\ddagger}$ at higher ionic strength may be attributed to a small negative contribution from prior ion-pair

formation. The activation parameters for isomerisation at low ionic strength ($\Delta H^{\ddagger}$ = 131.4 ± 1.2 kJ mol^{-1}; $\Delta S^{\ddagger}$ = 103 ± 5 J K^{-1} mol^{-1}) are in reasonable agreement with $\Delta H^{\ddagger}$ = 128.0 ± 1.2 kJ mol^{-1} and $\Delta S^{\ddagger}$ = 88 ± 4 J K^{-1} mol^{-1} found previously[4] for the corresponding exchange process. For this process, then, a D mechanism again seems likely.

Finally, it is of interest to compare the effect of pressure on the isomerisation in the present system with the *trans* to *cis* conversion of diaquo-dioxalato-chromium III in aqueous solvent.[10] The measured value $\Delta V^{\ddagger}$ = -16 ± 1 cm^3 mol^{-1} is interpreted in terms of a solvent-assisted ring opening mechanism (I_a). The associative nature for the Cr III system is in marked contrast with the dissociative character found in the Co III system. This contrast in behaviour appears to be a characteristic feature of the two metal ions. For example, Hunt and Taube[11] from their measurement $\Delta V^{\ddagger}$ = + 1.2 ± 0.2 cm^3 mol^{-1} for the water exchange of $Co(NH_3)_5OH_2^{3+}$ favour a dissociative interchange mechanism. However, for the analogous process with $Cr(NH_3)_5OH_2^{3+}$, $\Delta V^{\ddagger}$ = -5.8 ± 0.2 cm^3 mol^{-1} and an associative interchange mechanism has been argued.[12] Similarly, the measured volumes of activation[13] for the aquation of pentaamminecobalt III ions strongly suggest an I_d process. In contrast, an I_a mechanism is favoured for the analogous reactions of pentaamminechromium III.[14]

2.4.2 Conclusion

The rate of *trans* to *cis* isomerisation of diaquobis-(ethylenediamine)cobalt III in aqueous solution has been investigated over a pressure range from 1 to 1380 bar at 34.5 to 50.5°C and ionic strengths 0.05 M, 0.5 M and 1.0 M, and a temperature range from 34.5°C to 55°C at 1 bar and ionic strengths 0.05 M and 1.0 M. The volume and compressibility coefficient of activation were determined to be + 13.3 ± 0.7 cm^3 mol^{-1} and 1.0 ± 0.2 cm^3 mol^{-1} $kbar^{-1}$ at 0.05 M ionic strength, + 14.2 ± 0.5 cm^3 mol^{-1} and 8 ± 2 cm^3 mol^{-1} $kbar^{-1}$ at 0.5 M ionic strength, and +14.2 ± 0.2 cm^3 mol^{-1} and 10 ± 3 cm^3 mol^{-1} $kbar^{-1}$ at 1.0 M ionic strength. The enthalpies and entropies of activation were found to exhibit respective values of 131.4 ± 1.2 kJ mol^{-1} and 103 ± 5 J $K^{-1}mol^{-1}$ at 0.05 M ionic strength and 121.7 ± 1.0 kJ mol^{-1} and 64 ± 4 J K^{-1} mol^{-1} at 1.0 M ionic strength. The activation parameters are discussed in terms of a dissociative mechanism. The changed mechanistic detail at higher ionic strengths is attributed to ion-pair formation.

References to Chapter 2

1. J. Bjerrum and S.E. Rasmussen, *Acta. Chem. Scand.*, 1952, 6, 1265.
2. S.F. Lincoln and D.R. Stranks, *Aust. J. Chem.*, 1968, 21, 1745.
3. R.C. Henney, *Inorg. Chem.*, 1969, 8, 389.
4. W. Kruse and H. Taube, *J. Amer. Chem. Soc.*, 1961, 83, 1280.
5. J.Y. Tong and P.E. Yankwich, *J. Amer. Chem. Soc.*, 1958, 80, 2664.
6. F. Basolo, *J. Amer. Chem. Soc.*, 1950, 72, 4393.
7. F. Basolo and Pearson, *"Mechanisms of Inorganic Reactions"*, *Wiley and Sons Inc.*, 2nd edition, pg. 279.
8. A. Sandercock, *private communication.*
9. B.S. El'yanov and U.G. Gonikberg, *Russ. J. Physical Chem.*, 1972, 46, 856.
10. E.G. Conze, H. Stieger and L.H. Kelm, *Chem. Ber.*, 1972, 105, 2334.
11. H.R. Hunt and H. Taube, *J. Amer Chem. Soc.*, 1958, 80, 2642.
12. T.W. Swaddle and D.R. Stranks, *J. Amer. Chem. Soc.*, 1972, 94, 8357.
13. W.E. Jones, L.R. Carey and T.W. Swaddle, *Canad. J. Chem.*, 1972, 50, 2739.
14. G. Guastalla and T.W. Swaddle, *Canad. J. Chem.*, 1973, 51, 821.
15. F. Basolo, J.W. Palmer and R.G. Pearson, *J. Amer. Chem. Soc.*, 1960, 82, 1073.

Chapter 3. The Effect of temperature and pressure on the rate of isomerisation of the aquoselenito bis(ethylenediamine)cobalt III ion.

3.1 Introduction

3.1.1 Reactions of Coordinated Selenites

Little is known about the chemistry of metal complexes containing selenite as the ligand and only the attempted preparation of [Co $en_2(OH_2)SeO_3$]X where X = NO_3^-, Cl^- or Br^- has been reported.[1] In these laboratories a number of selenitoamminecobalt III complexes have been prepared recently and a start made on the reactions of these complexes.

Selenite may function as either a monodentate, as with $Co(NH_3)_5OSeO_2^+$ and Co $en_2(OH_2)OSeO_2^+$, or a bidentate, as with Co $en_2O_2SeO^+$ and Co $tn_2O_2SeO^+$. Infra-red studies[2,3] on all these crystalline selenito products have shown the selenite to be oxygen bonded to the metal ion. The bidentate selenito ligands are relatively inert to both acid and base catalyzed hydrolysis and favourable free energies of formation apply from pH1 to pH10. By contrast, monodentate selenito complexes undergo rapid hydrolysis in both acidic and basic media and significant equilibrium concentrations of monodentate complexes are only established from pH 6.5 to pH 8.5.

Fowless[2] has studied the rates of formation for the series of reactions

$$Co\ L_2X(H_2O)^{3+} + OSeO_2^{2-} \rightarrow CoL_2X\ OSeO_2^+ + H_2O \qquad 3.1$$

(where L_2 = en_2, tn_2 or $(NH_3)_4$ and X = NH_3 or H_2O) in relation to the degree of protonation of both the metal-aquo nucleophile and

the selenite substrate, and the stereochemistry of the aquo-complex. The half lives of these reactions are quite short, being of the order of milliseconds. The formation of these selenito products is considered to involve the rapid initial formation of an ion-pair followed by rate-determining aquo substitution at the selenium IV centre. Most substitutions of the selenite species were found to exhibit activation enthalpies, $\Delta H^{\ddagger}$, in the region of 40-50 kJ mol^{-1}, indicative of O-Se bond rupture.

The activation parameters for the base hydrolysis[3] of $Co(NH_3)_5OSeO_2^+$, $\Delta H^{\ddagger}$ = 48.1 ± 1.4 kJ mol^{-1}, $\Delta S^{\ddagger}$ = - 121 ± 4 J K^{-1} mol^{-1}, and $\Delta V^{\ddagger}$ = -20.8 ± 1.0 cm^3 mol^{-1}, are in marked contrast to those for the base hydrolysis of $Co(NH_3)_5OSO_3^+$, $\Delta H^{\ddagger}$ = 110 ± 3 kJ mol^{-1}, $\Delta S^{\ddagger}$ = +99.8 ± 3.4 J K^{-1} mol^{-1} and $\Delta V^{\ddagger}$ = +21.4 ± 1.1 cm^3 mol^{-1}, which is generally believed to proceed by a dissociative, conjugate base mechanism. Since the charge of the reactant species in the two systems do not differ, positive $\Delta S^{\ddagger}$ and $\Delta V^{\ddagger}$ values of comparable magnitudes might be expected if the same mechanism were operative for the base hydrolysis of the selenito complex. The experimental negative values for both $\Delta S^{\ddagger}$ and $\Delta V^{\ddagger}$ were taken as strong evidence for an associative mechanism involving attack by hydroxide ion at the selenium centre.

3.1.2 Behaviour of the Co $en_2/OSeO_2$ *System*

Both *cis* and *trans* isomers of Co $en_2(OH_2)OSeO_2H^{2+}$ have been identified. The rates of formation[2] of these species at varying acidities are summarized in Table 3.1.

Table 3.1

Formation rate constants of Co $en_2(H_2O)OSeO_2^+$

$[Co\ en_2(H_2O)_2]_0^{3+}$ = 0.01 M ; $[SeO_3]_0^{2-}$ = 0.1 M ; Temperature = 25°C

$\mu(NaClO_4)$ = 1 M.

pH	Predominant Species		$k_{subs}(sec^{-1})$	
			cis	*trans*
1	$R(OH_2)_2^{3+}$	H_2SeO_3	0.63	6.9
	100%	96%		
3	$R(OH_2)_2^{3+}$	$HSeO_3^-$	14	46
	100%	80%		
7	$ROH.OH_2^{2+}$	$HSeO_3^-$	1.7	2.2
	86%	91%		
10	$R(OH)_2^+$	SeO_3^{2-}	0.06	0.23
	98%	99%		
	(R≡Co(en)$_2$)			

The data imply that substitution of $HSeO_3^-$ by the diaquo species proceeds at the greatest rate. Furthermore, there is a significant *trans* effect the magnitude of which depends on the degree of protonation of reactants.

At 25°C, pH3 and in a 1 M $NaClO_4$ medium, the formation constants for the *trans* and *cis* selenito species have been measured as 45 M^{-1} and 50 M^{-1} respectively. When *trans*-Co $en_2(OH_2)_2^{3+}$ reacts with selenite anion, the reaction proceeds in two steps;

trans-Co $en_2(H_2O)_2^{3+}$ + $HSeO_3^-$ $\xrightarrow{k_1}$ *trans*-Co $en_2(H_2O)OSeO_2H^{2+}$

$$\xrightarrow{k_{isom}} \quad cis\text{-Co en}_2(H_2O)OSeO_2H^{2+} \qquad (3.2)$$

where k_{isom} is 10^3 times slower than k_1. The present investigation aimed at elucidating, from both a temperature and pressure dependence study, the reaction mechanism for this isomerisation process.

3.2 Experimental

3.2.1 Materials

trans-[Co $en_2(H_2O)OSeO_2H](ClO_4)_2$ was prepared by the method of Fowless[2]. Selenous acid (2.0g) was dissolved in a minimum volume of cold water and to this was added solid *trans*-[Co $en_2(OH)OH_2$] $(ClO_4)_2$(5.0 g). A dark green-grey solution was rapidly formed and within seconds a grey product precipitated. The precipitate was collected, washed with ethanol and air-dried. The crude product was recrystallised from a dilute selenous acid solution by ice cooling, collected and washed with ethanol and ether. Overall yield was 40%.

cis-[Co $en_2(OH_2)OSeO_2H](ClO_4)_2$

Equimolar quantities of selenous acid (2.0 g) and *cis*-[Co $en_2(OH)H_2O](ClO_4)_2$ (5.0 g) were mixed as for the *trans* preparation. On cooling a red-purple oil formed which precipitated as a pink-purple solid on the addition of successive amounts of ethanol. The product was collected and washed with ethanol, ether and air dried. There was a tendency for the solid to revert to an oil if left on the pump for too long. The crude product was recrystallised from a minimum volume of hot water and obtained in an overall yield of 40%.

Trizma buffer

Trizma base solutions ('Trizma' base is a proprietory term for the nitrogen base tris(hydroxymethyl) aminomethane) were prepared

from Reagent grade Trizma base supplied by the Sigma Chemical Company. Trizma buffer was prepared by the addition of appropriate volumes[4] of Trizma base solutions of the required concentration and nitric acid of the same concentration.

HNO_3

All nitric acid solutions for the Trizma buffer were prepared from concentrated Analar nitric acid by dilution with doubly distilled water and standardised against A.R. mercuric oxide.

3.2.2 Apparatus

pH Meter

All pH measurements were made using an Automatic Titrator, type TTT1 in combination with a Scale Expander, Model PHA 630T. The electrode used was a combination glass and calomel electrode. Buffer solutions for standardising the instrument before use were prepared from buffer tablets for the desired pH range, supplied by Marconi Instruments Ltd., England.

Temperature Control

Below 25°C, temperature control to ± 0.01°C was achieved by a Rheinische Thermostatic Refridgerator unit Type TK1 operating continuously in opposition to a solid-state proportional heater, regulated by a thermistor probe. At higher temperatures, satisfactory temperature control was maintained by the heating

unit alone.

Optical Vessel

The description and operation of the optical pressure vessel is given in Appendix I.

All other equipment used in these studies have been previously described (Section 2.2.2).

3.2.3 Procedure for Kinetic Runs

Temperature dependence study

To initiate a run, a weighed amount of the selenito complex was dissolved in deionised distilled water and transferred to a 1 cm silica cell placed inside the cell compartment of a Unicam, SP800 recording spectrophotometer. The solution was allowed to stand for thirty minutes to attain thermal equilibrium.

Runs were followed spectrophotometrically at 510 nm by recording on a Riken Denshi Speedex Model SP-G3 slave recorder the change with time in optical absorbance of the solution.

Pressure dependence study

Reaction solutions were prepared by dissolution of the selenite salt in deionised distilled water (pH 3.3) or Trizma buffer solution (pH 7.0). Solution samples were transferred to the sample cuvette of the optical vessel, the Teflon cap placed on the cell and the pressure raised to the desired value.

After an equilibrating period of thirty minutes, reaction

rates were determined at 510 nm (pH 3.3) and 530 nm (pH 7.0) as above.

3.2.4 Procedure for Equilibrium Measurements

Atmospheric pressure

A solution of the *trans* selenito salt (10^{-2} M), adjusted to an ionic strength of 1 M with sodium perchlorate, was allowed to stand overnight at 25°C to attain equilibrium and the optical absorbance measured at 510 nm using the Shimadzu QR-50 spectrophotometer.

Determination of K at High Pressures

The pressure cell was filled with the sample solution prepared as above and mounted inside the thermostatted cell compartment of a Unicam SP 800 spectrophotometer equipped with an SP 850 Scale Expansion Accessory. The solution was brought to the desired temperature and the apparent absorbance noted on a Riken Denshi Speedex slave recorder. The pressure was slowly increased (over about 2 minutes for each 340 bar pressure interval) and any change in optical absorbance noted on the recorder. The scale was expanded by a factor of 10. Under these conditions, for optical absorbance of 0.87 to 0.89 the uncertainty was typically ± 0.002.

As the pressure was increased some heating of the solution occurred. It was found that about five minutes was needed before a steady reading could be obtained. The measurements were repeated while decreasing the pressure over the same

pressure interval and were in good agreement to those recorded while increasing the pressure.

3.3 Results

3.3.1 Visible Absorption Spectra

The visible spectra of *cis* and *trans*-[Co $en_2(OH_2)OSeO_2H]^{2+}$ (pH 3.3) and [Co $en_2(OH_2)OSeO_2]^+$ (pH 7.0) are shown in Fig. 3.1 Absorption maxima occur at 588 nm (ε_{max} = 39 M^{-1} cm^{-1}) and 438 nm (ε_{max} = 31 M^{-1} cm^{-1}) for *trans*-[Co $en_2(OH_2)OSeO_2H]^{2+}$, 510 nm (ε_{max} = 92 M^{-1} cm^{-1}) and 358 nm (ε_{max} = 84 M^{-1} cm^{-1}) for *cis*-[Co $en_2(OH_2)OSeO_2H]^{2+}$, 590 nm (ε_{max} = 50 $M^{-1}cm^{-1}$) for *trans*-[Co $en_2(OH_2)OSeO_2]^+$, and 530 nm (ε_{max} = 110 M^{-1} cm^{-1}) for *cis*-[Co $en_2(OH_2)OSeO_2]^+$. The presence of other bands are obscured by strong charge transfer bands beyond 350 nm.

The spectra of solutions of *trans*-[Co $en_2(OH_2)OSeO_2H]^{2+}$ and [Co $en_2(OH_2)OSeO_2]^+$ changed with time, with isosbestic points at 584 nm, 453 nm, 425 nm and 378 nm at pH 3.3 and at 589 nm, 450 nm and 403 nm at pH 7.0. These corresponded exactly to the common points in the spectra of *cis* and *trans*-[Co $en_2(OH_2)OSeO_2H]^{2+}$ and [Co $en_2(OH_2)OSeO_2]^+$ and the process is identified as a *trans* $\rightleftarrows$ *cis* isomerisation.

3.3.2 Evaluation of Kinetic Data

For both the temperature and pressure dependence study the Guggenheim method[5] of analysis was employed (see Section 2.3.1). Plots of ln (OD_t - $OD_{t+\Delta}$) against time were linear so that the reaction exhibits first order or pseudo first order kinetic behaviour.

FIG. 3.1 Visible absorption spectra of the species:

A: *trans*-Co $en_2(OH_2)OSeO_2H^{2+}$

B: *cis* - Co $en_2(OH_2)OSeO_2H^{2+}$

C: *trans*-Co $en_2(OH_2)OSeO_2^{+}$

D: *cis* - Co $en_2(OH_2)OSeO_2^{+}$

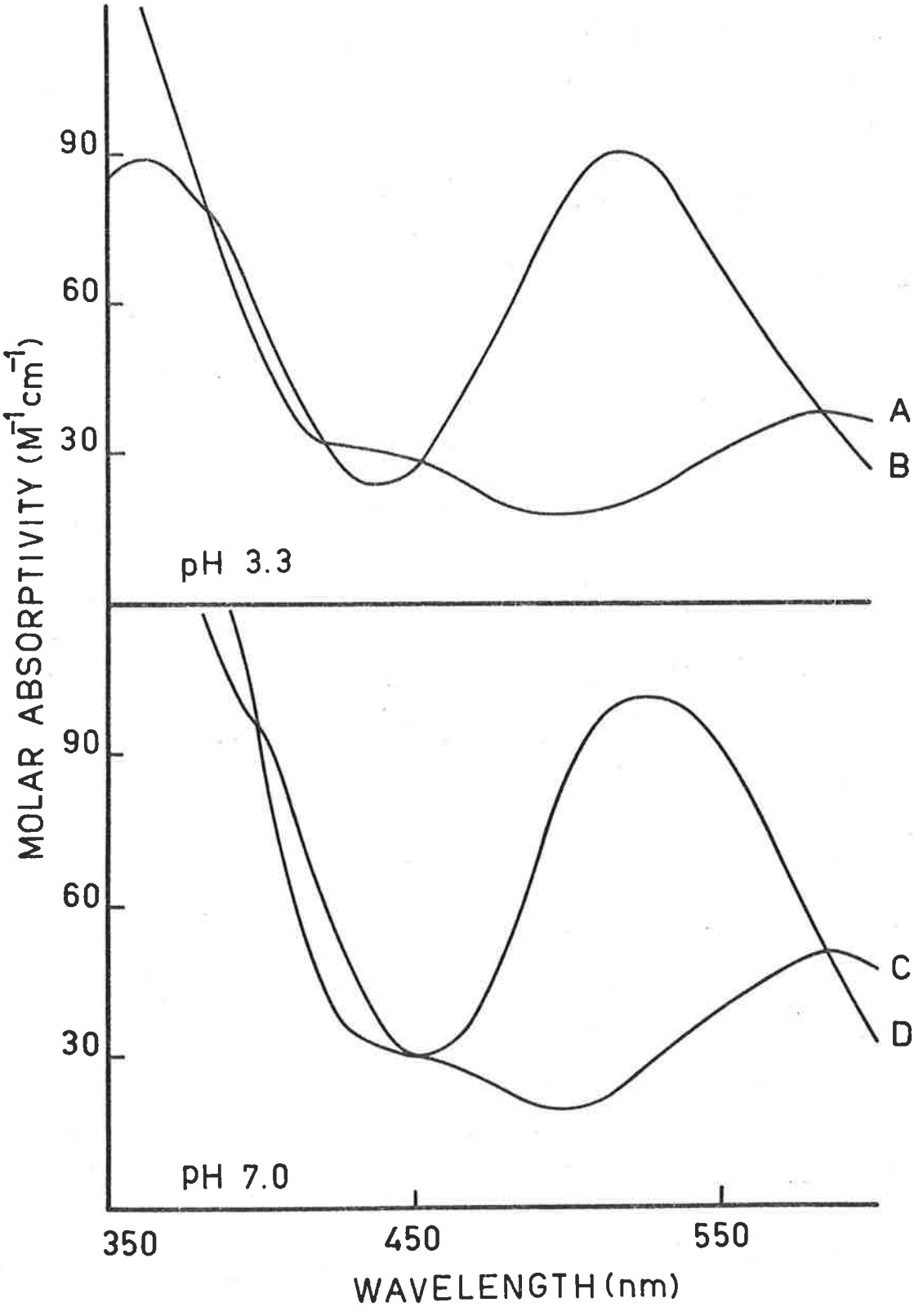
MOLAR ABSORPTIVITY ($M^{-1}cm^{-1}$)
90
60
30
A
B
pH 3.3
90
60
30
C
D
pH 7.0
350
450
550
WAVELENGTH (nm)

3.3.3 The Effect of Temperature on the Isomerisation Rate

It has previously been mentioned (Section 2.3.2) that the measured isomerisation rate constant, k_{isom}, for a *trans* to *cis* isomerisation process contains contributions from both the forward (k_{t-c}) and back (k_{c-t}) reaction. The individual values for k_{t-c} and k_{c-t} may be evaluated from measured values of k_{isom} and K_{isom}, the *cis/trans* equilibrium ratio. K_{isom} was evaluated from the values at 510 nm ; ε_{max} = 92 $M^{-1}cm^{-1}$ for the *cis* isomer, ε_{max} = 20 $M^{-1}cm^{-1}$ for the *trans* isomer and an optical absorbance of an equilibrated solution OD_{eq} = 0.87. In addition, OD_{eq} is constant over a temperature range of 21°C to 35°C. It then follows that the reverse rate constant, k_{c-t}, contributes only 7% to the observed isomerisation coefficient, k_{isom}, over this temperature range. Any change in k_{isom} with temperature may, therefore, be ascribed as arising entirely from variations in k_{t-c}.

The temperature dependence on the isomerisation rate coefficient, k_{isom}, was studied between 21°C and 35°C using a reactant concentration of 1.2 x 10^{-3} M for the selenito complex. The results obtained at four different temperatures are listed in Table 3.2. A number of runs at each temperature

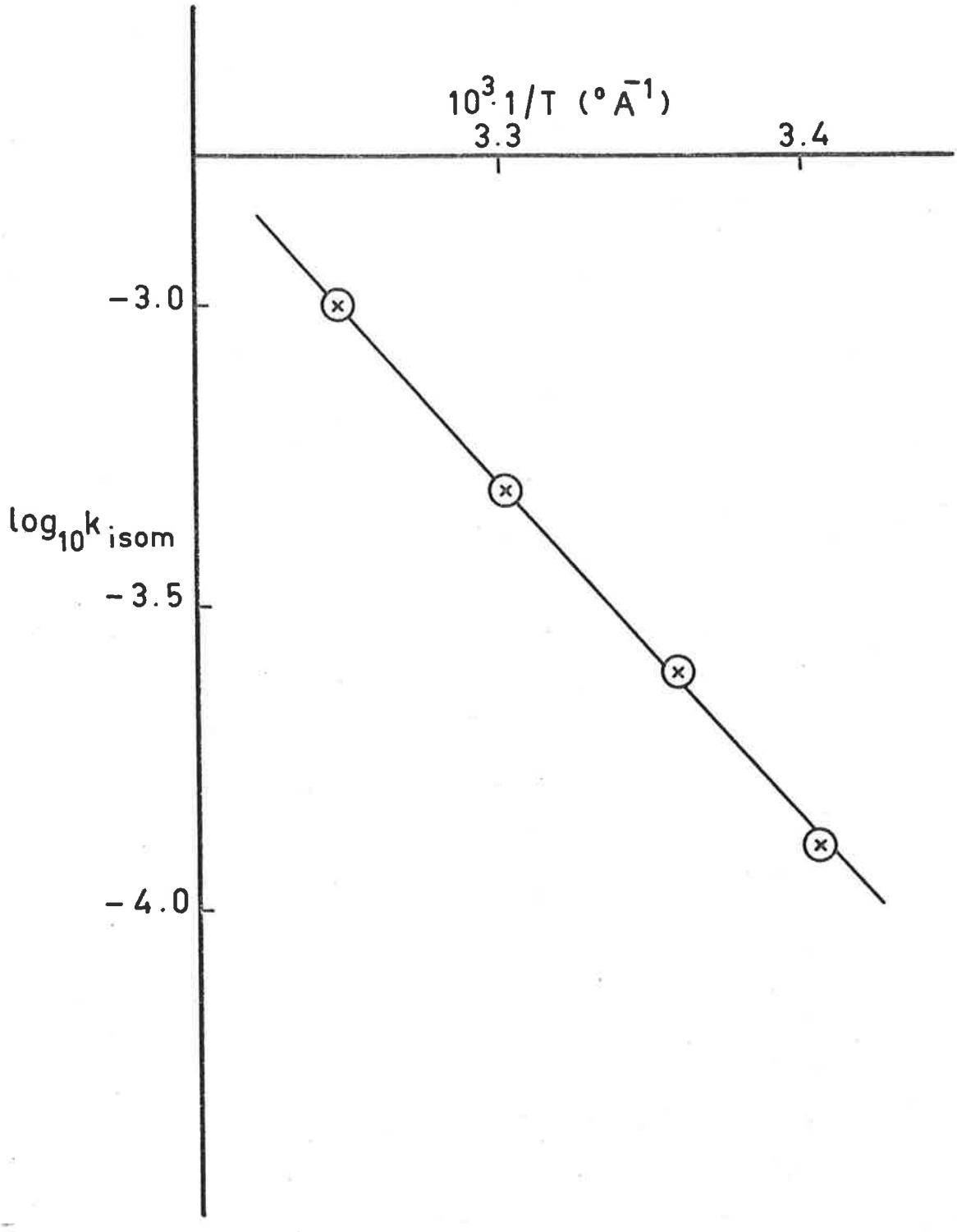

FIG. 3.2 Variation of k_{isom} with temperature.

Table 3.2

Variation of k_{isom} with temperature

$[Co\ en_2(H_2O)OSeO_2H]_0^{2+}$ = 0.012 M ; pH 3.3

Temp (°C)	$10^4.k_{isom}$ (sec^{-1})	nos. of runs
21.0	1.20 ± 0.02	4
25.0	2.42 ± 0.02	5
30.0	4.77 ± 0.05	5
35.0	9.87 ± 0.10	4

revealed that k_{isom} was reproducible to ± 3%.

Figure 3.2 is the Arrhenius plot of the data in Table 3.2 from which the enthalpy and entropy of activation, $\Delta H^{\ddagger}$ and $\Delta S^{\ddagger}$, were calculated by a least squares analysis to be:

$$\Delta H^{\ddagger} = 109.6 \pm 1.3 \text{ kJ mol}^{-1}$$

$$\Delta S^{\ddagger} = 53.1 \pm 4.2 \text{ J K}^{-1}\text{mol}^{-1}$$

3.3.4 The Effect of Pressure on the cis/trans Equilibrium.

The pressure dependence on K_{isom} was studied between 1 and 1360 bar at 25°C and pH 3.3 and pH 7.0. The results are shown in Table 3.3 and the isosbestic curves in Figures 3.3 and 3.4.

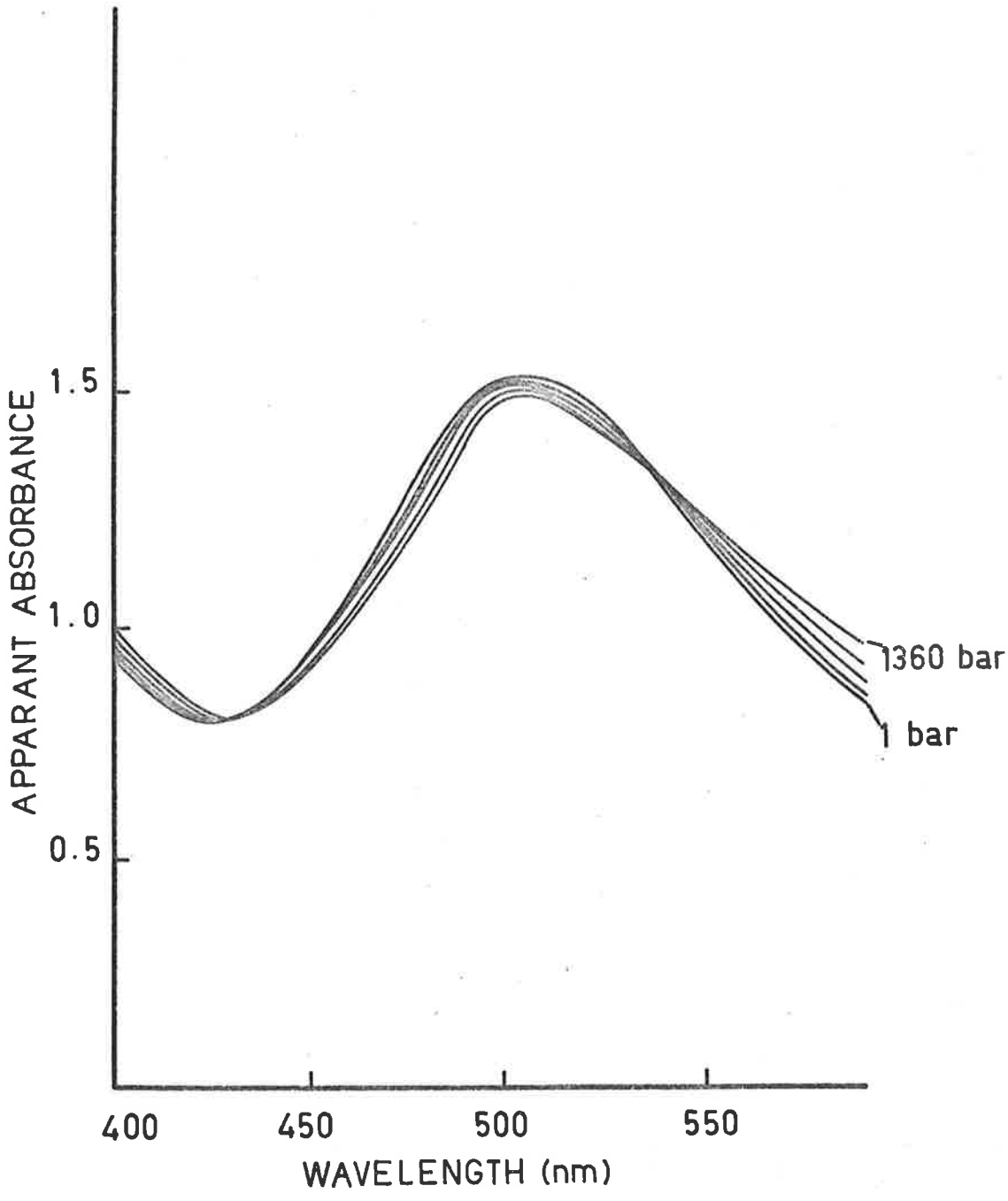

FIG. 3.3 Isosbestic plot at pH 3.3.

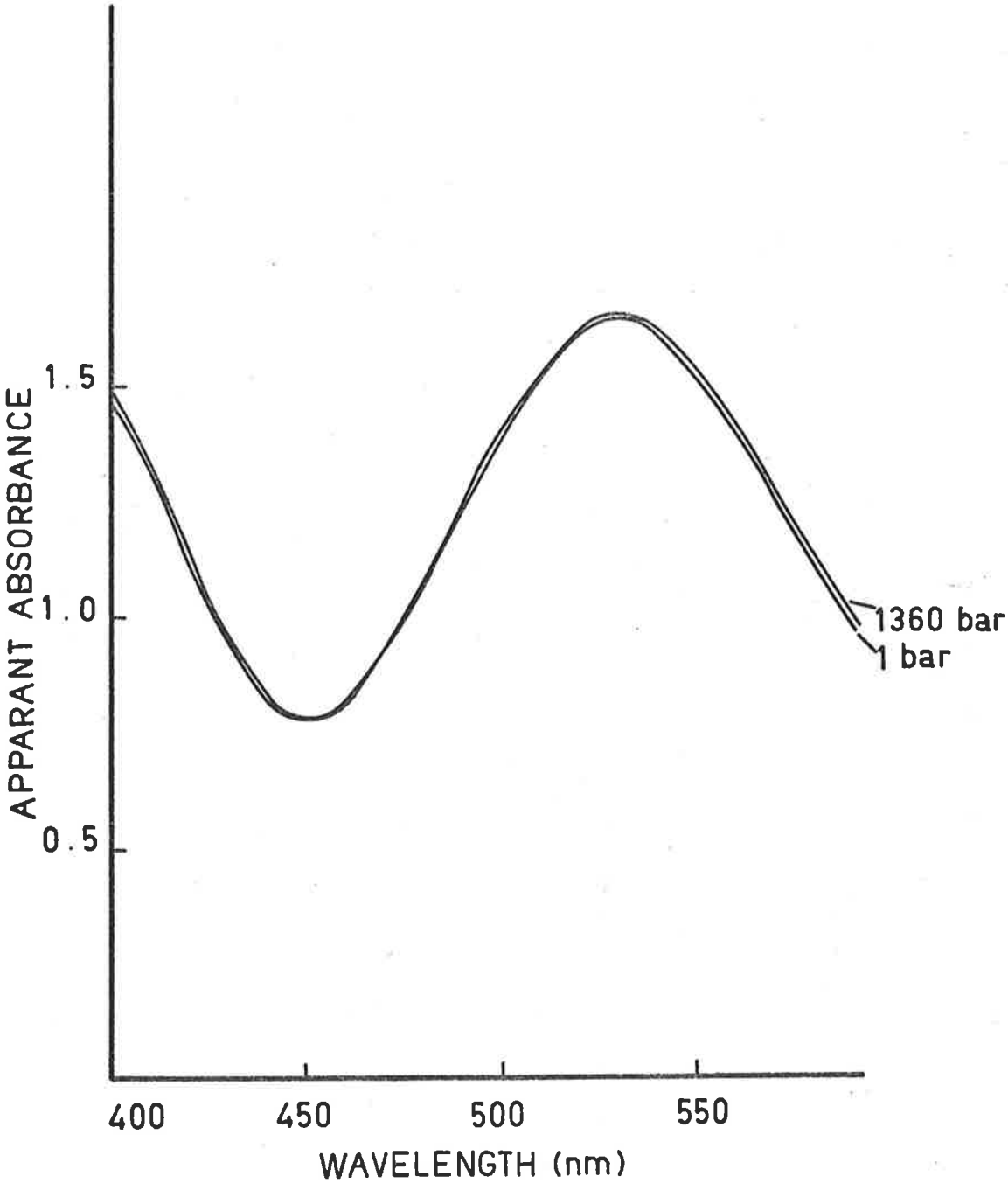

FIG. 3.4 Isosbestic plot at pH 7.0.

Table 3.3

Variation of K_{isom} with Pressure at 25.0°C

trans-[Co $en_2(OH_2)OSeO_2H]^{2+}$ = 0.01 M; μ = 1.0 M ($NaClO_4$); pH 3.3

trans-[Co $en_2(OH_2)OSeO_2]_0^+$ = 0.01 M; μ = 1.0 M ($NaClO_4$); pH 7.0

	pH 3.3		pH 7.0	
Pressure (bar)	Absorb. Measured OD_∞	K_{isom} (M^{-1})	Absorb. Measured OD_∞	K_{isom} (M^{-1})
1	0.872	13.5	0.910	70
340	0.875	15.0	0.910	70
680	0.878	16.2	0.912	90
1020	0.880	17.0	0.912	90
1360	0.884	19.0	0.912	90
	(± 0.002)	(± 1.0)	(± 0.002)	(± 20)

In this the absorbance values in columns 2 and 4 are the mean values of at least four determinations at each pressure.

At 25°C, pH 3.3 and in a 1 M $NaClO_4$ medium, the following overall equilibrium scheme exists:

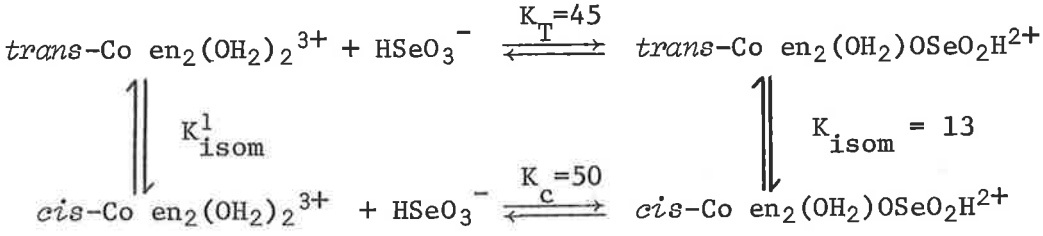

At these reaction conditions, the rate of isomerisation of the diaquo species is some 35 times slower than the *trans* to *cis* interconversion of the selenitoaquo cation and the increase in optical absorbance found at pH 3.3 may then be attributed to the effect of pressure on K_{isom}. There is no variation (within experimental uncertainty) in K_{isom} with pressure at the higher acidity where the selenitoaquo species exists almost exclusively (99%) in the *cis* form.

The pressure variation of the isomerisation equilibrium constant at pH 3.3 is shown in Figure 3.5 where log K_p/K is plotted against pressure. The value of ΔV_{isom} was evaluated from the slope of this plot to be

$$\Delta V_{K_{isom}} = -5.8 \pm 0.4 \text{ cm}^3 \text{ mol}^{-1}$$

3.3.5 Pressure Dependence on the Rate of Isomerisation

In one series of experiments the pressure effect on the isomerisation rate constant, k_{isom}, was determined between 0 and 2 kbar at 25°C and pH 3.3. At this pH, the reactant is *trans*-Co $en_2(OH_2)SeO_2H^{2+}$. In a second set of data the pressure effect was studied over the same pressure range at pH 7.0, 15°C and ionic strength 0.5 M. At this pH, the reactant is *trans*-Co $en_2(OH_2)OSeO_2^{+}$. Trizma base buffer was used to maintain the ionic strength and pH at the desired value. Column 3 of Table 3.4 lists the data determined by a least squares analysis. In both series runs conducted in the pressure assembly at atmospheric pressure gave the same results, within experimental uncertainty,

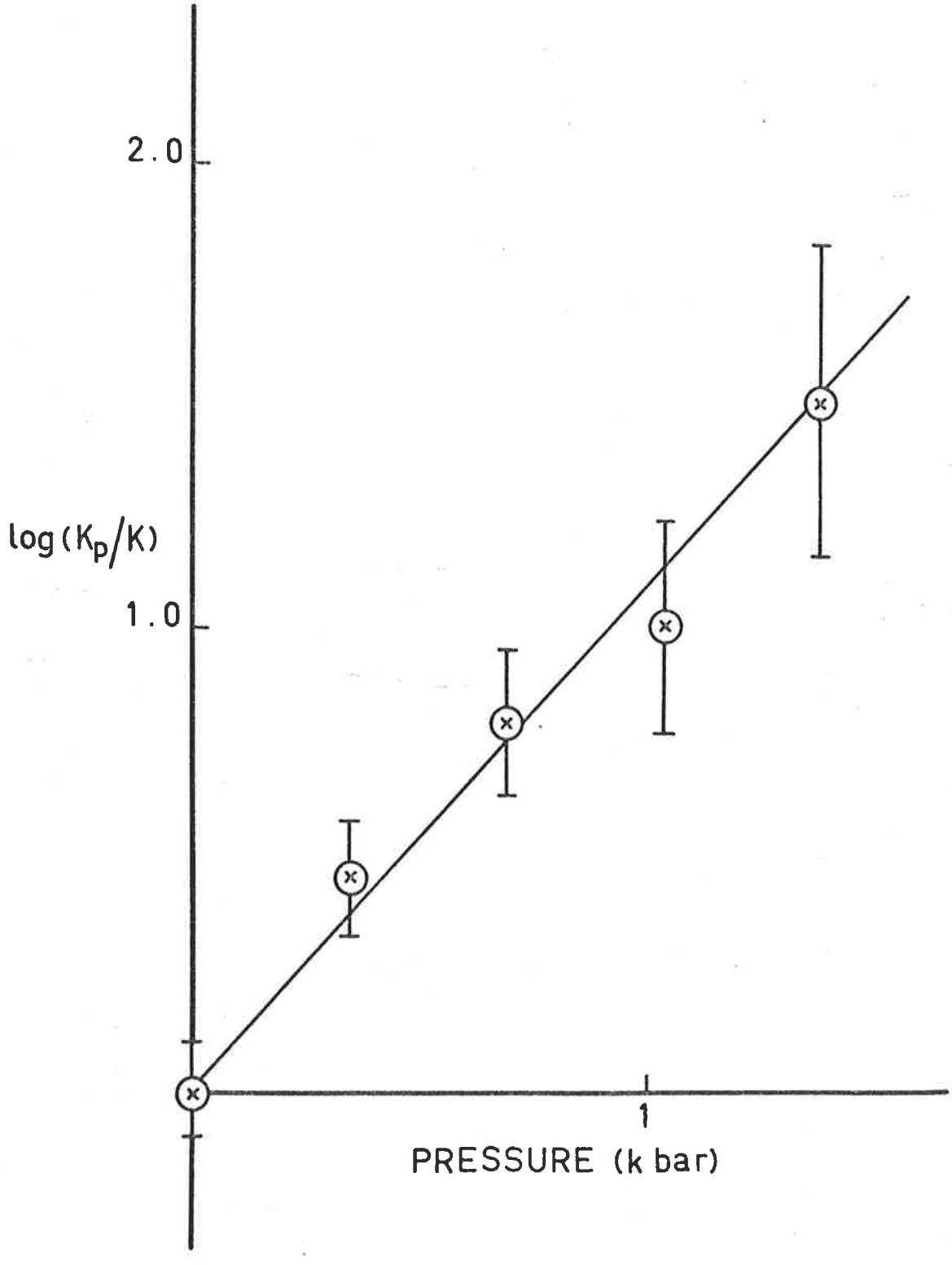

FIG. 3.5 The effect of pressure on K_{isom}.

Table 3.4

Variation of k_{isom} with pressure

trans-$[Co\ en_2(H_2O)OSeO_2H]_0^{2+}$ = 0.012 M, pH 3.3

Temp (°C)	Press (bar)	$10^4.k_{isom}$ (sec^{-1})	nos. of runs
25.0	1[a]	2.34 ± 0.05	3
	1	2.40 ± 0.04	5
	340	2.15 ± 0.04	5
	680	1.93 ± 0.05	5
	1020	1.71 ± 0.03	5
	1360	1.56 ± 0.04	5
trans-$[Co\ en_2(H_2O)OSeO_2]_0^{+}$ = 0.012 M; pH 7.0; μ = 0.5 M (Trizma base)			
15.0	1[a]	2.80 ± 0.04	3
	1	2.83 ± 0.05	4
	340	2.52 ± 0.06	4
	680	2.28 ± 0.04	5
	1020	2.03 ± 0.03	4
	1360	1.85 ± 0.04	5

a - analysed by a sampling technique.

as control experiments performed with the solution in a stoppered flask and analysed spectrophotometrically by a sampling technique. In most cases the standard deviation of each mean value of the rate coefficient is about ± 2%. To achieve this level of accuracy it was necessary to conduct at least four individual runs at each set of reaction conditions.

The measured isomerisation rate coefficient, k_{isom}, can be written in terms of the rate coefficients for the forward, k_{t-c}, and back, k_{c-t}, reactions, i.e.,

$$k_{isom} = k_{t-c} + k_{c-t} \qquad 3.3$$

Also, the equilibrium constant, K, which is given by

$$K = \frac{[cis\text{-selenitoaquo}]}{[trans\text{-selenitoaquo}]} \qquad 3.4$$

can be written in terms of k_{t-c} and k_{c-t}:

$$K_{isom} = k_{t-c}/k_{c-t} \qquad 3.5$$

Hence, values of k_{t-c} and k_{c-t} at each pressure may be obtained by using the data for the variation of K_{isom} with pressure previously determined in Section 3.3.4. The values of k_{t-c} and k_{c-t}, calculated from equations 3.3 and 3.5, are listed in Table 3.5 for the data at pH 3.3.

Table 3.5

Variation of k_{t-c} and k_{c-t} with pressure at pH 3.3

Temp: 25.0 ± 0.1°C.

Press (bar)	$10^4.k_{t-c}$ (sec^{-1})	$10^4.k_{c-t}$ (sec^{-1})
1	2.23 ± 0.04	0.17 ± 0.0_1
340	2.02 ± 0.04	0.13 ± 0.0_1
680	1.82 ± 0.04	0.11 ± 0.0_1
1020	1.71 ± 0.03	0.10 ± 0.0_1
1360	1.56 ± 0.03	0.08 ± 0.0_1

The variation of k_{isom} at pH 7.0 is shown in Figure 3.6 where log k_{isom} has been plotted against pressure. In Figures 3.7 and 3.8 the variations of k_{t-c} and k_{c-t} with pressure at pH 3.3 are shown. A least squares analysis of the data in Tables 3.4 and 3.5 yielded $\Delta V^{\ddagger}_{t-c}$ = + 7.5 ± 0.2 cm^3 mol^{-1} and $\Delta V^{\ddagger}_{c-t}$ = +12.7 ± 1.0 cm^3 mol^{-1} for isomerisation of *trans*-Co $en_2(OH_2)OSeO_2H^{2+}$ at pH 3.3 and $\Delta V^{\ddagger}_{t-c} = \Delta V^{\ddagger}_{c-t}$ = + 7.3 ± 0.2 cm^3 mol^{-1} for isomerisation of *trans*-Co $en_2(OH_2)OSeO_2^{+}$ at pH 7.0.

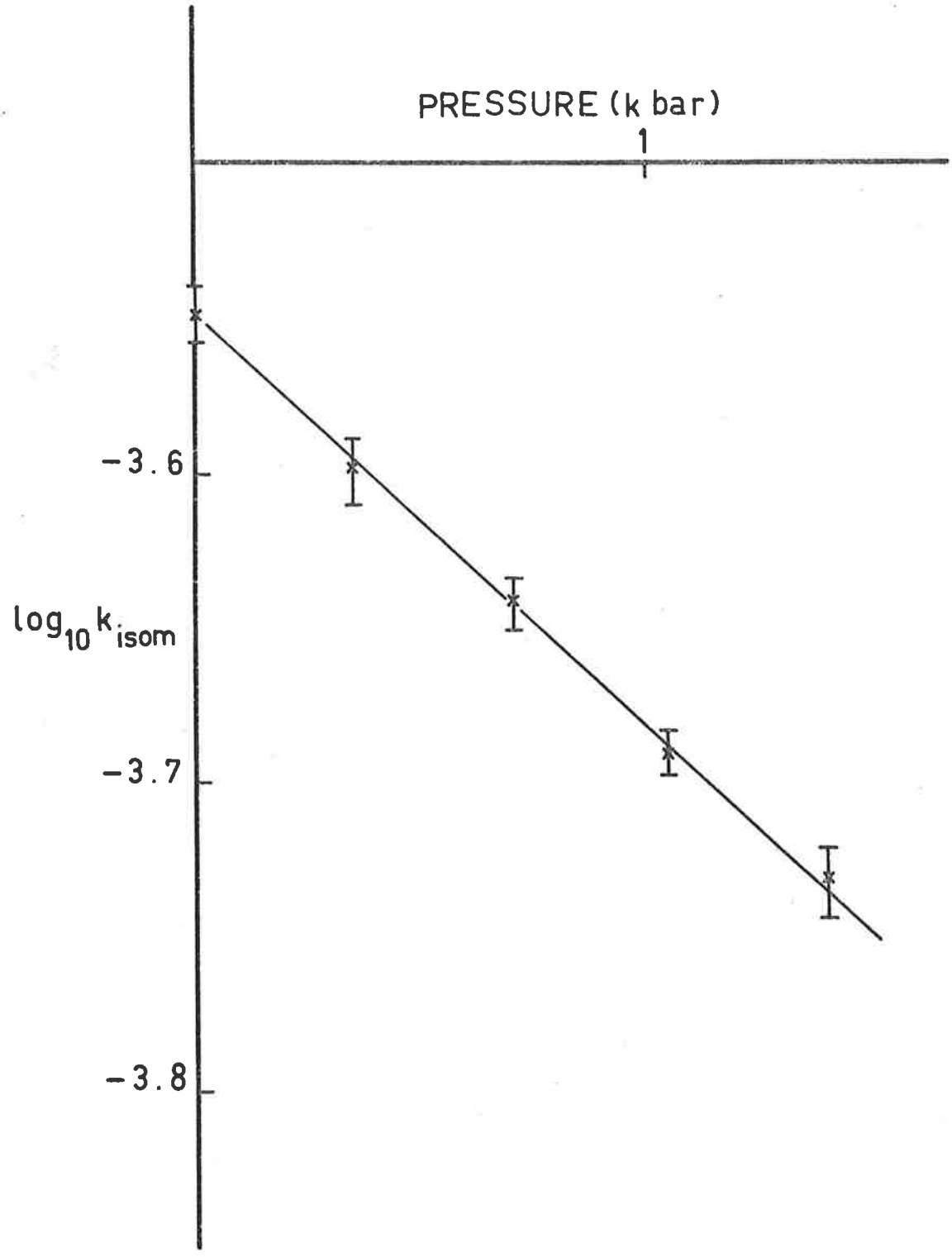

FIG. 3.6 The effect of pressure on k_{isom} at pH 7.0.

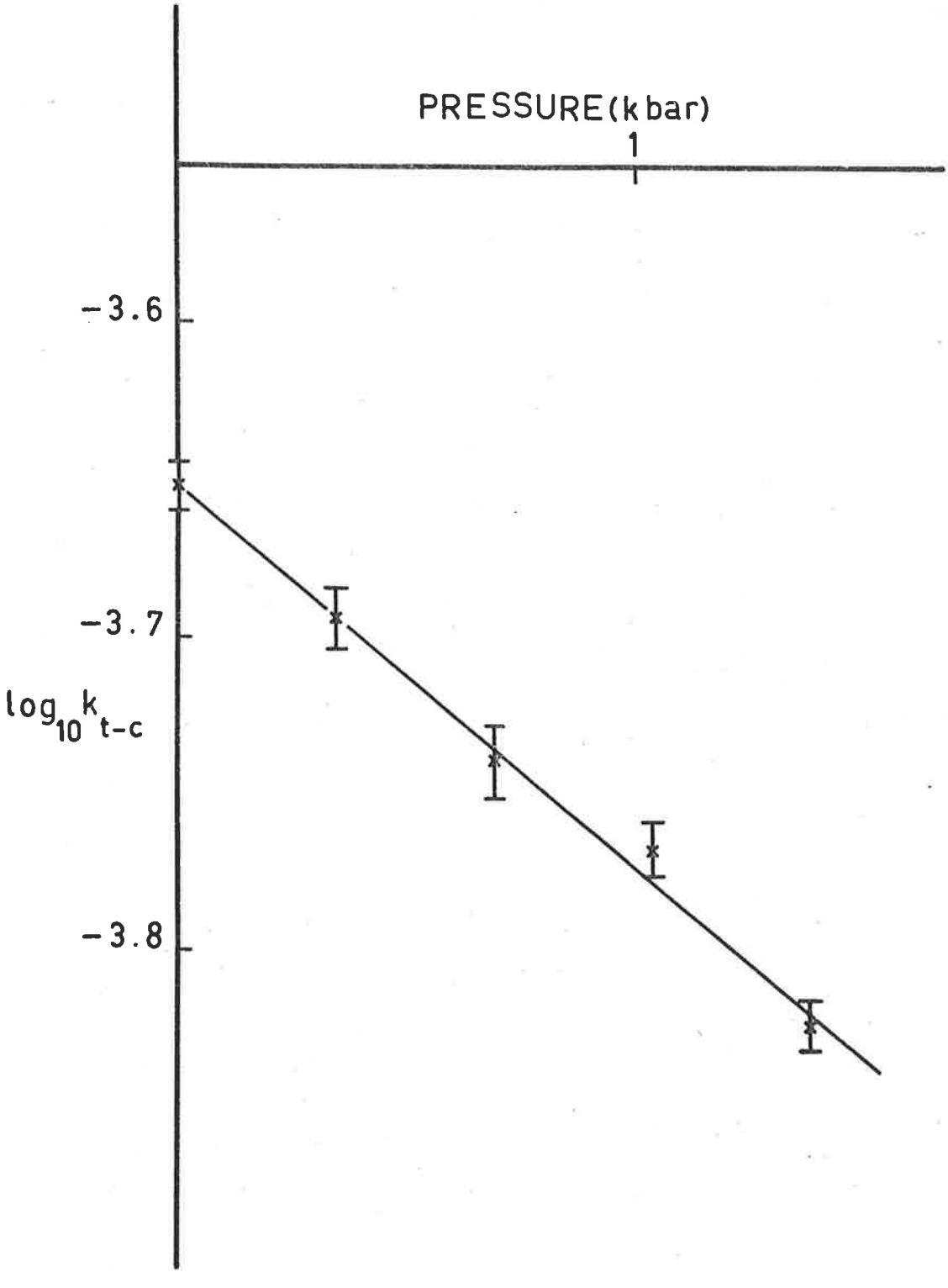

FIG. 3.7 Variation of k_{t-c} with pressure at pH 3.3.

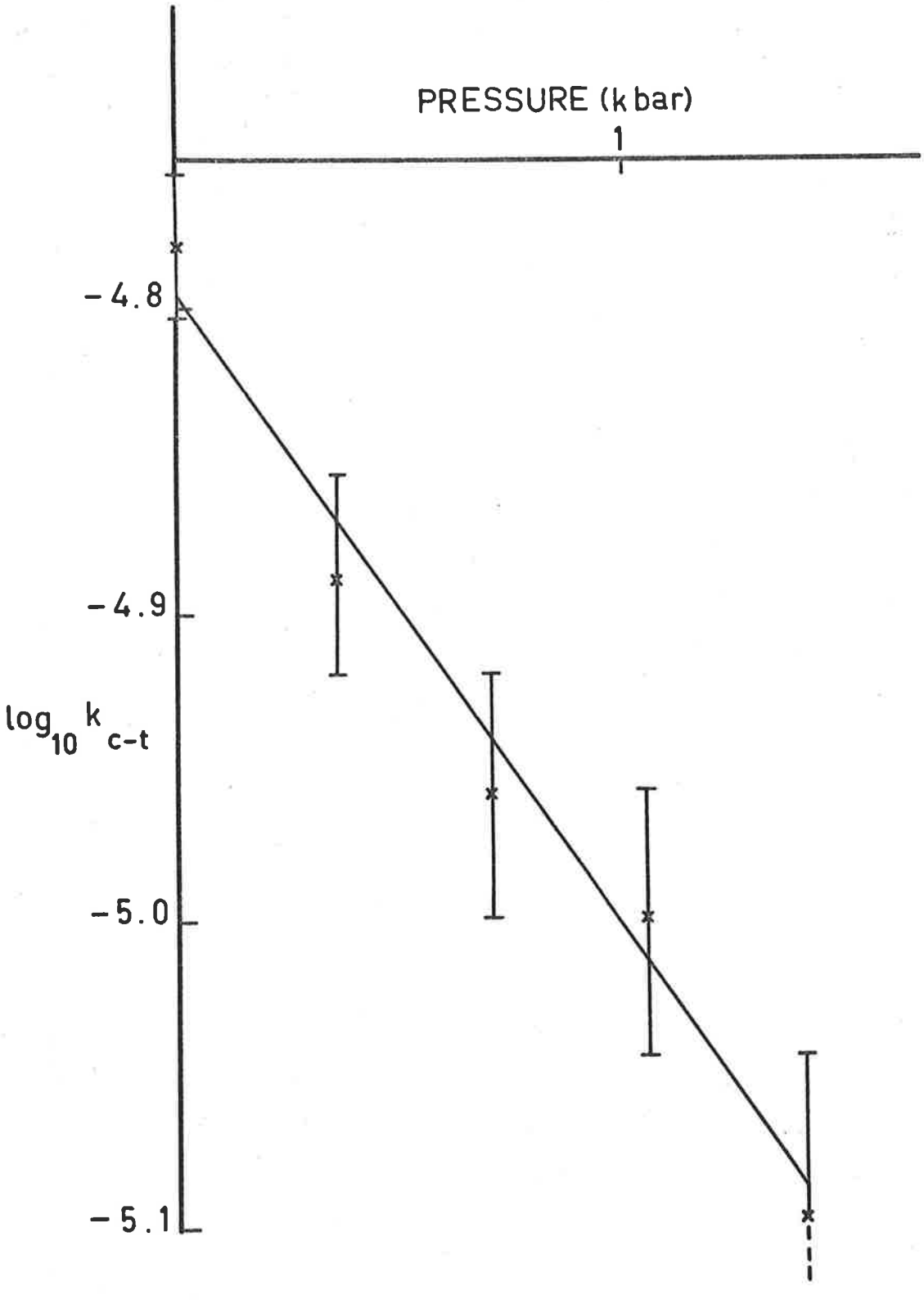

FIG. 3.8 Variation of k_{c-t} with pressure at pH 3.3.

3.4 Discussion

3.4.1 The Effect of Temperature and Pressure on the Isomerisation Rate at pH 3.3.

In the previous chapter it has been mentioned that isomerisation reactions occupy a unique position with regard to pressure studies. Changes in electrostrictive effects during the isomerisation should be quite minor and measured volumes of activation readily explained in terms of volume changes of the reacting molecules. Since the species *cis* and *trans*-Co $en_2(H_2O)OSeO_2H^{2+}$ are closely analogous to *trans*-Co $en_2(OH_2)_2^{3+}$, varying only in the overall charge and the nature of the ligand in one coordinated position, these features are equally relevant in the present system.

Clearly, the experimental values $\Delta V^{\ddagger}_{t-c} = + 7.5 \pm 0.2$ $cm^3\ mol^{-1}$ and $\Delta V^{\ddagger}_{c-t} = + 12.7 \pm 1.0\ cm^3\ mol^{-1}$ implies that the transition state for these isomerisation processes occupies a markedly larger volume than the reactants. At 25°C and pH 3.3 the rate of exchange[6] of amine protons in *cis*-$Co(en)_2NH_3Cl^{2+}$, *cis*-$Co(trien)NH_3Cl^{2+}$ and *cis*-Co $en_2(NH_3)_2^{3+}$ with D_2O are some 100 times slower than the rate of *trans* to *cis* selenito isomerisation and some 10 times slower than the reverse process at the same reaction conditions. Likewise, at 35°C and pH 3.3, the analogous exchange process[7] with *trans*-Co $en_2(OH_2)SO_3^{+}$ is respectively 10^4 and 10^3 times slower than *trans* to *cis* and *cis* to *trans* interconversion of Co $en_2(OH_2)OSeO_2H^{2+}$ at the same temperature and pH. The increase

in volumes observed cannot, therefore, be explained by decreased electrostriction arising from a ring opening mechanism to form a species $[(H_2NH_2CH_2CNH_2)Co\ en\ (OSeO_2H)]^{2+}$ of increased ionic radius.

Isomerisation could proceed by the rate determining release of the selenito ligand from the primary coordination sphere of the complex. However, this would involve increased electrostriction around the transition state species $^{\ddagger}[Co\ en_2OH_2{}^{3+}\ \ ^{-}OSeO_2H]$ and in such a case $\Delta V^{\ddagger}$ should be sharply negative and $\Delta\beta^{\ddagger}$ should have a measurable value. Since $\Delta V^{\ddagger}$ is positive and $\Delta\beta^{\ddagger} = 0$ (within experimental uncertainty), this mechanism is considered unlikely. Moreover (as shown in Section 3.4.2) $\Delta V^{\ddagger}_{t-c}$ is unaffected by the degree of protonation of the selenito ligand and electrostrictive effects must be negligible.

The experimental data for both *trans* to *cis* and *cis* to *trans* selenito isomerisation can be taken to indicate dissociatively activated processes involving aquo-cobalt bond rupture in the transition state. It has been argued in Chapter 2 that an interchange mechanism may exhibit values for $\Delta V^{\ddagger}$ in the range $-15\ cm^3\ mol^{-1}$ to $+\ 15\ cm^3\ mol^{-1}$ and $\Delta\beta^{\ddagger}$ should be $\leqslant 0.1\ cm^3\ mol^{-1}\ kbar^{-1}$. The observed activation parameters, $\Delta V^{\ddagger}_{t-c} = +7.5 \pm 0.2\ cm^3\ mol^{-1}$ and $\Delta\beta^{\ddagger}_{t-c} \simeq 0$, and $\Delta V^{\ddagger}_{c-t} = +\ 12.7 \pm 1.0\ cm^3\ mol^{-1}$ and $\Delta\beta^{\ddagger}_{c-t} \simeq 0$, is thus consistent with a dissociative interchange mechanism for both reactions. The value of $\Delta V^{\ddagger}$ for trans to cis isomerisation implies that the aquo-cobalt bond is significantly stretched in the activated complex. The higher value of $\Delta V^{\ddagger}$ for

the reverse process suggests that this same bond is almost completely dissociated in the transition state for this reaction. This effect is attributed to intramolecular hydrogen bonding possible in the *cis* isomer which requires the aquo ligand to be almost wholly moved from the vicinity of the adjacent selenito group before isomerisation may proceed.

The activation enthalpy for the selenito isomerisation process, $\Delta H^{\ddagger}$ = 109.6 ± 1.3 kJ mol^{-1}, is typical for the dissociative aquo release from diamagnetic cobalt III complexes[8], but some 40 kJ mol^{-1} higher than for the substitution[9] of the S-bonded *trans*-Co $en_2(OH_2)SO_3^+$ cation by SO_3^{2-} which is also considered to proceed by aquo-cobalt bond rupture. The unusually low $\Delta H^{\ddagger}$ value was attributed to special π-bonding effects of the S atom. The higher $\Delta H^{\ddagger}$ value for the O-bonded selenito species presumably originates from the greater energy required to rearrange the Co $en_2(\ )OSeO_2H^{2+}$ moiety to form the *cis*-Co $en_2(OH_2)OSeO_2H^{2+}$ complex via a trigonal pyramid intermediate since no π-bonding is possible with the O atom. Additionally, the O-bonded selenito ligand exhibits a less pronounced *trans* labilising effect on the aquo ligand as compared to the sulphito ligand. At 25°C, release of the aquo-ligand from *trans*-Co $en_2(OH_2)SO_3^+$ is 3700 times faster than from *trans*-Co $en_2(OH_2)OH^{2+}$. However, aquo release from *trans*-Co $en_2(OH_2)OSeO_2H^{2+}$ is some 15 times slower than from the *trans* aquo hydroxo species. Finally, the entropy of activation for isomerisation, $\Delta S^{\ddagger}$ = + 53.1 ± 4.2 J K^{-1} mol^{-1} is compatible

with a positive $\Delta V^{\ddagger}$.

3.4.2 The Effect of Pressure on the Rate of Isomerisation at pH 7.0.

By an analogous argument to that presented in the previous section, the experimental values $\Delta V^{\ddagger}_{t-c} = \Delta V^{\ddagger}_{c-t} = + 7.3 \pm 0.2$ cm^3 mol^{-1} is consistent with a dissociative interchange mechanism for the isomerisation reactions at neutral pH of the species *trans* and *cis* Co $en_2(OH_2)OSeO_2^+$. The lower value of $\Delta V^{\ddagger}$ for *cis* to *trans* isomerisation at pH 7.0 compared to the analogous process at pH 3.3 stems from the fact that no intramolecular hydrogen bonding is possible in the *cis* isomer at this pH since the selenito ligand is not protonated.

The high degree of linearity of Figure 3.6 for the isomerisation data at pH 7.0 implies that the pressure dependence of $\Delta V^{\ddagger}$ i.e. $(\partial \Delta V^{\ddagger}/\partial P)_T = \Delta\beta^{\ddagger}$ is zero regardless of whether a supporting electrolyte is present. By contrast, $\Delta\beta^{\ddagger}$ for the analogous *trans* to *cis* interconversion of Co $en_2(OH_2)_2^{3+}$ is about 10 times larger for a 20 fold increase in electrolyte concentration. This effect for the Co $en_2(OH_2)_2^{3+}$ cation is considered to originate from the substantial loosening of secondary water molecules about the 3^+ cation in the transition state. The failure of the selenito isomerisation process to exhibit this feature may originate from hydrogen bonding possible between the coordinated selenito group and secondary water molecules; this bonding not being significantly affected in forming the transition state. There is evidence for specially strong hydrogen bonding between selenites and water[16]. In addition, the smaller charge of the complex cation Co $en_2(OH_2)OSeO_2^+$ would result in less

defined solvation sheaths about this species.

3.4.3 The Effect of Pressure on the cis/trans Equilibrium Constant.

Most recent interpretations[10] of partial molal volumes of ions, $\bar{V}_{ion}$, as a function of size and charge regard $\bar{V}_{ion}$ as being composed of two major components

$$\bar{V}_{ion} = \bar{V}_{int} + \bar{V}_{el} \qquad 3.6$$

where $\bar{V}_{int}$ and $\bar{V}_{el}$ represent the intrinsic and electrostrictive partial molal volumes of the ions repectively. For the present equilibrium system electrostrictive effects are likely to be absent since the charge of the isomers do not differ. On this basis the experimental value $\Delta V = -5.8 \pm 0.4$ cm^3 mol^{-1} must result from the larger intrinsic volume of the *trans* isomer as compared to the *cis* form since

$$\Delta V_{isom} = \bar{V}_{cis} - \bar{V}_{trans} = -5.8 \text{ cm}^3 \text{ mol}^{-1}$$

$$\text{i.e. } \bar{V}_{trans} = \bar{V}_{cis} + 5.8 \text{ cm}^3 \text{ mol}^{-1}$$

The molar volumes of hydrogen-bonded compounds are found[11] to be always smaller than those of non-associated compounds of similar molecular size. Hamann[12] has estimated the contraction involved in the formation of a hydrogen bond to be about 3.8 cm^3 mol^{-1}. This fact has been used to explain[13] the lower molar volume change for the base dissociation (equation 3.7) of Trizma base as compared to other nitrogen bases

$$BH^+ + H_2O \overset{K_b}{\rightleftarrows} B + H_3O^+ \qquad 3.7$$

At 25°C and 1 bar, ΔV_b = - 17.9 $cm^3\ mol^{-1}$ for Trizma base,[13] -28.9 $cm^3\ mol^{-1}$ for ammonia,[12] - 26.4 $cm^3\ mol^{-1}$ for monomethylamine,[12] -27.2 $cm^3\ mol^{-1}$ for dimethylamine[12] and - 28.1 $cm^3\ mol^{-1}$ for trimethylamine.[12] The small effect of Trizma buffer is attributed to the existance of hydrogen bonds between the three -OH groups in the tris(hydroxymethyl) aminomethane molecule for which Benesch and Benesch[14] proposed the following model:

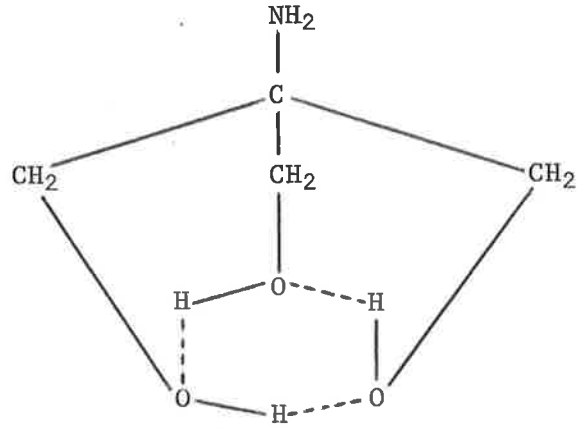

Likewise, the measured volume contraction of - 7.5 $cm^3\ mol^{-1}$ for the effect of pressure on the keto-enol tautomerism of aceto-acetic ester[15] at 25°C

$$CH_3 - \underset{\underset{O}{|}}{C} - CH_2CO_2C_2H_5 \rightleftarrows CH_3 - \underset{\underset{OH}{||}}{C} = CH\ CO_2C_2H_5 \qquad 3.8$$

keto enol

was interpreted in terms of hydrogen bonding between the hydroxy group of the *enol* isomer and the surrounding water molecules.

In the present equilibrium system, the smaller intrinsic volume of the *cis* isomer may then be explained by intramolecular

hydrogen bonding between the adjacent coordinated selenite and aquo ligands, as represented below:

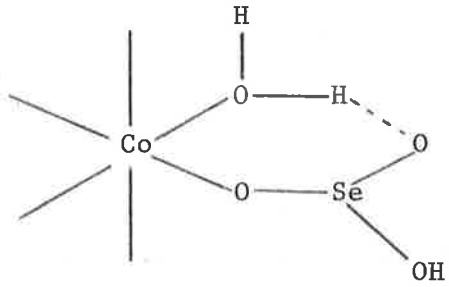

Intramolecular hydrogen bonding cannot occur in the *trans* species. In fact, this isomer may contain an additional volume as a result of intermolecular hydrogen bonding between the free oxygen of the selenito group and surrounding solvent molecules.

3.4.4 Conclusion

In aqueous solution both *trans*-Co $en_2(OH_2)OSeO_2H^{2+}$ and *trans*-Co $en_2(OH_2)OSeO_2^{+}$ isomerise almost completely to the *cis* forms. The isomerisation rate parameters for *trans*-Co $en_2(OH_2)OSeO_2H^{2+}$ at pH 3.3 are $k_{(25°C)} = 2.42 \times 10^{-4}$ sec^{-1}, $\Delta H^{\ddagger} = 109.6 \pm 1.3$ kJ mol^{-1}, $\Delta S^{\ddagger} = + 53.1 \pm 4.2$ J K^{-1} mol^{-1}, $\Delta V^{\ddagger}_{t-c} = + 7.5 \pm 0.2$ cm^3 mol^{-1} and $\Delta V^{\ddagger}_{c-t} = + 12.7 \pm 1.0$ cm^3 mol^{-1}. For *trans*-Co $en_2(OH_2)OSeO_2^{+}$ at pH 7.0 and ionic strength 0.5 M, $k_{(15°C)} = 2.83 \times 10^{-4}$ sec^{-1} and $\Delta V^{\ddagger}_{t-c} = \Delta V^{\ddagger}_{c-t} = + 7.3 \pm 0.2$ cm^3 mol^{-1}. For both systems $\Delta V^{\ddagger}$ shows no measurable pressure dependence.

The data are consistent with a dissociative interchange process for the *trans* to *cis* and reverse reactions. At pH 3.3, the equilibrium concentration of the *cis* isomer is favoured with increasing pressure and $\Delta V_{t-c} = -5.8 \pm 0.4$ cm^3 mol^{-1}.

References to Chapter 3.

1. P. Ray and A.N. Ghosh, *Indian Chem. Soc.*, 1936, 13, 494.
2. A.D. Fowless, *Ph.D. Thesis, University of Adelaide*, 1973.
3. J.V. Dubrawski, *Honours Report, University of Adelaide*, 1972.
4. *Handbook of Chemistry and Physics*, 50th Edition, 1969-70.
5. A.A. Frost and R.G. Pearson, *"Kinetics and Mechanism"*, *John Wiley and Sons, Inc.*, 2nd Edition, pg. 49.
6. F. Basolo, J.W. Palmer and R.G. Pearson, *J. Amer. Chem. Soc.*, 1960, 82, 1073.
7. A.C. Sandercock, *Honours Report, University of Adelaide*, 1970.
8. F. Basolo and R.G. Pearson, *"Mechanism of Inorganic Reactions"*, *John Wiley and Sons, Inc., New York*, 2nd Edition, Chapter 3.
9. D.R. Stranks and J.K. Yandell, *Inorg. Chem.*, 1970, 9, 751.
10. J.F. Millero, *Chem. Reviews*, 1971, 71, 147.
11. G.C. Pimentel and A.L. McClellan, *"The Hydrogen Bond"*, *Freeman & Co., San Francisco*, pg. 53.
12. S.D. Hamann, *"High Pressure Physics and Chemistry"*, Vol. 2., *Academic Press INc., New York*, 1963 ed., R.S. Bradley.
13. A. Disteche, *"The Effect of Pressure on Organisms"*, *Symposia of the Society for Experimental Biology*, Nos. XXVI, *Cambridge University Press*, 1972, pg. 27.
14. R.E. Benesch and R. Benesch, *J. Amer. Chem. Soc.*, 1955, 77, 2749.
15. M.I. Kabachnik, S.E. Yaknshkina and N.V. Kislyakova, *C.R. Acad. Sci. U.R.S.S.*, 1954, 96, 1169.

16. A. Simon and R.Z. Paetzold, *Anorg. Allgem Chem.*, 1959, 301, 246.

Chapter 4. The Effect of Pressure on the Nucleophilic Substitution of diaquobis(ethylenediamine) cobalt III cation by oxalate ions.

4.1 Introduction

4.1.1 Mechanisms of Anation Reactions

It has been found[1] that the anation rate of most aquo-amine cobalt III complexes , RH_2O^{n+}, by many different anions, Y^{m-}, first increases linearly with anion concentration and then gradually reaches a limiting value. The general rate law is given by the expression,

$$\text{Rate} = a[Y^{m-}][RH_2O^{n+}]/(1 + b[Y^{m-}]) \qquad 4.1$$

where a and b are two suitable parameters. In the reciprocal form,

$$1/k_{obs} = b/a + 1/a[Y^{m-}] \qquad 4.2$$

where Rate = k_{obs} $[RH_2O^{n+}]$ in excess nucleophile Y^{m-}. Thus a and b may be evaluated from the slope and intercept of the straight line plot of $1/k_{obs}$ against $1/[Y^{m-}]$.

A classical associative, A, mechanism between an aquo-metal ion and entering anion is not consistent with the appearance of limiting rates in these reactions. The rate law is compatible with a limiting dissociation, D, of an aquo complex followed by competition between solvent water and entering anion for the five coordinate

intermediate;

$$RH_2O^{n+} \xrightarrow[\text{slow}]{k_1} R^{n+} + H_2O \qquad 4.3$$

$$R^{n+} + H_2O \xrightarrow{k_{-1}} RH_2O^{n+} \qquad 4.4$$

$$R^{n+} + Y^{m-} \xrightarrow{k_2} RY^{(n-m)+} \qquad 4.5$$

Assuming the rate of hydrolysis of $RY^{(n-m)+}$ is negligible, a steady-state treatment yields the rate law:

$$\text{Rate} = k_1k_2[Y^{m-}][RH_2O^{n+}]/(k_{-1}[H_2O] + k_2[Y^{m-}]) \qquad 4.6$$

and hence, from equation 4.2,

$$1/k_{obs} = 1/k_1 + k_{-1}[H_2O]/k_1k_2[Y^{m-}] \qquad 4.7$$

where

$$a = k_1k_2/k_{-1}[H_2O] \text{ and } b = k_2/k_{-1}[H_2O]$$

However the same rate law (equation 4.1) is also consistent with a rapid pre-equilibrium formation of an ion-pair between the cationic complex and entering anion, followed by an interchange, I, between the leaving group and the anion within the ion pair,

$$RH_2O^{n+} + Y^{m-} \underset{\text{fast}}{\overset{K_{I.P.}}{\rightleftharpoons}} RH_2O^{n+}.\ Y^{m-} \qquad 4.8$$

$$RH_2O^{n+}.\ Y^{m-} \xrightarrow[\text{slow}]{k_{an}} RY^{(n-m)+} + H_2O \qquad 4.9$$

where $K_{I.P.}$ denotes the ion-pair formation constant and k_{an} the interchange rate constant. The corresponding rate law is given by,

$$\text{Rate} = k_{an}K_{I.P.}[Y^{m-}][RH_2O^{n+}]/(1 + K_{I.P.}[Y^{m-}]) \qquad 4.10$$

where the term $K_{I.P.}[Y^{m-}]/1 + K_{I.P.}[Y^{m-}]$ represents the fraction of RH_2O^{n+} existing as the ion-pair. It follows immediately from equation 4.2 that $a = k_{an} K_{I.P.}$ and $b = K_{I.P.}$

and
$$1/k_{obs} = 1/k_{an} + 1/k_{an}.K_{I.P.}[Y^{m-}] \qquad 4.11$$

By the principle of microscopic reversibility, it is unlikely that an I_a mechanism would operate in anation reactions. Hence nucleophilic substitution reactions are essentially dissociative (D or I_d) in nature.

The two reaction pathways discussed above exhibit similar rate behaviour. At low $[Y^{m-}]$, both give second-order reactions, and at high $[Y^{m-}]$ both yield limiting rates. There are, however, some indicative differences between the two mechanisms. Whereas for the D pathway the limiting rate must equal the independently measurable water exchange rate, k_{ex}, the limiting rate for the I_d process lies below k_{ex} by an appropriate statistical factor related to the population of the outer sphere. This is because the Y^{m-} group occupies only one outer-sphere coordination position in the encounter complex, the rest being occupied by water. On dissociation of the aquo ligand, water exchange is likely to be the more probable reaction. A further distinguishing feature is that the Y^{m-} dependence of the I_d path must match the independently measurable counter equilibrium which is not especially sensitive to any characteristic of Y^{m-} other than its charge. However, for the D pathway, variations in Y^{m-} changes the ligand attacking a

relatively stable intermediate. The resultant differences may be large but not parallel to 'ion-pairing' tendencies.

4.1.2 Nucleophilic Substitution of Co $en_2(OH_2)_2^{3+}$ *by Oxyanions*

The anations of Co $en_2(OH_2)_2^{3+}$ by both SO_4^{2-} and SeO_4^{2-} have been found[2] to involve extensive ion-pairing between the reactants. The enthalpy and entropy of activation of the anation process were measured to be $\Delta H^{\ddagger}$ = 146.0 ± 4.2 kJ mol^{-1} and $\Delta S^{\ddagger}$ = 100.4 ± 12.6 J K^{-1} mol^{-1} in each case. At 25°C and pH 3.5, the rate of anation, $k_{an} = 2.34 \times 10^{-4}$ min^{-1}, was found to be seven times slower than the estimated first order rate coefficient for water exchange, $k_{ex} = 15.9 \times 10^{-4}$ min^{-1}, at the same reaction conditions.

Lincoln[3] has studied the analogous reaction by PO_4^{3-} at 47.9°C and pH 6.94, where the predominant species are *cis* and *trans* [Co $en_2(OH)OH_2]^{2+}$. He concluded that the major path to phosphate anation is through the *trans*-[Co $en_2(OH)OH_2]^{2+}$.HPO_4^{2-} ion pair. The enthalpy and entropy of activation were found to exhibit respective values of 125.5 ± 2.5 kJ mol^{-1} and + 79.5 ± 12.6 J K^{-1} mol^{-1}. The measured specific anation rate coefficient, k_{an} = 0.255 min^{-1}, was 1/20 the estimated value for water exchange, $k_{ex} \simeq 5$ min^{-1}, for the unassociated *trans* hydroxo cation at the same reaction conditions.

In contrast to the behaviour of the oxyanions discussed above, the rate of nucleophilic substitution[4] by SeO_3^{2-} at 25°C and between pH 1 and 10 is very much greater than water exchange rate for the corresponding aquo species. For example, the value k_{an} = 6.9 sec^{-1}

for substitution of *trans*-Co $en_2(OH_2)_2^{3+}$ by $HSeO_3^-$ at 25°C and pH 1 is 10^4 times faster than $k_{ex} = 6.8 \times 10^{-4}$ sec^{-1} under identical conditions. In addition, these substitutions of selenite exhibit activation enthalpies, $\Delta H^{\ddagger}$, in the region 40 - 50 kJ mol^{-1} which is very much smaller to that found for anation by other oxyanions. The rate-determining process for the formation of the selenito products is considered to involve aquo substitution at selenium IV. There is evidence[5] to suggest that anation by AsO_4^{3-} proceeds via the same mechanism.

A: *The Effect of Pressure on the Anation of diaquobis(ethylenediamine)cobalt III by oxalate in Aqueous Acidic Medium.*

4.2 *Introduction*

In aqueous acidic medium (pH < 1), the reaction

$$Co\ en_2(H_2O)_2^{3+} + HC_2O_4^- \rightarrow Co\ en_2C_2O_4^+ + H^+_{aq} \qquad 4.12$$

proceeds essentially to completion. The anation is believed[6] to involve an ion-pair mechanism (equations 4.8 and 4.9) and the reaction scheme is depicted as

$$cis\text{-}Co\ en_2(H_2O)_2^{3+} + HC_2O_4^- \underset{}{\overset{K_{I.P.}}{\rightleftharpoons}} cis\text{-}Co\ en_2(H_2O)_2^{3+}.HC_2O_4^- \qquad 4.13$$

$$cis\text{-}Co\ en_2(H_2O)_2^{3+}.\ HC_2O_4^- \xrightarrow{k_{an}} Co\ en_2C_2O_4^+ + H^+_{aq} \qquad 4.14$$

In this scheme $HC_2O_4^-$ represents the two predominant oxalate species $H_2C_2O_4$ and $HC_2O_4^-$, and the interchange rate constant, k_{an}, is assumed to be the same for both associated species. The association constants for the reactant pairs $Co\ en_2(H_2O)_2^{3+}.\ H_2C_2O_4$ and $Co\ en_2(H_2O)_2^{3+}.\ HC_2O_4^-$ are, at 60°C, 7 and 64 respectively. The activation parameters for reactions 4.13 and 4.14 are $k_{an}(60°C) = 4.8 \times 10^{-4}\ sec^{-1}$, $\Delta H^{\ddagger}_{an} = 103.8 \pm 2.1\ kJ\ mol^{-1}$, $\Delta S^{\ddagger} = 6.3 \pm 6.3\ J\ K^{-1}\ mol^{-1}$ and $\Delta H_{I.P.} = 25.1 \pm 12.6\ kJ\ mol^{-1}$. At 40°C and ionic strength of 1 M, the water exchange rate[7], $k_{ex} = 7.7 \times 10^{-5}\ sec^{-1}$, is faster than the anation rate by a factor close to 4.

The oxalate substitution reaction is of special interest in relation to the *trans* to *cis* isomerisation of $Co\ en_2(H_2O)_2^{3+}$ discussed in Chapter 2 since it involves the same parent cation. Oxalate substitution is considered to be the replacement of an

aquo ligand by oxalate as compared with replacement by another water molecule in the previous system. This reaction provides, therefore, a useful comparison for volumes of activation of related systems involving nucleophilic substitution by water and oxalate.

4.3 Experimental

4.3.1 Materials

[Co en_2CO_3]Cl was prepared by the method of Dwyer, Sargeson and Reid.[8]

[Co en_2CO_3]NO_3

A suspension of [Co en_2CO_3]Cl (8 g) in water (60 ml) was shaken for five minutes with silver nitrate (3.7 g) in water (20 ml). The silver chloride was removed, alcohol added to the filtrate and the [Co $en_2C\overset{O}{\emptyset}_3$]$NO_3$ which crystallised collected, washed with alcohol and dried. Yield 60%.

cis-[Co $en_2(H_2O)_2$]$(NO_3)_3$

cis-[Co $en_2(H_2O)_2$]$(NO_3)_3$ was prepared directly from [Co en_3CO_3]NO_3 by the addition of nitric acid. Solutions obtained in this way gave extinction coefficients at 492 nm which compared favourably with those reported by Bjerrum and Rasmussen[9] (ε_{492} = 80.9 M^{-1} cm^{-1}).

All other reagents have been previously described or were commercial products of good quality and were used without further purification.

4.3.2 Apparatus

Pressure vessel

The high pressure sampling vessel (see Appendix I) was used in all experiments.

Spectrophotometer

All absorbance measurements were made using a Shimadzu spectrophotometer, Model QR-50 (see Section 2.2.2).

Temperature control

Temperature control to ± 0.01°C was achieved in the same manner as described in Section 2.2.2.

4.3.3 Procedure for Kinetic Runs

Atmospheric pressure

An aliquot of diaquobis(ethylenediamine)cobalt III was thermostated in a volumetric flask, immersed in a water bath at the desired temperature, and an equivalent volume of thermostated oxalate solution added rapidly with stirring. The ionic strength was controlled by the addition of requisite amounts of sodium nitrate. Aliquot samples were withdrawn at regular time intervals and discharged into ice-chilled tubes to quench the reaction. The samples were analysed spectrophotometrically at 500 nm where the respective extinction coefficients for the species *cis*-Co $en_2(OH_2)_2^{3+}$ and Co $en_2C_2O_4^{+}$ are 80.9 M^{-1} cm^{-1} and 113 M^{-1} cm^{-1}.[6]

Higher pressures

Equal aliquots from both the stock diaquo and oxalate reaction solutions were mixed and placed in the Perspex reaction vessel. The teflon plunger was placed in position and the entire apparatus lowered into the pressure vessel. The pressure was raised to

the desired value and the reaction solution left at this pressure for at least 30 minutes to attain thermal equilibrium. Aliquot samples were discharged, at regular time intervals, into ice-chilled tubes; the pressure being quickly readjusted with the pump after each sample removal.

Sample analysis was the same as above.

4.4 Results

4.4.1 Evaluation of the Kinetic Data

Plots of $\log(OD_\infty - OD_o / OD_\infty - OD_t)$ against time, where OD_∞, OD_o and OD_t represents the optical absorbances at infinite, zero and time t respectively, were linear. Since the concentration of the oxalate anion (0.015 M - 0.06 M) was always much greater than that of the diaquo species (5.81×10^{-3} M), the reaction displays pseudo-first order behaviour. This observation was in agreement with Brown and Harris[6] who also observed first order kinetics.

The OD_t values were taken over two reaction half-times while the OD_∞ reading obtained after at least six half times.

4.4.2 Pressure Dependence on the Anation Reaction

The pressure dependence on oxalate anation (equations 4.13 and 4.14) was studied between 0 and 2 kbar at 60°C from sets of runs at different $[HC_2O_4^-]$ and pressures. Table 4.1 lists such data determined, at four different pressures, by a least-squares procedure.

In most cases, the standard deviation of each mean value of the rate coefficient is close to ± 2%. To achieve this level of accuracy, it was necessary to conduct at least four individual runs at a particular set of reaction conditions. The results at atmospheric pressure are in satisfactory agreement with values quoted by Brown and Harris[6] at the same reaction conditions (see Table 4.1).

Table 4.1

Variation of k_{obs} with pressure

Temp. = 60.0 ± 0.1°C ; $[HNO_3]$ = 0.5 M ; $\mu(NaNO_3)$ = 2.0 M

Applied Pressure (bar)	Oxalate conc.	$10^5.k_{obs}$ (sec^{-1})	nos. of runs
1[a]	0.015	9.03	2
	0.020	10.9	-
	0.030	14.0	2
	0.060	21.2	3
1	0.015	9.18 ± 0.15	4
	0.020	11.37 ± 0.17	4
	0.030	14.18 ± 0.26	5
	0.060	20.90 ± 0.38	4
552	0.015	7.88 ± 0.21	4
	0.020	9.90 ± 0.21	4
	0.030	12.28 ± 0.26	4
	0.060	18.62 ± 0.30	4
1034	0.015	7.10 ± 0.09	5
	0.020	9.16 ± 0.22	4
	0.030	10.95 ± 0.15	4
	0.060	16.80 ± 0.41	4
1517	0.015	6.39 ± 0.20	6
	0.020	8.06 ± 0.16	5
	0.030	9.96 ± 0.24	5
	0.060	15.04 ± 0.33	3

a - values from Brown and Harris[6] at the same reaction conditions

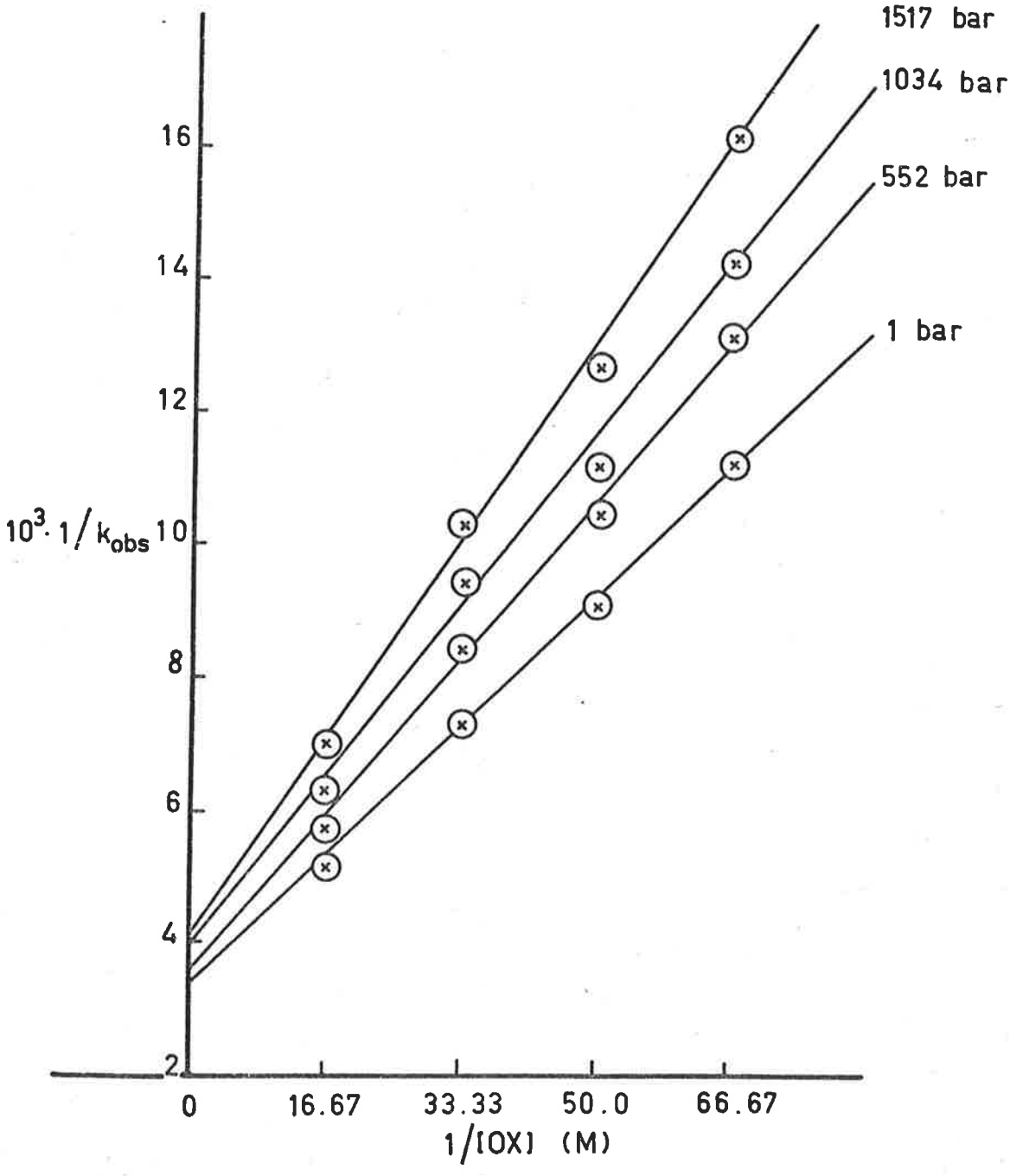

FIG. 4.1 Variation of k_{obs} with pressure.

The data in Table 4.1 were analysed using equation 4.11 (see Figure 4.1) to yield values for the two unknown quantities k_{an} and $K_{I.P.}$; these are summarised in Table 4.2.

Table 4.2

Variation of k_{an} and $K_{I.P.}$ with pressure

Applied Pressure (bar)	$10^5 . k_{an}$ (sec^{-1})	$K_{I.P.}$ (M^{-1})
1	34.9 ± 1.2	23.8 ± 1.2
552	32.1 ± 1.5	21.8 ± 1.4
1034	28.8 ± 2.2	22.1 ± 2.5
1517	26.9 ± 1.5	20.6 ± 1.7

The errors in both k_{an} and $K_{I.P.}$ become larger than those in the individual values of k_{obs} but a clear decrease in both k_{an} and $K_{I.P.}$ with increasing pressure is observed. In Figures 4.2 and 4.3 the variation of $\log_{10} k_{an}$ and $\log_{10} K_{I.P.}$ with pressure are shown as straight lines of best fit drawn through the experimental data. The values of $\Delta V^{\ddagger}_{an}$ and $\Delta V_{I.P.}$ were calculated from the slopes of these lines using equation 1.10. A least-squares analysis of the data in Table 4.2 yielded,

$$\Delta V^{\ddagger} = + (4.8_0 \pm 0.2_3) \text{ cm}^3 \text{ mol}^{-1}$$

$$\Delta V_{I.P.} = + (2.3 \pm 0.6) \text{ cm}^3 \text{ mol}^{-1}$$

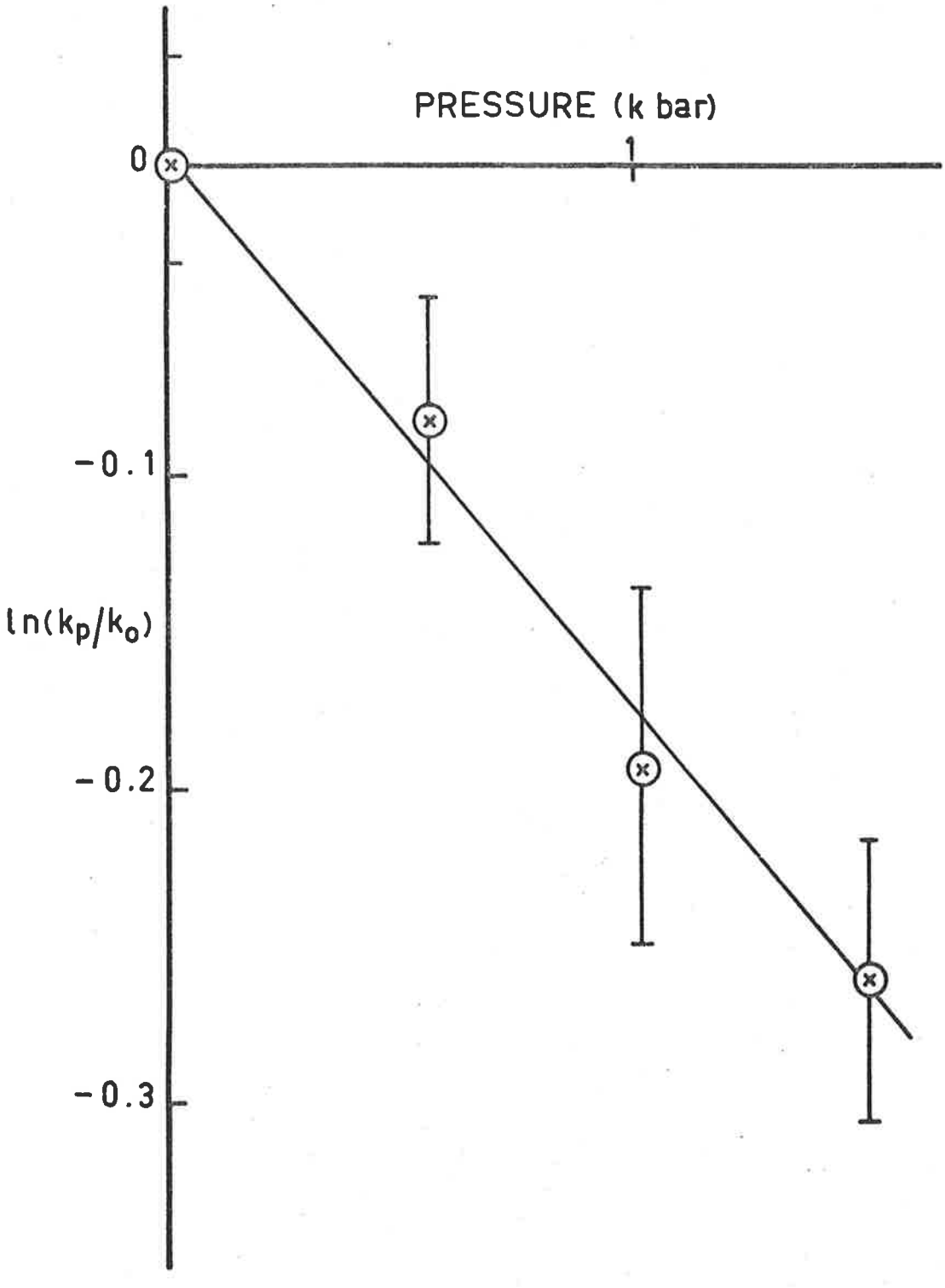

FIG. 4.2 The effect of pressure on k_{an}.

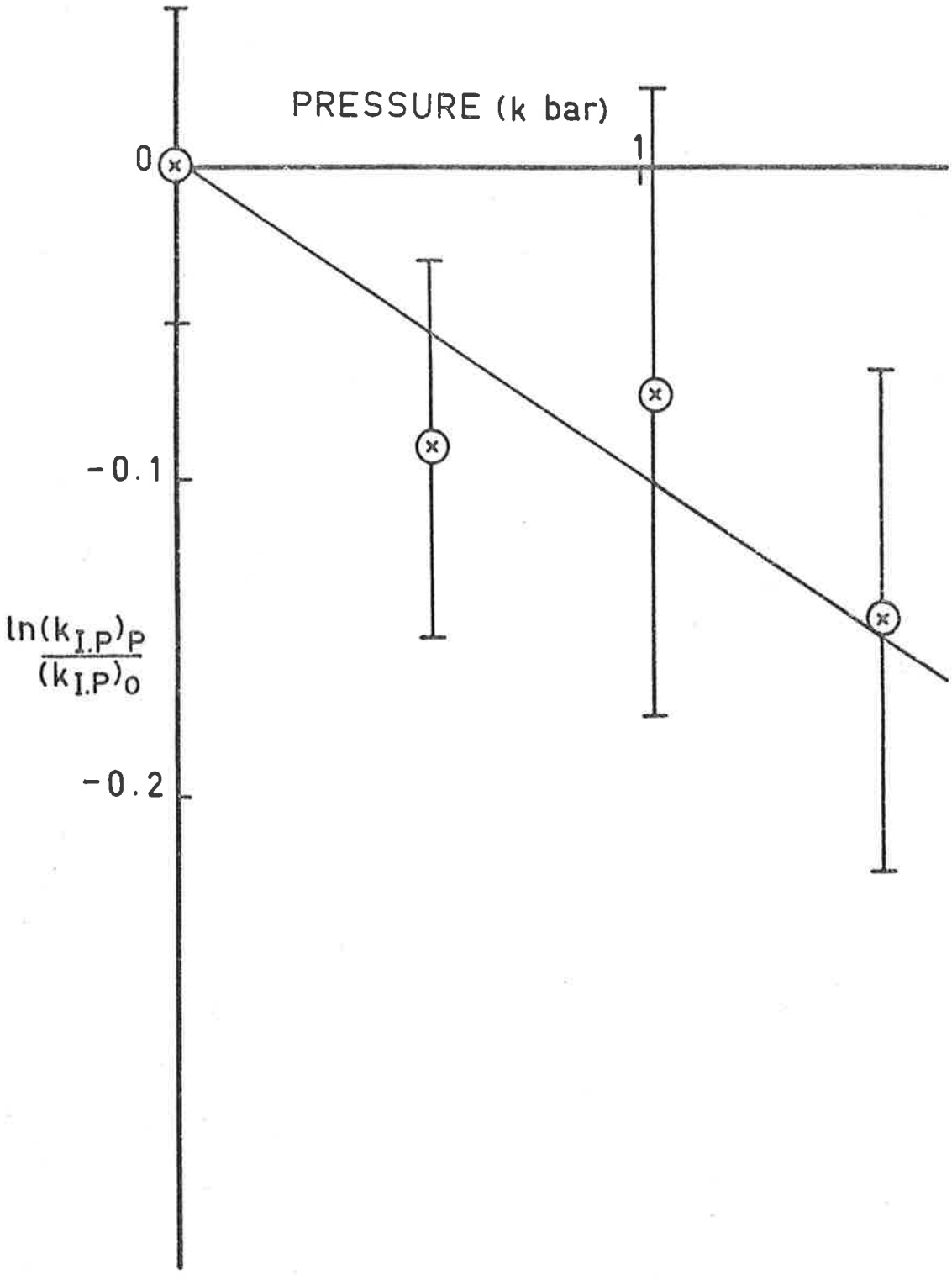

FIG. 4.3 Pressure dependence of the ion-pair equilibrium constant.

the variance of each value being quoted. If 95% confidence limits are applied, then the values become $\Delta V^{\ddagger}$ = +(4.8 ± 0.67) $cm^3\ mol^{-1}$ and $\Delta V_{I.P.}$ = +(2.3 ± 1.2) $cm^3\ mol^{-1}$.

4.5 *Discussion*

4.5.1 *The Effect of Pressure on Oxalate Anation in Aqueous Acidic Medium.*

For the nucleophilic substitution of *cis*-Co $en_2(OH_2)_2^{3+}$ by $HC_2O_4^-$ (reaction 4.12) two alternative mechanisms have been proposed. These can each be considered in terms of the measured volume of activation determined in the present studies.

A limiting dissociative, D, mechanism (equations 4.3 to 4.5) involves the synchronous loss of an aquo ligand from *cis*-Co $en_2(OH_2)_2^{3+}$ to form an intermediate of reduced coordination and the release of electrostricted water to the bulk solvent. The *trans* to *cis* isomerisation of Co $en_2(OH_2)_2^{3+}$, discussed in Chapter 2, has been assigned this mechanism and at high ionic strength $\Delta V^{\ddagger}$ and $\Delta\beta^{\ddagger}$ have been determined as + 14.2 $cm^3\ mol^{-1}$ and 10 $cm^3\ mol^{-1}\ kbar^{-1}$ respectively. This is not in accord with the measured values in the present system of $\Delta V^{\ddagger}$ = 4.7 ± 0.7 $cm^3\ mol^{-1}$ and $\Delta\beta^{\ddagger} \leqslant 0.1\ cm^3\ mol^{-1}\ kbar^{-1}$ at comparable conditions and a D mechanism does not seem likely. This finding is consistent with the view of Brown and Harris[6] who eliminated the ~~seem~~ same mechanism from a consideration of the competition ratio between oxalic acid and water for the intermediate Co $en_2(\ )OH_2^{3+}$. The second order rate coefficient for substitution of a metal-aquo complex, k_s, is related to the rate of water loss, k_{H_2O} by the equation

$$k_s = K_{I.P.}\ k_{H_2O} \qquad 4.15$$

where $K_{I.P.}$ is the equilibrium quotient for the formation of the outer-sphere ion-pair. Using the value[6] 7 M^{-1} for K_3 and assuming the concentration of water in solvent water is about 55 M, it follows that $H_2C_2O_4$ should be some 400 times more reactive than H_2O in competing for the intermediate, quite contrary to reasonable expectation.

The alternative interchange, I, pathway (equation 4.8 and 4.9) entails the rapid prior formation of an outer-sphere ion-pair followed by a rate-determining interchange between coordinated water and oxalate nucleophile. It has been argued (Chapter 1) that the interchange of an aquo ligand between the primary and secondary coordination spheres of a 3+ metal ion may exhibit values of $\Delta V_0^{\ddagger}$ in the range + 15 cm^3 mol^{-1} to - 15 cm^3 mol^{-1}. In the present system $\Delta V_0^{\ddagger}$ = + 4.7 cm^3 mol^{-1} and it seems very likely that substitution of *cis*-Co $en_2(OH_2)_2^{3+}$ by $HC_2O_4^-$ proceeds by an I_d mechanism i.e., the aquo ligands are dissociated in the transition state but not to the limit for complete release of OH_2 into the first hydration sphere.

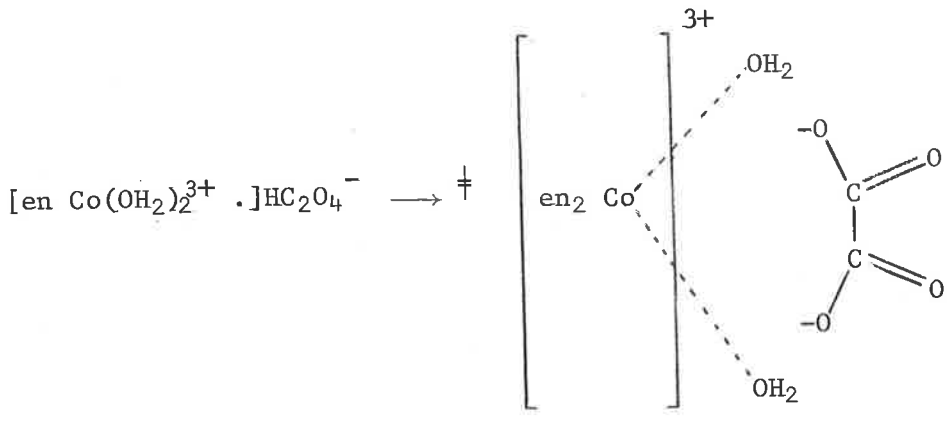

There is a good correlation between $\Delta V_0^{\ddagger}$ and $\Delta S^{\ddagger}$. At 2.0 M ionic strength, Brown and Harris[6] have determined $\Delta S^{\ddagger}$ to be 6.3 ± 6.3 J K^{-1} mol^{-1}. The value of $\Delta V^{\ddagger}$ is significantly more than twice that reported for the dissociative exchange of a single aquo ligand in $Co(NH_3)_5OH_2^{3+}$ ($\Delta V_0^{\ddagger}$ = + 1.2 ± 0.2 cm^3 mol^{-1}). An additional positive contribution to $\Delta V_0^{\ddagger}$ could arise from partial desolvation of $HC_2O_4^-$ on formation of the transition state. This would involve electrostrictive effects and in such a case, $\Delta\beta^{\ddagger}$ should have a measurable value. Since $\Delta\beta^{\ddagger} \leqslant 0.4$ cm^3 mol^{-1} $kbar^{-1}$, it appears that this effect is unimportant.

An expression for estimating the volume change for the formation of an ion-pair (reaction 4.8) can be obtained by differentiating the Fuoss[10] equation for the association of two ions with respect to pressure. Hemmes[11] has shown that

$$\Delta V_{I.P.} = RT[(/Z_+Z_-/e^z/a\varepsilon kT)(\partial \ln\varepsilon/\partial P)_T - \kappa_s] \qquad 4.16$$

where $\Delta V_{I.P.}$ is the volume change in a medium of dielectric contrast ε and temperature T of two spheres of closest encounter distance a and charge Z_+e and Z_-e, k represents the Boltzman constant and κ_s the solution compressibility. In equation 4.16 activity coefficients have been ignored. Using the values[12] $\partial \ln\varepsilon/\partial P$ = 51.05 x 10^{-6} bar^{-1}, ε = 66.76 and κ_s = 44.5 x 10^{-6} bar^{-1}, all at 60°C, and putting $/Z_+Z_-/$ = 3 and a = 7Å, equation 4.16 evaluates to + 3.2 cm^3 mol^{-1}.

There is experimental evidence that suggests a large variation of $\Delta V_{I.P.}$ with ionic strength.[13] For example, the measured volume change $\Delta V_{I.P.}$ = + 18.9 cm^3 mol^{-1} for the outer sphere binding of SO_4^{2-} to $Co(NH_3)_5OH_2^{3+}$ at 0.1 M ionic strength is lowered to $\Delta V_{I.P.}$ = + 12.9 cm^3 mol^{-1} in a 1 M $NaClO_4$ medium. Nevertheless, the value $\Delta V_{I.P.}$ = + 2.6 ± 1.2 cm^3 mol^{-1} found in the present study is in accord with that predicted from the electrostatic model.

The equilibrium 4.8 involves the association of two ions to form a product of larger intrinsic volume and for such a process a negative value for $\Delta V_{I.P.}$ might be expected. The small positive value found implies that the major contribution to $\Delta V_{I.P.}$ arises from decreased electrostriction as a result of the neutralisation of the +3 and -1 charges. For this step, therefore, $\Delta\beta^{\ddagger}$ should have a measurable value. However, the large uncertainties associated with $K_{I.P.}$ together with the small value observed for $\Delta V_{I.P.}$ requires, within the limit of the measurements, that $\Delta\beta$ be close to zero.

Several high pressure studies on the nucleophilic substitution of aquated metal cations have been reported in the literature (see Table 1.2). As a single comparison system, the substitution reaction[14]

$$Cr(OH_2)_6^{3+} + HC_2O_4^- \rightleftarrows Cr(OH_2)_4C_2O_4^+ + H^+_{aq} \qquad 4.17$$

is cited since this involves ions of identical charge to reaction 4.12. At 25°C, pH 2.7 and ionic strength 1.0 M, $\Delta V^{\ddagger}$ was measured to be - 2.2 ± 1 cm^3 mol^{-1}. A major criticism of this study is that

reaction 4.17 very likely proceeds by an ion-pair mechanism but the individual volume changes for the two steps was not evaluated.

Since

$$\Delta V^{\ddagger}_{obs} = \Delta V_{I.P.} + \Delta V^{\ddagger}_{0} \qquad 4.18$$

and assigning a value of + 3 $cm^3\ mol^{-1}$ to $\Delta V_{I.P.}$ seems reasonable, it follows from equation 4.18 that $\Delta V^{\ddagger} \simeq -5\ cm^3\ mol^{-1}$. This estimated value of $\Delta V^{\ddagger}_{0}$ is consistent with an I_a mechanism for the reaction

$$Cr(OH_2)_6^{3+}.HC_2O_4^{-} \rightarrow Cr(OH_2)_4C_2O_4^{+} + H^{+}_{aq} \qquad 4.19$$

and again demonstrates the contrast between the dissociative nature of Co III complex ions and the associative nature of Cr III for analogous reactions.

4.5.2 Conclusion

The substitution of *cis*-Co $en_2(OH_2)_2^{3+}$ by $HC_2O_4^{-}$ to form Co $en_2C_2O_4^{+}$ was studied at 60°C and pressures between 0 and 2 kbar. The activation parameters are $\Delta V^{\ddagger}_{0} = +4.8 \pm 0.7\ cm^3\ mol^{-1}$, $\Delta\beta^{\ddagger} \leqslant 0.1\ cm^3\ mol^{-1}\ kbar^{-1}$ and $\Delta V_{I.P.} = +2.3 \pm 1.2\ cm^3\ mol^{-1}$. The data are consistent with a dissociative interchange mechanism.

B: The Effect of Temperature and Pressure on the Anation of aquohydroxobis(ethylenediamine)cobalt III ion by oxalate in basic aqueous solution.

4.6 Introduction

In strongly acidic medium, the reactant species for the oxalate anation process is limited to *cis*-Co $en_2(OH_2)_2^{3+}$ and the oxalate species $H_2C_2O_4$ and $HC_2O_4^-$. Above pH 7, the diaquo 3+ ion exists as a mixture of *cis* and *trans*-Co $en_2(OH_2)(OH)^{2+}$ and Co $en_2(OH)_2^+$ as defined by the appropriate equilibrium constants (see section 2.1) and the only oxalate species present in measurable amounts is $C_2O_4^{2-}$; the anation reaction is then considered[15] to proceed as,

$$Co\ en_2(OH)OH_2^{2+} + C_2O_4^{2-} \xrightleftharpoons{K_{I.P.}} Co\ en_2(OH)OH_2^{2+}.\ C_2O_4^{2-} \qquad 4.20$$

$$Co\ en_2(OH)OH_2^{2+}\ .\ C_2O_4^{2-} \xrightarrow{k_0} Co\ en_2(OH)C_2O_4^{0} + H_2O \qquad 4.21$$

$$Co\ en_2(OH)C_2O_4^{0} \xrightarrow{k_1} Co\ en_2C_2O_4^{+} + OH^- \qquad 4.22$$

Furthermore, since the reaction is accelerated at lower pH, reaction 4.22, which involves chelate-ring formation by a monodenate oxalato ligand, is considered to proceed through an acid-base pre-equilibrium (4.23) followed by the rapid release of the aquo ligand (4.24),

$$Co\ en_2(OH)C_2O_4^{0} + H^+_{aq} \xrightleftharpoons{1/K_a} Co\ en_2(OH_2)C_2O_4^{+} \qquad 4.23$$

$$Co\ en_2(OH_2)C_2O_4^{+} \xrightarrow{k_1^1} Co\ en_2C_2O_4^{+} \qquad 4.24$$

such that $k_1 = k_1^1/K_a$

At 25°C, ionic strength of 0.37 M and 7.3 < pH < 8.1, k_0 and $K_{I.P.}$ were found to exhibit relatively constant values of 9.4 ± 0.6 x 10^{-4} sec^{-1} and 5.6 ± 0.3 M^{-1} respectively, indicative of substitution with only the monohydroxocobalt species. The value for k_0 is about half the estimated water exchange rate, $k_{ex} \simeq 2 \times 10^{-3}$ sec^{-1}, for Co $en_2(OH_2)OH^{2+}$ at similar reaction conditions. The activation parameters for ring closure are $k_1 = 1.5 \times 10^{-3}$ sec^{-1} (50°C, pH 7.8), $\Delta H_1^{\ddagger} = 106.2 \pm 2.1$ kJ mol^{-1}, and $\Delta S_1^{\ddagger} = -27.2 \pm 4.2$ J K^{-1} mol^{-1}.

In this section the pressure and temperature dependence of k_0 and $K_{I.P.}$ together with the pressure dependence of k_1 are presented.

4.7 *Experimental*

4.7.1 *Materials*

cis-[Co $en_2(OH)H_2O](NO_3)_2$ was prepared from *trans*-[Co en_2Cl_2]Cl by the method of Kruse and Taube.[7]

Resin

The resin column consisted of Dowex 50 W - X8, 20 - 50 mesh in the Na^+ form supplied by the Dow Chemical Company.

Trizma buffer

The preparation of Trizma buffer solutions have been previously described (Section 3.2.1).

All other materials were A.R. or Reagent grade and were used without further purification.

4.7.2 *Apparatus*

Description of the high pressure sampling vessel (Appendix I), spectrophotometers (Section 2.2.2) and pH Meter (Section 3.2.2), and method of temperature control (Section 2.2.2) have been previously given in the indicated sections.

4.7.3 *Procedure for Kinetic Runs*

Experimental procedures similar to that of Chan and Harris[15] were employed.

Temperature dependence on the anation rate

Weighed quantities of the aquohydroxo salt, sodium oxalate and sodium nitrate were dissolved in a known volume of Trizma buffer solution and brought to the reaction temperature. The ionic strength was maintained at a constant value partially by the Trizma base and by sodium nitrate. When thermal equilibrium was established aliquot samples were withdrawn, at regular time intervals, and passed down a column of cationic exchange resin. The effluent containing only the uncharged intermediate was acidified with nitric acid and made up to a known volume by washing of the column with distilled water. The resultant solutions were allowed to stand for two days before analysis for the final product ion, Co $en_2C_2O_4^+$, by absorbance measurements at 500 nm (ε_{500} = 113 M^{-1} cm^{-1}).

Pressure dependence on the anation rate

The reactant solution was prepared as above and placed in the Perspex reaction vessel. The Teflon plunger was placed in position, the apparatus lowered into the pressure vessel and the pressure raised to the desired value. After thermal equilibrium was attained (usually after thirty minutes) aliquot samples were removed at regular time intervals, passed down the cationic ion-exchange column and analysed as above.

Pressure dependence on the rate of disappearance of Co $en_2(OH)C_2O_4^0$

A solution of the intermediate at the desired pH and ionic

strength was prepared in situ and placed in the Perspex reaction vessel. The apparatus was appropriately loaded in the pressure vessel and the pressure raised to the desired value. As soon as thermal equilibrium was established (30 minutes) aliquot samples were withdrawn and passed through a column of cationic ion-exchange resin. The column was washed thoroughly with water and acidified with dilute acetic acid. Determination of the product $Co\ en_2C_2O_4^+$ was effected by elution with 1 M $NaNO_3$ and spectrophotometric analysis at 500 nm.

4.8 Results

4.8.1 Evaluation of Kinetic Data

Temperature and pressure dependence on the anation rate

The kinetic data was treated in an identical manner to that described in Section 4.4.1. The OD_t values were taken over two half-life times while the OD_∞ readings taken after six half-lives. Complications due to pH drift as found by Chan and Harris[15] were avoided by using Trizma base buffer.

Pressure dependence on the rate of ring closure of Co $en_2(OH)C_2O_4^0$

Conventional first-order plots (Section 4.4.1) were again linear. Since the concentration of oxalate was always in excess of the cobalt complex, pseudo first order kinetics was observed.

Reactions were followed over one half-time and final absorbance measurements taken after at least four half times.

4.8.2 The Effect of Temperature on the Rate of Formation of Co $en_2(OH)C_2O_4^0$

The rate of appearance of the uncharged oxalato intermediate was investigated as a function of oxalate concentration between 20°C and 35°C and an ionic strength of 0.32 M. The results at four different oxalate concentrations, listed in Table 4.3, were obtained by a computer program fitted with a least squares subroutine. A number of runs at each temperature and oxalate concentration revealed that the mean value for k_{obs} was reproducible to ± 2%.

Table 4.3

Variation of k_{obs} with temperature

$$Co\ en_2OH\ OH_2^{2+} + C_2O_4^{=} \rightarrow Co\ en_2OH\ C_2O_4^{0} + OH_2$$

μ = 0.37 M $[Co\ en_2(OH)(H_2O)]_0^{2+}$ = 0.004 M

Temp (°C)	[OX] (M)	$k_{obs} \cdot 10^4$ (sec^{-1})	nos. of runs
20	0.02	-	-
	0.03	0.55 ± 0.01	3
	0.04	0.69 ± 0.01	3
	0.06	0.97 ± 0.02	3
25	0.02	0.87 ± 0.02	3
	0.03	1.24 ± 0.02	4
	0.04	1.58 ± 0.03	4
	0.06	2.12 ± 0.04	3
30	0.02	1.17 ± 0.01	4
	0.03	1.66 ± 0.03	3
	0.04	2.17 ± 0.05	3
	0.06	3.05 ± 0.06	4
35	0.02	1.57 ± 0.02	4
	0.03	2.18 ± 0.04	3
	0.04	2.94 ± 0.04	3
	0.06	4.34 ± 0.08	4

In Figure 4.4, $1/k_{obs}$ has been plotted against 1/[OX] for each temperature. The straight lines drawn through these data are the lines of best fit calculated using the "least squares" method. The values of k_0 and $K_{I.P.}$ and their standard deviations, obtained from the slope and intercept, are listed in Table 4.4. In this the values of k_0(corr.) and $K_{I.P.}$(corr.) are derived by dividing k_0 and $K_{I.P.}$ by f, the fraction of the aquo cobalt III complex which is in the reactive form Co $en_2(OH)(H_2O)^{2+}$ at the specified pH.

Table 4.4

Variation of k_o and $K_{I.P.}$ with temperature

Temp (°C)	pH	f	$k_0.10^4$ (sec^{-1})	k_0(corr.)10^4 (sec^{-1})	$K_{I.P.}$ (M^{-1})	$K_{I.P.}$(corr.) (M^{-1})
20	7.4	0.82	3.97	$4.9 \pm 0.1_4$	5.3	6.5 ± 0.5
25	7.3	0.83	7.84	$9.4 \pm 0.1_8$	6.2	7.5 ± 0.4
30	7.2	0.85	15.0	$17.6 \pm 0.7_5$	4.2	4.9 ± 0.4
35	7.1	0.85	28.3	$33.2 \pm 2.0_5$	2.9	3.4 ± 0.8

The values for k_0(corr.) and $K_{I.P.}$(corr.) measured at 25°C are in good agreement with k_0(corr.) = 9.9×10^{-4} sec^{-1} and $K_{I.P.}$(corr.) = 5.8 M^{-1} reported previously[15]. The errors in both k_0(corr.) and $K_{I.P.}$(corr.) are relatively larger than those of the individual runs and are greater at the higher temperatures where $1/k_{obs}$ becomes quite small.

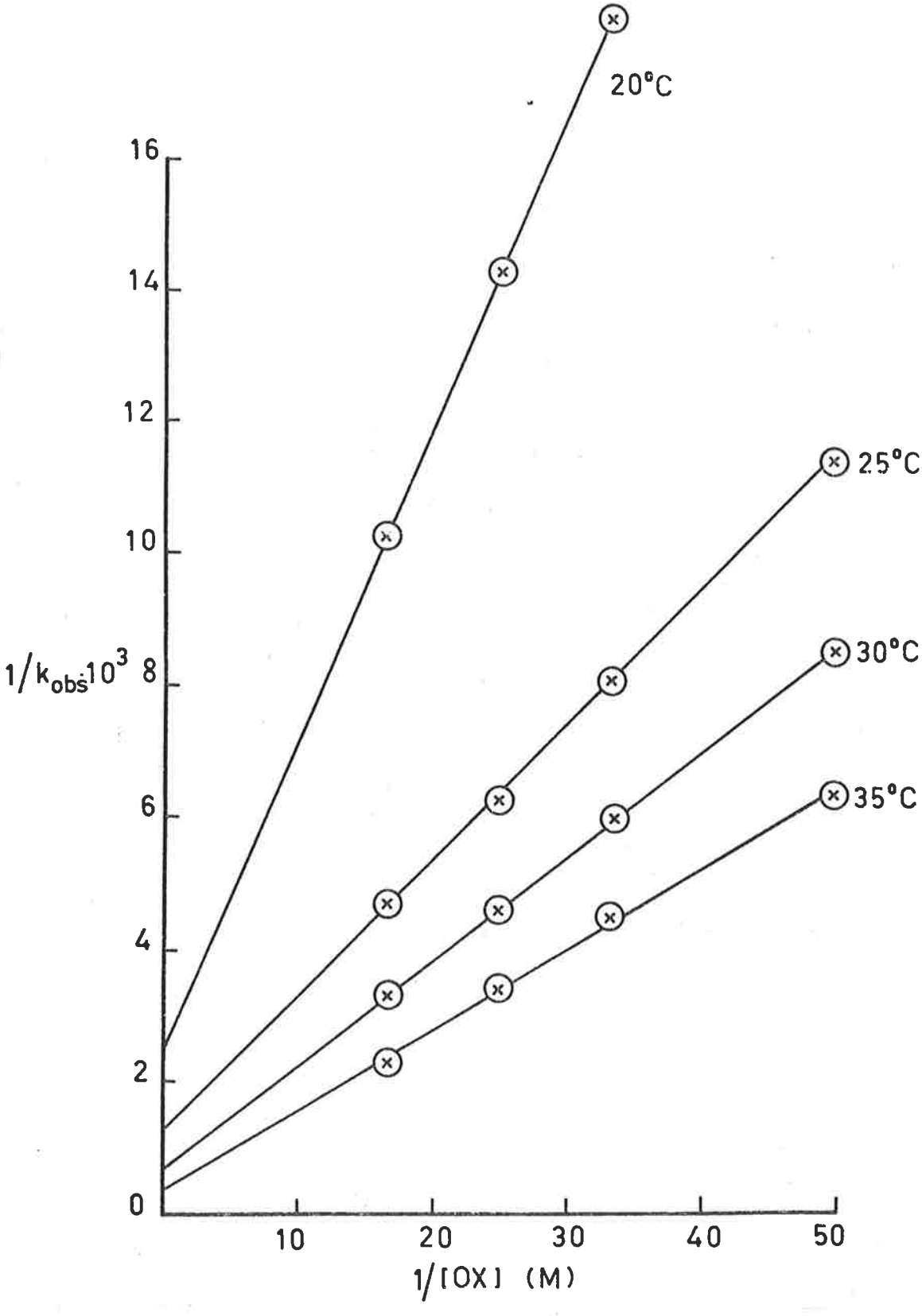

FIG. 4.4 Variation of k_{obs} with temperature.

Figures 4.5 and 4.6 are the Arrhenius plots of the data in columns 5 and 7 of Table 4.4 from which the enthalpy and entropy of activation, $\Delta H^{\ddagger}$ and $\Delta S^{\ddagger}$, were calculated to be,

$$\Delta H^{\ddagger}_{k_0(corr)} = 92.9 \pm 1.7 \text{ kJ mol}^{-1}$$

$$\Delta S^{\ddagger}_{k_0(corr)} = 9.6 \pm 4.2 \text{ J K}^{-1} \text{ mol}^{-1}$$

$$\Delta H_{I.P.\ (corr)} = -33.5 \pm 16.7 \text{ kJ mol}^{-1}$$

4.8.3 The Effect of Pressure on the Rate of Formation of Co $en_2(OH)C_2O_4^0$

The reaction was studied as a function of oxalate concentration between 0 and 2 kbar at an ionic strength of 0.32 M and temperature of 30°C. The results are given in Table 4.5, where each value represents the mean of two or three runs.

Table 4.5

Variation of k_{obs} with Pressure

Co $en_2OH\ OH_2^{2+}$ + $C_2O_4^{2-}$ → Co $en_2OH\ C_2O_4^0$ + OH_2

Temp = 30.0 ± 0.1°C ; μ = 0.32 M ; $[Co\ en_2(OH)H_2O]_0^{2+}$ = 0.004 M

Pressure (bar)	[OX] (M)	$k_{obs}.10^4$ (sec^{-1})
1	0.02	1.17 ± 0.03
	0.03	1.66 ± 0.04
	0.04	2.17 ± 0.04
	0.06	3.05 ± 0.06

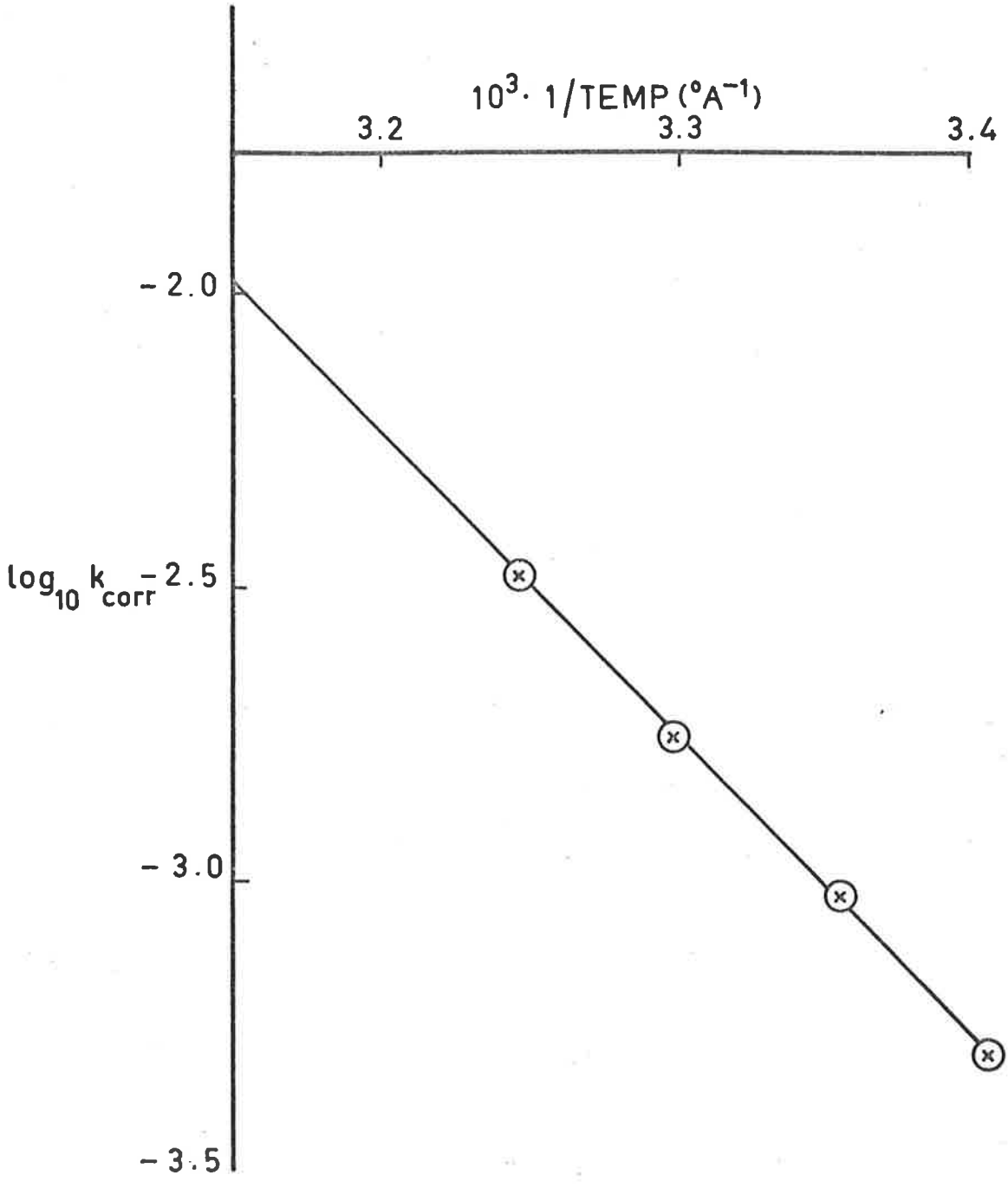

FIG. 4.5 The effect of temperature on k_{an}.

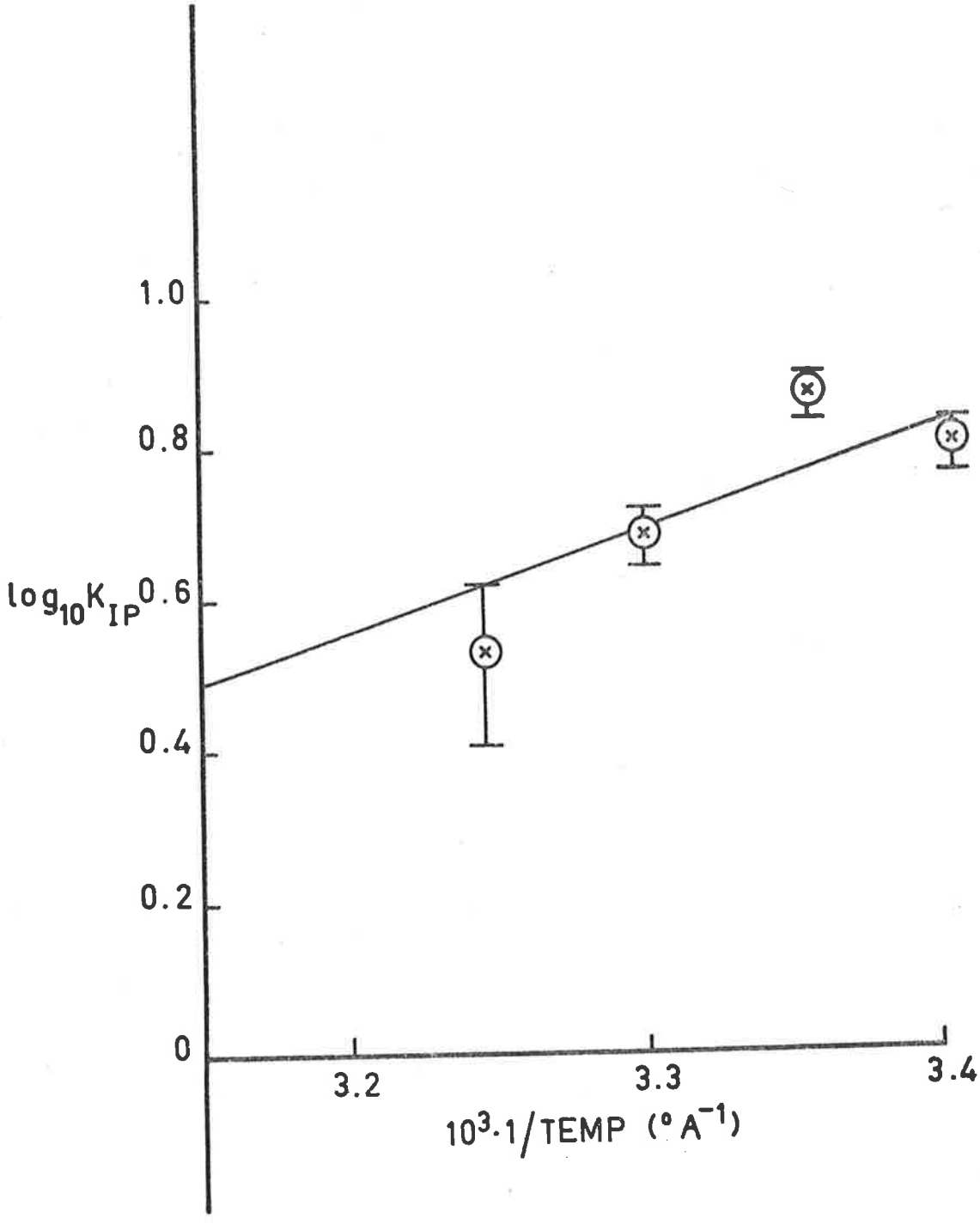

FIG. 4.6 Variation of $K_{I.P.}$ with temperature.

517	0.02	1.06 ± 0.02
	0.03	1.54 ± 0.02
	0.04	1.99 ± 0.04
	0.06	2.73 ± 0.05
1034	0.02	0.93 ± 0.03
	0.03	1.36 ± 0.02
	0.04	1.74 ± 0.04
	0.06	2.41 ± 0.04
1551	0.02	0.82 ± 0.02
	0.03	1.17 ± 0.03
	0.04	1.53 ± 0.03
	0.06	2.15 ± 0.04

The data in Table 4.5 were analysed using equation 4.11 (see Figure 4.7) to yield the values of k_0(corr) and $K_{I.P.}$(corr) presented in Table 4.6.

Table 4.6

Variation of k_o and $K_{I.P.}$ with Pressure

Temp. = 30.0°C

Press (bar)	pH	f	$k_0.10^4$ (sec^{-1})	k_0(corr).10^4 (sec^{-1})	$K_{I.P.}$ (M^{-1})	$K_{I.P.}$(corr) (M^{-1})
1	7.2	0.85	15.0	17.6 ± 0.8	4.2	4.9 ± 0.4
517	7.2	0.85	13.8	16.2 ± 0.6	4.1	4.8 ± 0.3
1034	7.1	0.85	12.4	14.6 ± 0.6	4.0	4.7 ± 0.3
1551	7.1	0.85	11.2	13.2 ± 0.5	3.9	4.6 ± 0.3

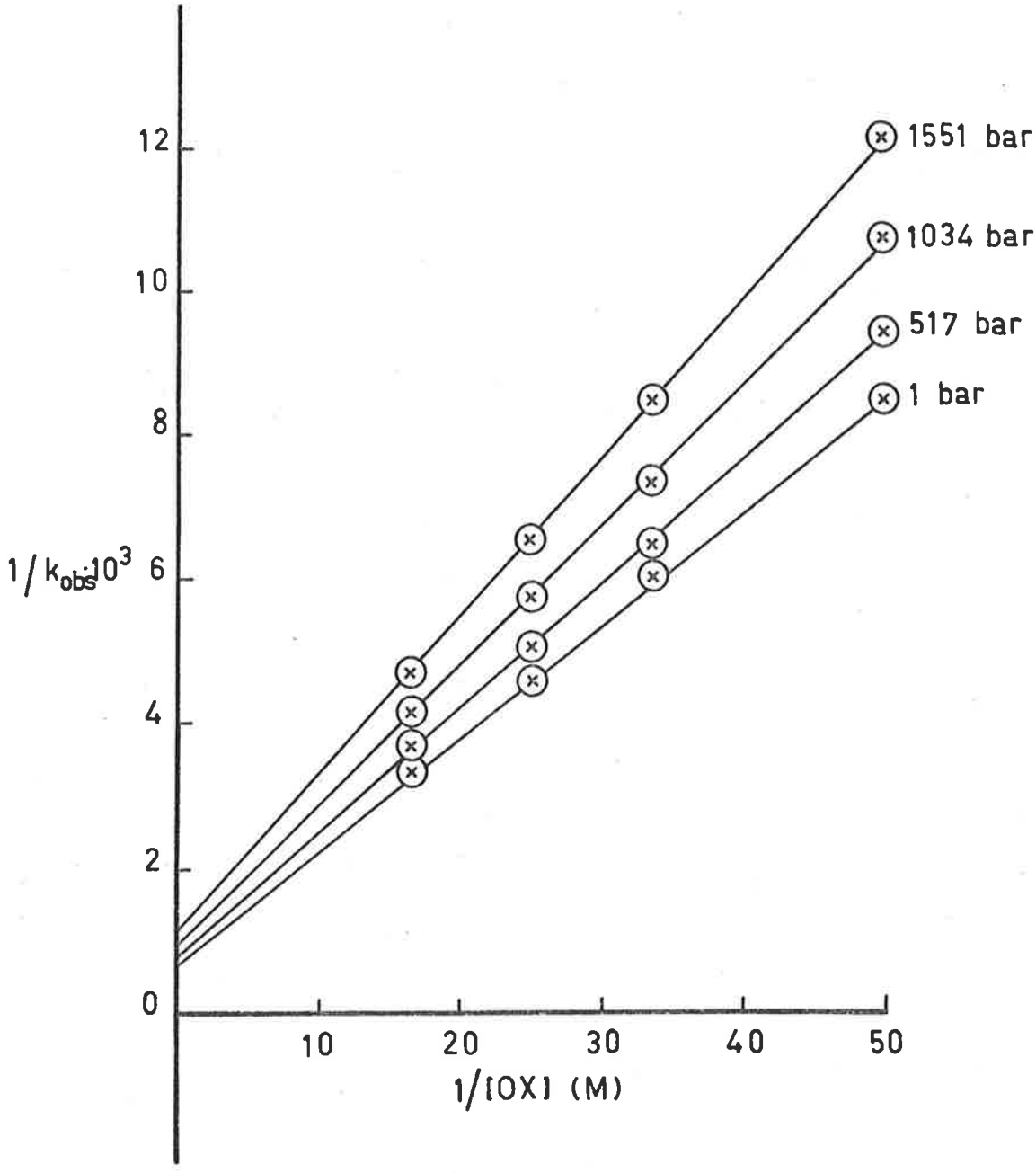

FIG. 4.7 Variation of k_{obs} with pressure.

In columns 3, 5 and 7 of Table 4.6 the results have been corrected for the pressure effects on the dissociation constant of Trizma base. Distèche[16] has measured the molal volume change, ΔV_a, for the reaction

$$TH^+ + H_2O \underset{\leftarrow}{\overset{K_a}{\rightarrow}} T + H_3O^+ \qquad 4.25$$

to be $-2.5\ cm^3\ mol^{-1}$. This value means the pH of a solution, "buffered" by Trizma base, falls by 0.023 pH unit for an increase of pressure of 517 bar.

The variation of k_0(corr) and $K_{I.P.}$(corr) are shown in Figures 4.8 and 4.9, where log k_0(corr) and log $K_{I.P.}$(corr) have been plotted against pressure. Because of the systematic uncertainties involved in estimating k_0(corr) and $K_{I.P.}$(corr) and their small dependence on pressure, a straight line of best fit has been drawn through the experimental data. The values of $\Delta V_0^{\ddagger}$ and $\Delta V_{I.P.}$ calculated from the slopes of these lines were found, by a least squares analysis, to be

$$\Delta V_0^{\ddagger} = +4.6 \pm 0.4\ cm^3\ mol^{-1}$$

$$\Delta V_{I.P.} \leqslant 1.0\ cm^3\ mol^{-1}.$$

4.8.4 The Effect of Pressure on the Rate of Ring Closure of $Co\ en_2(OH)C_2O_4^{\oplus}$

The pressure dependence on the rate of disappearance of the uncharged intermediate $Co\ en_2(OH)C_2O_4^{\oplus}$ was studied between 0 and 2 kbar using freshly prepared solutions of the monodentate oxalato intermediate

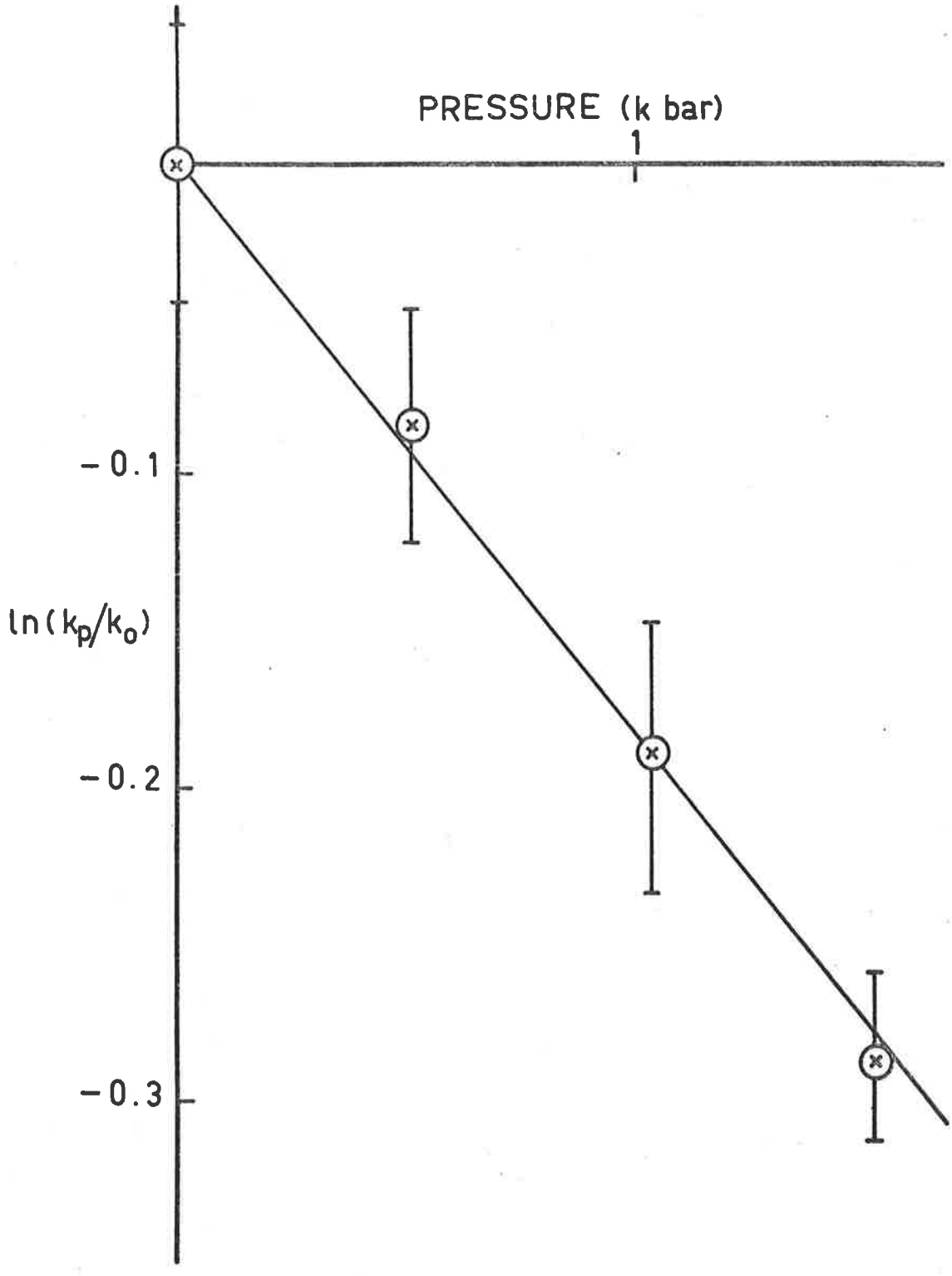

FIG. 4.8 Pressure dependence of the anation rate.

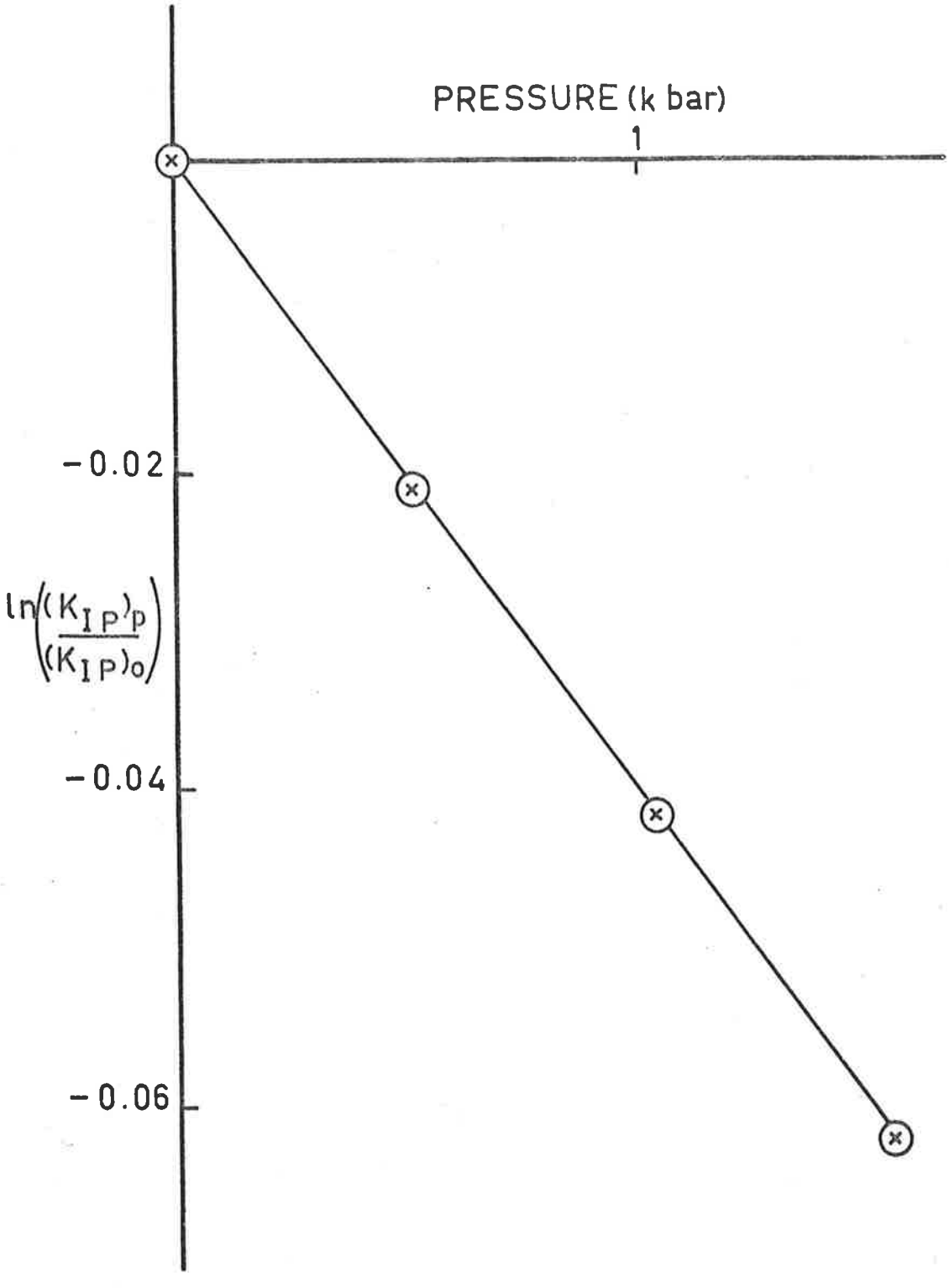

FIG. 4.9 The effect of pressure on the ion-pair equilibrium constant.

at an ionic strength of 0.37 M, pH 7.8 and temperature of 50°C. The variation of the observed rate coefficient with pressure is listed in Table 4.7.

The results show that within experimental uncertainty there is no detectable difference in rates between glass and perspex vessels. A number of runs at each pressure revealed that the mean value of the rate coefficient was reproducible to better than ± 4%. In columns 6 - 8 of Table 4.7 the data have been corrected for the pressure effects on the dissociation constant of Trizma base (Section 4.8.3). The rate coefficient $k_1(corr)$ was derived from k_{obs} on the assumption that all ring closure is according to reaction 4.24, whence

$$k_1(corr) = k_{obs}/f^1 \qquad 4.26$$

where f^1 is the fraction of the monodentate oxalato complex in the form of Co $en_2(OH_2)C_2O_4^+$.

The values of $k_1(corr)$ listed in Table 4.7 are, in fact, the effect of pressure on reactions 4.23 and 4.24 combined. Because of the assumptions used in the evaluation of these rate constants, the data are subject to an estimated uncertainty of 10%. Nevertheless a small decrease in rate coefficient with increasing pressure is observed.

The volume of activation, $\Delta V^{\ddagger}_{obs}$, was calculated from equation 1.10 by a least squares analysis. The resultant plot, shown in Figure 4.10, yields

$$\Delta V^{\ddagger}_{obs} = + 2.6 \pm 0.6 \text{ cm}^3 \text{ mol}^{-1}$$

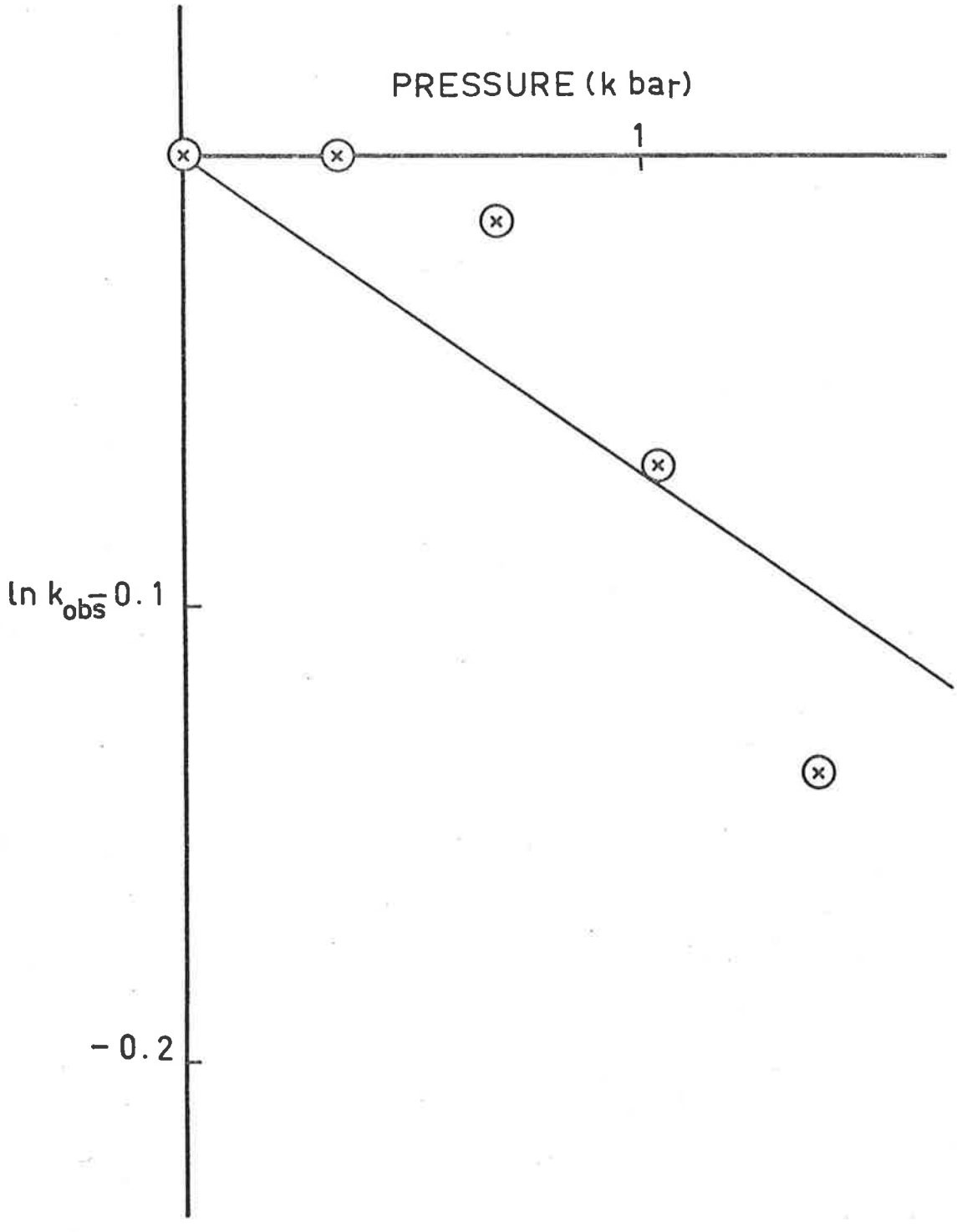

FIG. 4.10 Pressure dependence of the rate of ring closure of Co $en_2(OH)C_2O_4^0$.

Table 4.7

Variation of k_{obs} with Pressure

temp; 50.0 ± 0.1°C μ = 0.37 M

Pressure (bar)	Reaction Vessel	nos. of runs	$10^5 . k_{obs}$ (sec^{-1})	pH	$pH_{(corr)}$	f^1	$10^3 . k_1$(corr) (sec^{-1})
0	glass	4	$6.2_8 \pm 0.1_0$	7.8	7.8	0.048	1.3_0
0	perspex	6	$6.3_6 \pm 0.1_2$	7.8	7.8	0.048	1.3_3
345	perspex	6	$6.6_4 \pm 0.1_0$	7.8	7.78	0.050	1.3_3
689	perspex	6	$6.6_8 \pm 0.1_3$	7.8	7.77	0.051	1.3_1
1034	perspex	6	$6.5_6 \pm 0.0_8$	7.8	7.75	0.053	1.2_4
1379	perspex	6	$6.2_4 \pm 0.1_0$	7.8	7.74	0.054	1.1_6

4.9 Discussion

4.9.1 The Effect of Temperature and Pressure on Oxalate Anation In Basic Aqueous Solution.

By an analogous argument to that presented in Section 4.5.1, the measured volume of activation for reaction 4.21 $\Delta V^{\ddagger} = + 4.6 \pm 0.4$ $cm^3\ mol^{-1}$ is consistent with an interchange mechanism. Since $\Delta\beta^{\ddagger}$ is zero within experimental uncertainty, it appears that there is no additional positive contribution to $\Delta V^{\ddagger}$ from the partial desolvation of $C_2O_4^{-}$ on formation of the activated complex. Hence, the small positive $\Delta V^{\ddagger}$ value observed may then be ascribed as arising entirely from the stretching of the aquo-cobalt bond in the transition state.

$[en_2Co(OH)OH_2^{2+}].C_2O_4^{2-} \longrightarrow$

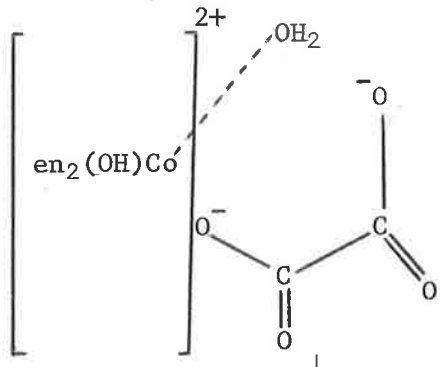

The measured values for the Arrhenius parameters, $\Delta H^{\ddagger} = 92.9 \pm 1.7$ kJ mol^{-1} and $\Delta S^{\ddagger} = 9.6 \pm 4.2$ J K^{-1} mol^{-1}, are compatible with the above interpretation. The enthalpy of activation observed is of similar magnitude to $\Delta H^{\ddagger}$ in the range 100 - 120 kJ mol^{-1} found for the substitution[1] of other diamagnetic cobalt III complexes proceeding by the dissociative release of an aquo ligand. The lower value reflects the labilizing influence of the hydroxo ligand. The small and positive value for $\Delta S^{\ddagger}$ found implies that the solvation of the +2 and -2 ions in

the ion-pair is not greatly different from that in the transition state, as previously argued from the $\Delta\beta^{\ddagger}$ value. There is again good correlation between $\Delta S^{\ddagger}$ and $\Delta V_0^{\ddagger}$.

An interesting finding is that the value of $\Delta V_0^{\ddagger}$ for oxalate anation in basic medium is of similar magnitude to $\Delta V_0^{\ddagger} = + 4.8 \pm 0.7$ $cm^3\ mol^{-1}$ found for substitution at low pH. This suggests that the formation of Co $en_2C_2O_4^+$ in the latter case may proceed via the complex ion Co $en_2(OH_2)C_2O_4^+$ which, once formed, rapidly ring closes.

Finally the errors in $K_{I.P.}$ mean that it is not yet possible to state whether there is any statistically significant change in the ion-association constant with pressure. Nevertheless an upper limit of $\Delta V_{I.P.} \leqslant 1\ cm^3\ mol^{-1}$ is suggested by the present data. An estimate for $\Delta V_{I.P.}$ at low ionic strength may be obtained from the Hemmes expression (equation 4.16). Putting $/Z_+Z_-/=4$ and $a = 7\mathring{A}$, and using the values[12] $(\partial \ln\varepsilon/\partial P) = 47.58 \times 10^{-6}\ bar^{-1}$, $\varepsilon = 76.58$ and $\kappa_s = 44.75 \times 10^{-6}\ bar^{-1}$, all at 30°C, equation 4.16 yields $\Delta V_{I.P.} = + 3.8\ cm^3\ mol^{-1}$.

3.9.2 The Effect of Pressure on the Rate of Ring Closure of Co $en_2(OH)C_2O_4^0$

It has been mentioned in Section 4.8.4 that ring closure of the uncharged intermediate Co $en_2(OH)C_2O_4^0$ is according to reactions 4.23 and 4.24. Hence,

$$\Delta V^{\ddagger}_{obs} = \Delta V^{\ddagger} - \Delta V_a \qquad 4.27$$

The molal volume change for the acid hydrolysis of the complex ion $Co(NH_3)_5OH_2^{3+}$ has measured value -2.6 ± 0.6 cm^3 mol^{-1} (see Chapter 5). If ΔV_a for reaction 4.23 is assigned the same value, then it follows from equation 4.27 that $\Delta V^{\ddagger} = (+ 2.6 \pm 0.6) + (-2.6 \pm 0.6) = 0.0 \pm 1.2$ cm^3 mol^{-1}. Although the estimated value of $\Delta V^{\ddagger}$ together with its large uncertainty does not permit an unambiguous designation of the mechanism for the ring-closure of Co $en_2(OH_2)C_2O_4^{+}$, an associative intramolecular concerted process is suggested as one possibility.

4.9.3 Conclusion

The rate of substitution of Co $en_2(OH)OH_2^{2+}$ by $C_2O_4^{2-}$ was investigated over a temperature range from 20°C to 35°C at 1 bar and ionic strength 0.32 M, and a pressure range from 1 to 1551 bar at 30°C and the same ionic strength. The activation parameters were found to be $\Delta H^{\ddagger} = 92.9 \pm 1.7$ kJ mol^{-1}, $\Delta S^{\ddagger} = + 9.6 \pm 4.2$ J K^{-1} mol^{-1}, $\Delta V^{\ddagger} = + 4.6 \pm 0.4$ cm^3 mol^{-1} and $\Delta\beta^{\ddagger} \leqslant 0.4$ cm^3 mol^{-1}, and $\Delta H_{I.P.} = - 33.5 \pm 16.7$ kJ mol^{-1} and $\Delta V_{I.P.} \leqslant 1.0$ cm^3 mol^{-1},

The rate of disappearance of Co $en_2(OH)C_2O_4^{0}$ involving the ring closing reaction Co $en_2(OH_2)C_2O_4^{+} \rightarrow$ Co $en_2C_2O_4^{+} + OH_2$ was studied at 50°C and pressures between 1 and 1379 bar. The volume of activation for ring closing in the aquo-oxalato complex was determined to be 0.0 ± 1.2 cm^3 mol^{-1}.

Both the rate of formation of Co $en_2(OH)C_2O_4^{0}$ and its rate of ring closure are discussed in terms of a dissociative interchange mechanism.

References to Chapter 4

1. F. Basolo and R.G. Pearson, *"Mechanism of Inorganic Reactions," John Wiley and Sons, Inc., New York, N.Y.*, 1967.
2. R.S. Murray, *PH.D. Thesis, University of Adelaide*, 1967.
3. S.F. Lincoln and D.R. Stranks, *Aust. J. Chem.*, 1968, 21, 1745.
4. A.D. Fowless, *Ph.D. Thesis, University of Adelaide*, 1973.
5. S.F. Lincoln, *private communication.*
6. P.M. Brown and G.M. Harris, *Inorg. Chem.*, 1968, 7, 1872.
7. W. Kruse and H. Taube, *J. Amer Chem. Soc.*, 1961, 83, 1280.
8. F.P. Dwyer, A.M. Sargeson and I.K. Reid, *J. Amer. Chem. Soc.*, 1963, 85, 1215.
9. J. Bjerrum and S.E. Rasmussen, *Acta. Chem. Scand.*, 1952, 6, 1265.
10. R.M. Fuoss, *J. Amer. Chem. Soc.*, 1958, 80, 5059.
11. P. Hemmes, *J. Phys. Chem.*, 1972, 76, 895.
12. B.B. Owen, R.C. Miller, C.E. Milner and H.L. Cogan, *J. Phys. Chem.*, 1961, 65, 2065.
13. T.G. Spiro, A. Revesz and J. Lee, *J. Amer. Chem. Soc.*, 1968, 90, 4000.
14. C. Schenk and H. Kelm, *J. Coord. Chem.*, 1972, 2, 71.
15. S.C. Chan and G.M. Harris, *Inorg. Chem.*, 1971, 10, 1317.
16. A. Disteche, *"The Effect of Pressure on Organisms", Symposia of the Society for Experimental Biology*, Nos. XXVI, *Cambridge University Press*, 1972, pg. 50.

Chapter 5: The Effect of Pressure on the Hydrolysis Equilibria of Aqueous Metal Ions.

5.1 Introduction

The effect of pressure on the dissociation of weak acids (equations 5.1 and 5.2) and electrically neutral bases (equation 5.3) has been the subject of many investigations.[1]

$$HA \rightleftarrows A^- + H^+ \qquad 5.1$$

$$HA^- \rightleftarrows A^{2-} + H^+ \qquad 5.2$$

$$B + H_2O \rightleftarrows HB^+ + OH^- \qquad 5.3$$

However data relating to the effect of pressure on acid hydrolysis constants K of aqueous metal ions (equation 5.4) has received little attention.

$$ML_5H_2O^{n+} \underset{\rightleftarrows}{\overset{K}{}} ML_5OH^{(n-1)+} + H^+ \qquad 5.4$$

In addition to their intrinsic interest, a detailed knowledge of the pressure dependence of equilibrium 5.4 is important in evaluating volumes of activation for substitution and redox reactions of metal ions in which hydrolytic pre-equilibria are involved. For example, the measurement of the activation volume for the ring closure of Co $en_2(OH)C_2O_4^0$ discussed in the previous chapter includes an unknown contribution from the acid-base pre-equilibrium of Co $en_2(H_2O)C_2O_4^+$. Similarly volumes of activation for the electron exchange reaction[2] between Fe^{3+}_{aq} and Fe^{2+}_{aq} must be corrected for the contribution by the parallel $FeOH^{2+}$ and Fe^{2+}_{aq} exchange path.

This chapter is aimed to help offset the dearth in information for metal ion hydrolysis. The effect of pressure on equilibrium 5.4 (where M = Fe^{3+}, Tl^{3+}, or Co^{3+}, and L = $(H_2O)_5$ or $(NH_3)_5$) have been investigated and the results collectively discussed in terms of current ion-dielectric theory.

A: A High Pressure Study on the First Hydrolysis Constant of Iron III.

5.2 Introduction

The initial stages of the hydrolysis of aquated ferric ion[3] may be described by the equilibria:

$$Fe(H_2O)_6^{3+} \underset{\leftarrow}{\overset{K_1}{\rightarrow}} Fe(H_2O)_5OH^{2+} + H^+_{aq} \qquad 5.5$$

$$Fe(H_2O)_5OH^{2+} \underset{\leftarrow}{\overset{K_2}{\rightarrow}} Fe(H_2O)_4(OH)_2^{+} + H^+_{aq} \qquad 5.6$$

$$2Fe(H_2O)_6^{3+} \underset{\leftarrow}{\overset{K_p}{\rightarrow}} Fe(H_2O)_4(OH)_2Fe(H_2O)_4^{4+} + 2H^+_{aq} \qquad 5.7$$

For solutions 10^{-4} M in iron (III) and acid concentrations between 10^{-2} and 10^{-3} M reaction 5.5 is alone important. At greater ferric and lower acid concentrations further hydrolysis and polymerisation reactions become significant.

The first hydrolysis constant, K_1, has been evaluated by electrometric,[4-10] spectrometric,[11-21] conductivity,[22-23] and magnetic susceptibility[24] measurements with values ranging from 3.5 to 50 x 10^{-3} M at 25°C and zero ionic strength; a similar lack of agreement is reported at other reaction conditions.

In the present studies K_1 has been redetermined under atmospheric pressure, using the method of Milburn and Vosburgh,[17] and a pressure dependence study conducted up to 2 kbar.

5.3 *Experimental*

5.3.1 *Materials*

Ferric Perchlorate, $Fe(ClO_4)_3 . 9H_2O$

A ferric perchlorate stock solution was prepared from Purum grade Fluka $Fe(ClO_4)_3 . 9H_2O$. The solution was acidified with perchloric acid to prevent hydrolysis.

Ferric ammonium sulphate solution

Stock solutions of A.R. ferric ammonium sulphate (1 ml. ≡ 0.1 mg. of Fe) were prepared by direct weighting of B.D.H. Analar ferric ammonium sulphate and dissolving in 0.1 M hydrochloric acid.

All other materials were A.R. or Reagent grade and were used without further purification.

5.3.2 *Apparatus*

Pressure Vessel

The optical reactor used in these studies is described in Appendix I.

Spectrophotometers

For complete spectra in the U.V. and visible regions, the Unicam S.P. 800 recording spectrophotometer (± 0.01 absorbance units) was used.

Accurate absorbance measurements at single wavelengths were made using a manually-operated Shimadzu spectrophotometer, Model QR - 50. Measurements on duplicate samples were reproducible to

± 0.001 optical absorbance units.

5.3.3 Procedure for Equilibrium Measurements at Atmospheric Pressure.

A stock ferric solution was prepared containing 51.6 mg of iron III perchlorate in a litre of 0.001 M perchloric acid. The fraction of iron III in the stock solution was determined by the O-phenanthroline method.[25] Calibration curves were prepared using A.R. ferric ammonium sulphate and analysed at 510 nm on a Shimadzu manual spectrophotometer, Model QR-50. Over the concentration range 3.6×10^{-5} M to 1.8×10^{-4} M for the standard salt, a Beer's Law plot was linear with an extinction coefficient of $1.1_5 \times 10^{-4}$ M^{-1} cm^{-1}.

To 10 ml aliquot samples of the stock solution were added solutions of perchloric acid (5 ml) and sodium perchlorate (5 ml) such that the overall acid concentration was varied between 1.00 and 20.0×10^{-3} M and the ionic strength maintained constant at 0.09 M. The solutions were allowed to attain thermal equilibrium and their optical absorbance measured at 340 nm and 25°C using the Shimadzu QR - 50 spectrophotometer. Although the absorbances of these solutions remained constant over a day, there were marked changes in daily measurements taken over a week. These variations were as high as 50% at the low acidities (below 8.00×10^{-3} M). As a result all solutions were discarded after a day. New measurements on freshly prepared solutions provided good agreement in equilibrium measurements.

Temperature control (± 0.1°C) of the optical cell was achieved by the rapid circulation of constant temperature water through the water channels surrounding the cell compartment. The reservoir of water was contained in a thermostatted bath and maintained at the desired temperature by a solid state proportional control heater.

5.3.4 Determination of K at High Pressures

The operation of the optical vessel in combination with a Unicam SP 800 recording spectrophotometer and SP 850 Scale Expansion Accessory for equilibrium measurements at high pressures has been previously described in Section 3.2.4.

For the present studies the scale was expanded by factors of 5 or 10 depending on the change in absorbance. Under these conditions, for optical absorbances of 0.06 to 0.012 the uncertainty was typically ± 0.0005. Good agreement in absorbance measurements was obtained when increasing or decreasing the pressure over the same pressure interval.

5.4 Results

5.4.1 Compression Studies

The optical absorbance of solutions under high pressure studies may change as a result of a chemical reaction, variations in the physical characteristics associated with the pressure vessel, changes in the band width, ε_{max}, or peak height, λ_{max}, of the absorption peak or from concentration effects. As a preliminary to the high pressure studies these contributions were investigated by consideration of the area under the absorption peaks of solutions of alkaline potassium chromate, λ_{max} 373 nm, $Co(NH_3)_6^{3+}$, λ_{max} 473 nm, and $Co(en)_3^{3+}$ which exhibits two absorption maxima at 333 nm and 465 nm respectively. These species were chosen as inert ions with simple absorption bands in both the ultra-violet and visible spectral region. The area under the absorption curve was taken to be proportional to the product of the peak height and the band width at half peak height, $\Delta\omega_{1/2}$. In each peak, an increase in area of 6% was observed for an increase of pressure of 1340 bar. From the known[26] compressibility of water at 45°C, namely 8.0×10^{-4} $cm^3\ mol^{-1}\ bar^{-1}$, it can be calculated that this 6% change is almost entirely due (90-95%) to compression of the solutions. Thus the effect of any distortion of the sapphire windows and any change in effective path length of the cell under high pressure is not greater than 0.3% in optical absorbance at least from 333 nm to 473 nm. This effect may then be neglected in the 0 - 2 kbar range for spectrophotometric measurements. Furthermore, this 6% change in observed

absorbance area is not influenced by a change in the frequency envelope of the absorption curve of the reference ions. From 0 - 1340 bar the half width, $\Delta\omega_{1/2}$, of the absorption peaks remained constant within the precision of the measurements.

5.4.2 Absorption Spectra of Fe^{3+}_{aq} and $Fe(OH)^{2+}$

The absorption spectrum of the hexaaquo ferric ion, Fe^{3+}_{aq}, has two absorption bonds, one with a maximum at 240 nm and another which extends into the region below 200 nm. The first hydrolysis product, $FeOH^{2+}$, also has two absorption bands, the maxima of which occur at 300 nm and 204 nm. The absorption spectra of both species are shown in Figure 5.1 and are in good agreement to those reported earlier.[20]

5.4.3 Evaluation of the Equilibrium Data

In 10^{-4} M ferric perchlorate solution and pH below 3, the only significant hydrolysis reaction is

$$Fe^{3+}_{aq} + H_2O \underset{\leftarrow}{\xrightarrow{K_1}} FeOH^{2+} + H^+_{aq} \qquad 5.8$$

For equilibrium 5.4 it follows that

$$1/O.D. = 1/C_{Fe}\varepsilon + [H^+]/C_{Fe}\, K_1\, \varepsilon \qquad 5.9$$

where O.D. denotes the optical absorbance for a 1 cm light path, C_{Fe} the total iron concentration, ε the molar extinction coefficient of $FeOH^{2+}$, $[H^+]$ the hydrogen ion concentration and the assumption is made that $\varepsilon_{Fe^{3+}_{aq}} << \varepsilon_{FeOH^{2+}}$. If equation 5.9 accurately describes the system, this is good evidence for no further hydrolysis or polymerisation. Plots of 1/O.D. versus $[H^+]$ were linear under all experimental conditions used in the evaluation of K_1.

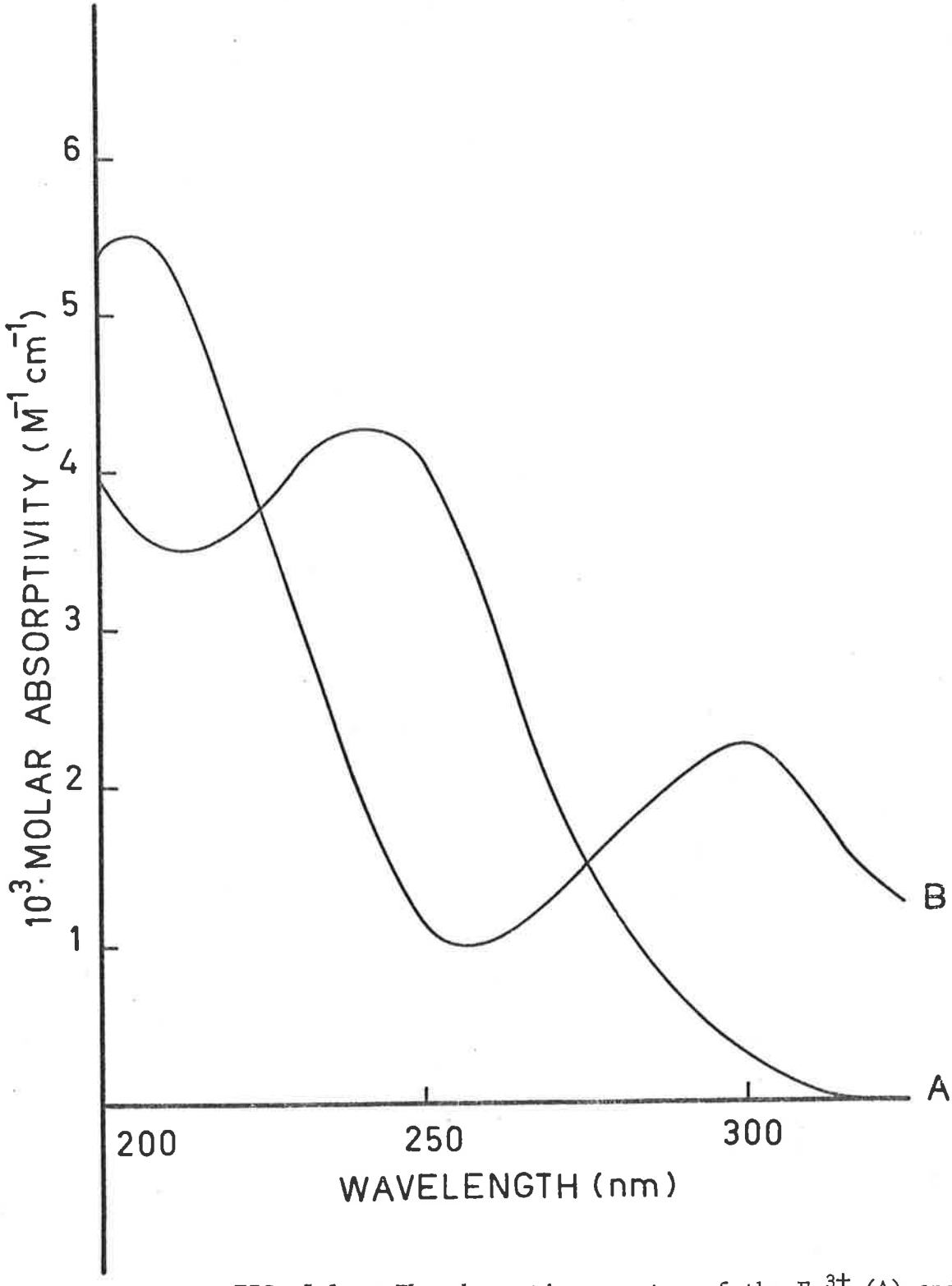

FIG. 5.1 The absorption spectra of the Fe^{3+}_{aq} (A) and $Fe\,OH^{2+}$ (B) ions.

5.4.4 Accuracy of Results

The accuracy of the results is somewhat limited by the small absorbance changes observed for the equilibrium measurements. Even for solutions of relatively large optical absorbance, the total change was never greater than 0.007 absorbance units. Furthermore, measurements were taken over a time range of 60 to 80 minutes, during which time slight drifts in the reading instrument were bound to occur. Nevertheless, it was possible to achieve good reproducibility of the absorbance measurements for each particular sample solution at pressures between 1 to 1723 bar both for increasing and decreasing cycles of pressure change.

5.4.5 Determination of the First Hydrolysis constant of iron III, K_1, and the molar extinction coefficient of $FeOH^{2+}$, ε, at atmospheric pressure.

Both K_1 and ε have been redetermined at 340 nm, 25°C and total ionic strength 0.09 M. For each series of measurements nine pairs of corresponding 1/O.D. and $[H^+]$ were fitted to equation 5.9 by a least squares computer program from which K_1 and ε were evaluated as $2.89 \pm 0.10 \times 10^{-3}$ and 980 ± 60 respectively. A typical series of data pair is given in Table 5.1 and its plot shown in Figure 5.2.

Table 5.1

Series pairs for determination of K_1 *and* $\varepsilon_{FeOH^{2+}}$

Temp. 25.0 ± 0.1°C ; μ = 0.09 M

$[H^+].10^3$	1/O.D.
1.25	15.3
2.23	18.9
4.00	24.4
6.25	33.0
8.20	40.0
10.25	48.8
12.18	53.2
15.25	63.3
20.15	80.0

These results are in good accord with those of Milburn and Vosburgh[17] (K_1 = 3.18 x 10^{-3} and $\varepsilon_{FeOH^{2+}}$ = 925) and Bray and Hershley[4] (K_1 = 2.46 x 10^{-3}) found previously at the same ionic strength.

5.4.6 The Effect of Pressure on K_1 *and* ε

The pressure dependence of K_1 was studied, under the same reaction conditions, up to 2 kbar. For solutions of acid concentrations between 10^{-2} and 10^{-3} M, where the individual optical density values are relatively large, small but definite increases in absorbance of, for example, 10 ± 1% at 1723 bar were observed. At acid concentrations greater than 10^{-2} M the absorbance values of the solutions were much

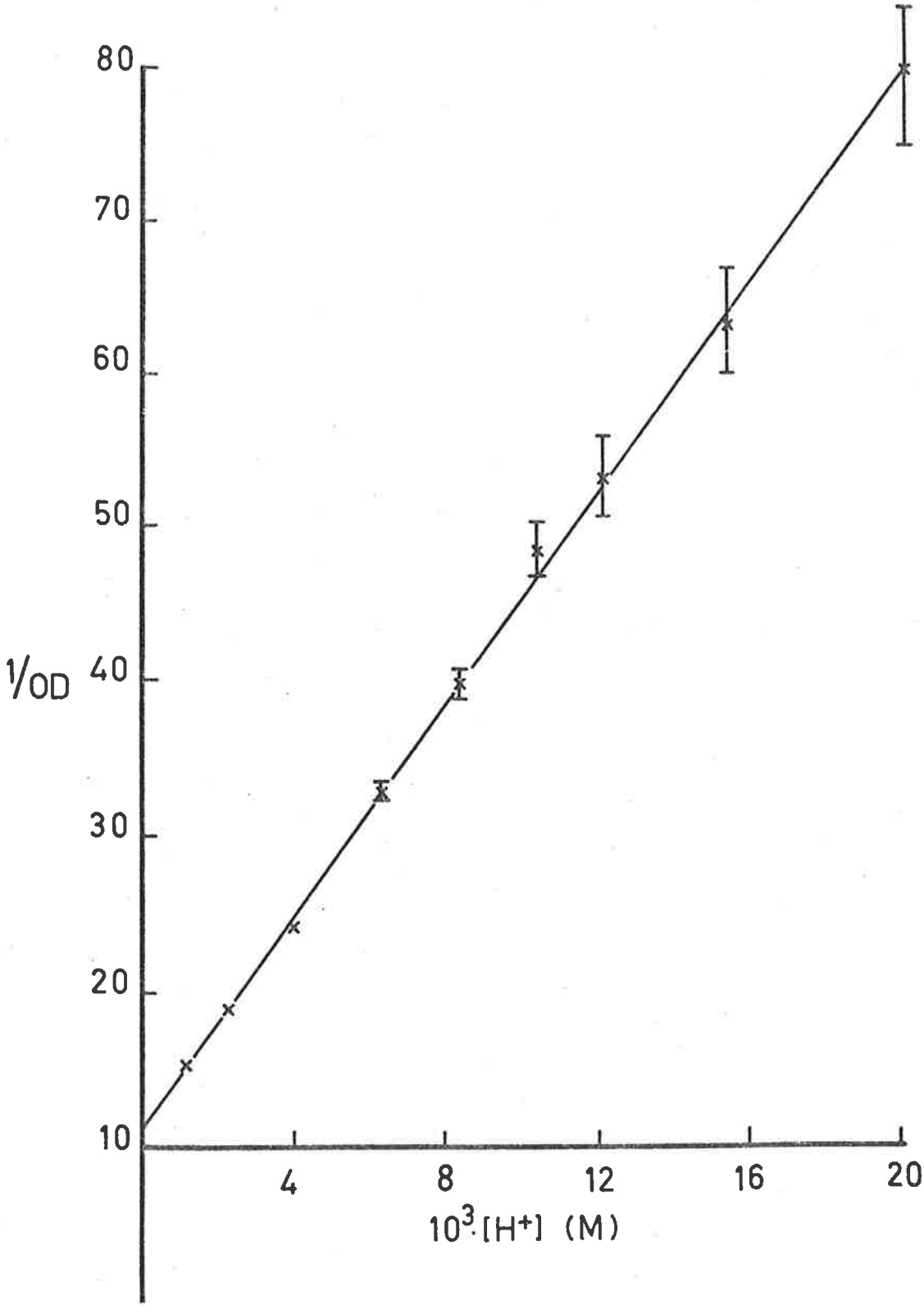

FIG. 5.2 Typical series of data for the determination of the first hydrolysis constant of Fe^{3+}_{aq}.

smaller (below 0.02) and apparent changes with pressure were not greater than the inherent instrument "noise". To overcome this difficulty a set of pressure runs was performed on freshly prepared solutions five times more concentrated in iron (III). For these more concentrated solutions equation 5.9 was also shown to apply. For example, an increase of 11 ± 1% in optical absorbance at 1723 bar was observed and this is consistent with that observed, at the lower ferric concentrations.

During the pressure runs adiabatic heating of the solution by compression could constitute a significant source of error. However any significant temperature drift would have been manifested by drifting optical absorbance readings. Furthermore, good agreements between absorbance measurements made with ascending and descending pressures was observed and this would not have resulted had re-equilibrium of the solutions and cell temperature not occurred during the course of the measurements.

The variations of K_1 and ε with pressure, together with their uncertainties, are listed in Table 5.2

Table 5.2

Effect of Pressure of K_1 and ε

Temp. 25.0 ± 0.1°C; μ = 0.09 M

Pressure (bar)	$K.10^3$ (M)	ε	nos. of individual measurements
1	2.89 ± 0.10	980 ± 60	6
1034	3.00 ± 0.07	1020 ± 50	6
1723	3.16 ± 0.10	1010 ± 60	6

In most cases, the standard deviation in the mean value of the individual measurements is close to ± 3%. In Figure 5.3, log K_p/K is plotted against pressure and represented by a straight line of best fit as calculated by the least squares procedure.' The presssure variation of a molar equilibrium constant, evaluated from solutions whose molar concentrations are expressed at a given pressure, is given by the relation:

$$RT\partial \ln K_c/\partial P = -\Delta V + RT\kappa_s \qquad 5.10$$

where ΔV is the excess of the partial molal volume of the products over the reactants and $RT\kappa_s$ corrects for the compressibility of the solvent. However the equilibrium measurements were conducted with solutions of constant molar composition expressed at 1 bar pressure and the term $RT\kappa_s$ cancels. The slope of the line (Figure 5.3) therefore evaluates directly the partial molal volume change for the acid hydrolysis and ΔV_a was evaluated as -1.2 cm^3 mol^{-1}. Although the computational analysis of the results suggest a standard deviation of ± 0.2 cm^3 mol^{-1}, a more realistic estimate of the uncertainty (based on 95% confidence levels) would be ± 0.5 cm^3 mol^{-1}.

Finally there appears to be no significant change (within experimental uncertainty) in ε with pressure as shown in column 3 of Table 5.2.

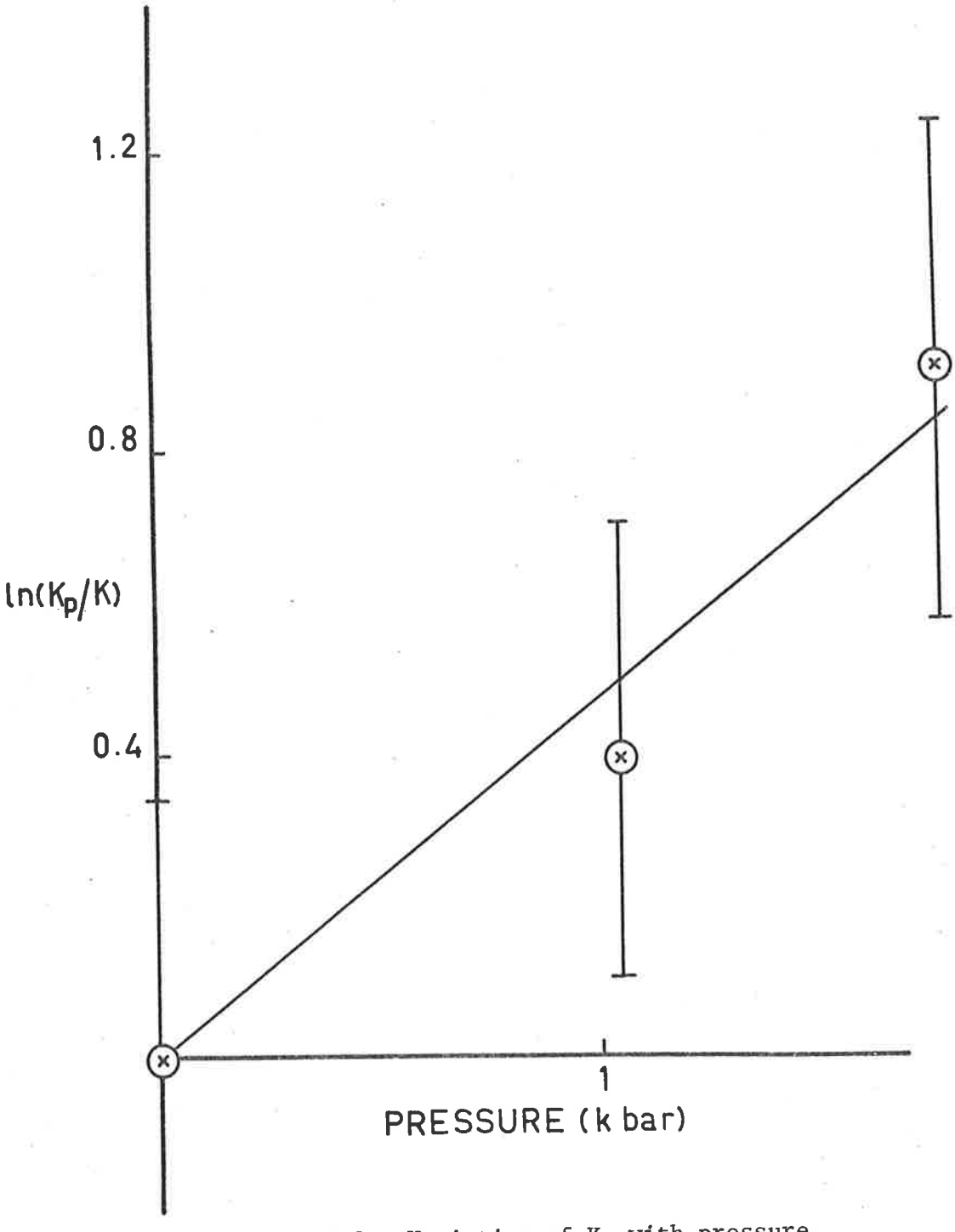

FIG. 5.3 Variation of K_a with pressure.

B: The Effect of Pressure on the First Hydrolysis Constant of Thallium III

5.5 Introduction

The first acid dissociation of the thallic aquo ion (5.11)

$$Tl^{3+}_{aq} \underset{\leftarrow}{\overset{K_1}{\rightarrow}} TlOH^{2+} + H^{+}_{aq} \qquad 5.11$$

has been previously investigated by potentiometric[27-28] and spectrophotometric[29-30] methods and the reported values for K_1 are listed in Table 5.3.

Table 5.3

Hydrolysis constants of Tl III in aqueous solution at 25.0°C

method	ionic strength (M)	K_1	ref.
potentiometric	3	0.072	27
potentiometric	3	0.066	28
spectrophotometric	3	0.069	29
	1.5	0.086	29
spectrophotometric	0.1	0.069	30

Where comparable, there is good agreement for K_1 with the two analytical methods. Furthermore, at acid concentrations greater than 5×10^{-2} M, equilibrium 5.11 is not complicated from higher stages of hydrolysis. This system provides, therefore, a further useful example to study the effect of pressure on the hydrolysis

equilibria of aqueous metal ions.

The present study was carried out at 25°C in solutions of total ionic strength 1.5 M using the spectrophotometric method of Rogers and Waind[29].

5.6 Experimental

5.6.1 Materials

Thallium Perchlorate

Thallium III perchlorate stock solutions 0.02 M were prepared by dissolution of B.D.H.(L.R. Grade) thallium III oxide in hot concentrated perchloric acid. The solution was heated using an infra-red lamp to avoid decomposition of perchlorate to chloride. Complete dissolution took 2-4 days.

The stock solutions were stored in dark bottles as suggested by Biedermann[31] to prevent reduction of thallium III by sunlight.

All other chemicals used have been previously described or were of analytical reagent quality.

5.6.2 Apparatus

Pressure Vessel

These studies were conducted in the optical pressure vessel, described in Appendix I.

Phase Separator

For the present studies it was desirable to work in the U.V. spectral region at wavelengths below 300 nm. In this region Ondina 17 oil absorbs strongly and cannot, therefore, serve as the pressure medium in the optical reactor. Instead n-hexane was used, with a phase separator between the pressure vessel and pump. This functioned to separate the two pressure media.

A detailed description of the phase separator is given in Appendix I.

All other equipment used ~~have~~ has been previously described.

5.6.3 Analysis of Stock Solutions

Thallium III analysis

The stock thallic perchlorate solutions were analysed by a gravimetric method[32] involving precipitation of the *tris*-(8-quinolinol) thallium III complex. Best results were obtained from solutions containing 0.1 mg. ml^{-1} thallium, (0.01 M Tl^{3+} ≡ 2.04 mg. ml^{-1}) using a small excess of 5% 8-quinolinol in ethanol. Duplicate assays were reproducible to within 0.5%.

Acid concentrations

The perchloric acid concentration of a stock thallic perchlorate solution was determined by a difference method. An aliquot sample of the stock solution was passed down an ion exchange column (Dowex 50 W - X2 resin in the H^+ form, 200-400 mesh). The acid concentration of the effluent and pure-water washings was determined by titration of an aliquot sample against red mercuric ~~II~~ oxide dissolved in potassium iodide solution to a methyl red end-point. The perchloric acid concentration in the stock solution was evaluated by subtracting the known number of equivalents of thallic perchlorate from the equivalents of hydrogen ion determined in this way.

5.6.4 Procedure for Equilibrium Measurements at Atmospheric and Higher Pressures.

To 10 ml aliquot samples of a stock solution containing 38.8 mg of thallic perchlorate in a litre of 0.096 M perchloric acid were added solutions of perchloric acid (5 ml) and sodium perchlorate (5 ml) such that the overall acid concentration was varied between 0.60 and 1.4 M and the ionic strength maintained constant at 1.5 M. The optical absorbances of these solutions were measured at 250 nm and 25°C using a Shimadzu QR-50 spectrophotometer. Daily measurements over a week provided good agreement in absorbance readings for the individual solutions.

The procedure for equilibrium measurements at higher pressures using the optical vessel have been previously described (Section 3.2.4). Apparent absorbance changes were recorded using a scale expansion factor of 2. For optical absorbances of 0.120 and 0.055 the uncertainty was ± 0.001.

5.7 *Results*

5.7.1 *Evaluation of the Equilibrium Data*

In acidic media from 0.06 M to 1.4 M, equilibrium 5.11 is not complicated from higher stages of hydrolysis. The concentrations of thallium III were always small compared with that of the formal acid; the contribution of hydrolysis to the acid concentration may then be neglected.

The absorption spectrum of the species $TlOH^{2+}$ exhibits a strong charge transfer band in the region below 280 nm. In contrast, the aquated thallic ion, Tl^{3+}_{aq}, absorbs strongly only below 240 nm. Furthermore, Rogers[29] has shown that at wavelengths longer than 240 nm the presence of small amounts of thallous (Tl^{+}) ion, a contaminant in stock thallic solutions, can be ignored. All measurements described below were therefore made at 250 nm. Then it follows that

$$1/OD = 1/C_{Tl}\varepsilon + [H^{+}]/C_{Tl}\,\varepsilon\,K_1 \qquad 5.12$$

where C_{Tl} represents the total thallium concentration, ε the molar extinction coefficient of $TlOH^{2+}$ and the assumption is made that $\varepsilon_{Tl^{3+}_{aq}} << \varepsilon_{TlOH^{2+}}$. All the other terms are previously defined in Section 5.4.3. The unknown quantities K_1 and ε were evaluated from the slope and intercept of straight line plots of 1/OD against $[H^{+}]$.

5.7.2 *Determination of K_1 and ε at atmospheric pressure.*

The quantities K_1 and ε were redetermined at 25°C and total ionic strength 1.5 M. Seven pairs of corresponding 1/OD and $[H^{+}]$

were fitted to equation 5.12 for each series of measurements. A least squares analysis yielded K_1 = 8.2 ± 0.4 x 10^{-2} and ε = 510 ± 20. Figure 5.4 is the plot of a typical data sample given in Table 5.4

Table 5.4

Series pairs for determination of K_1 and $\varepsilon_{TlOH^{2+}}$

Temp. 25.0 ± 0.1°C; μ = 1.5 M

$[H^+]$	1/OD
0.600	8.13
0.694	9.17
0.788	10.41
0.956	12.20
0.995	12.66
1.193	14.93
1.381	16.95

These results are in good agreement with those of Rogers and Waind,[29] K_1 = 8.6 x 10^{-2} and ε = 520, 1.5 M $NaClO_4$, 25°C, and Burns and Whitaker,[33] ε = 513, 3.0 M $NaClO_4$, 22°C.

5.7.3 Effect of Pressure on K_1 and ε

With aqueous solvent, of absolute optical absorbance 0.000, in the sample cuvette, an increase in optical absorbance of 0.1 ± 0.01 absorbance units at 1723 bar and 250 nm was observed.

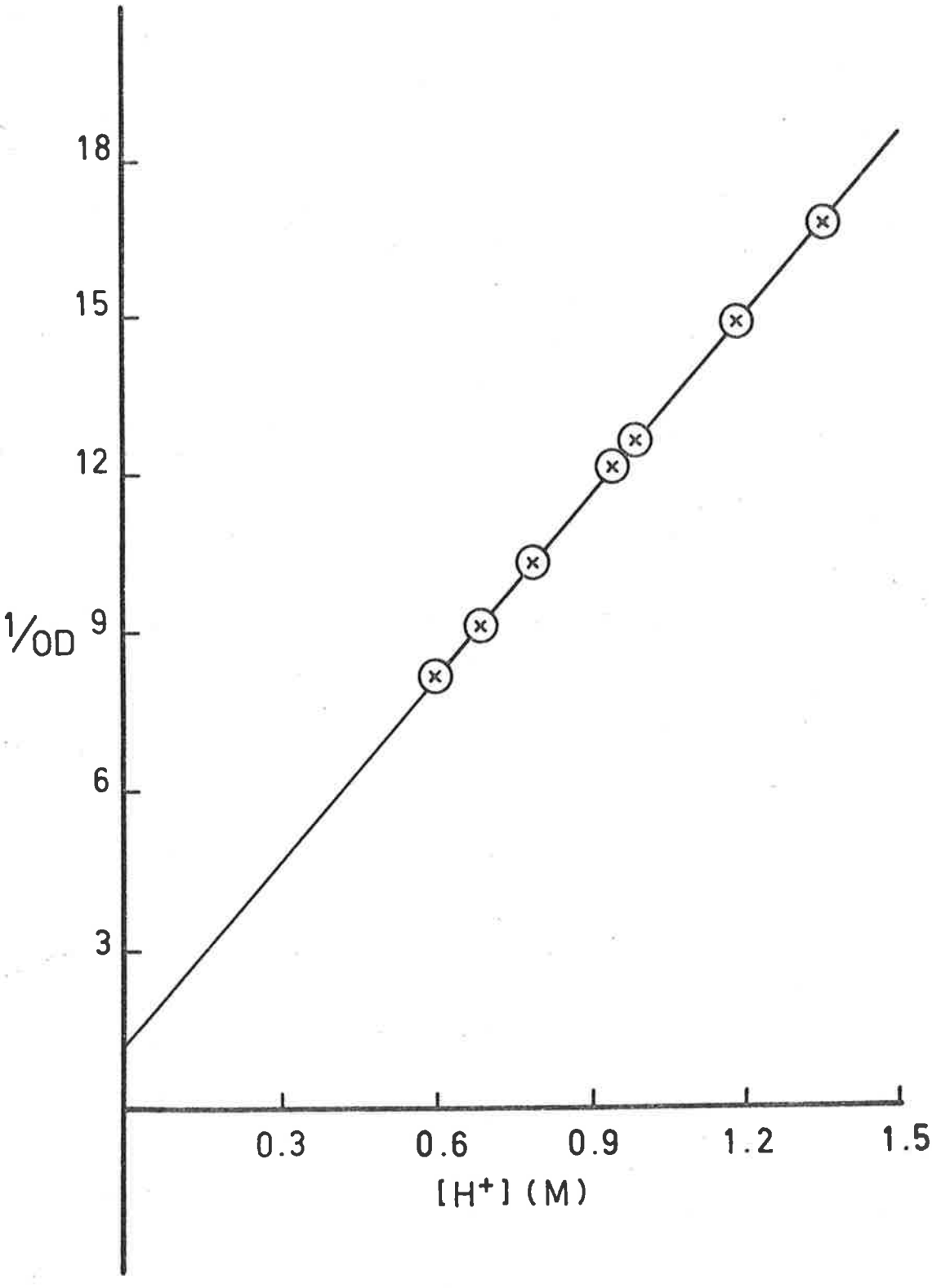

FIG. 5.4 Typical data series for the determination of the first hydrolysis constant of Tl^{3+}_{aq}.

This background effect is considered to arise from light scattering as a result of concave deformation of the sapphire windows in addition to compression effect on the solution (see section 5.4.1); the former effect being significant only in the ultra-violet spectral region below 290 nm. For this reason, the effect of pressure on equilibrium 5.11 was determined at 25°C, 250 nm and ionic strength 1.5 M by a difference method. To the apparent absorbance increase measured for each individual sample solution at a particular pressure was subtracted the absorbance increase of aqueous solvent at the same pressure. Since this method is subject to larger uncertainties and the apparent absorbance increase measured in this way was very slight in all cases, K_1 and ε were determined only at 1723 bar. The data are summerised in Table 5.5. The standard deviation of the mean value for K_1 at 1723 bar is close to ± 11%.

Table 5.5

Effect of pressure on K_1 and ε

Temp. 25.0 ± 0.1°C; μ = 1.5 M

Pressure (bar)	$10^2.K$ (M)	ε	nos. of individual measurements
1	8.2 ± 0.4	510 ± 20	4
1723	10.3 ± 0.6	520 ± 20	4

Assuming a linear dependence of log K_p upon pressure for the data in Table 5.5, the partial molal volume change together with the standard deviation, was calculated to be -3.2 ± 0.9 $cm^3\ mol^{-1}$.

Finally, for a pressure increase of 1723 bar there is no significant change in ε as shown in column 3 of Table 5.5.

C: *The Effect of Pressure on the Hydrolysis Constant of aquopentaamminecobalt III.*

5.8 *Introduction*

The hydrolysis of the mixed aquo-metal complex ion $Co(NH_3)_5OH_2^{3+}$ may be described by the equilibrium

$$Co(NH_3)_5OH_2^{3+} \underset{}{\overset{K_a}{\rightleftharpoons}} Co(NH_3)_5OH^{2+} + H^+_{aq} \qquad 5.13$$

Potentiometric[34] and spectrophotometric[34,35] techniques have been used to determine K_a; the range in reported values[35] are K_a = 2.0×10^{-6} at zero ionic strength and 25°C; $K_a = 2.8 \times 10^{-7}$ 1 M ($NaNO_3$), 25°C; $K_a = 2.6 \times 10^{-7}$, 2 M (NH_4NO_3), 30°C; $K_a = 3.9 \times 10^{-7}$, 1 M (NH_4NO_3), 30°C; $K_a = 5.6 \times 10^{-7}$, 0.5 M (NH_4NO_3), 30°C; and $K_a = 6.9 \times 10^{-7}$, 0.25 M (NH_4NO_3), 30°C. No evidence has been found for polynuclear species in solution.

The partial molal volume change for equilibrium 5.13 may be estimated from the dilatometric measurement[36], at low ionic strength, of $\Delta V = 20.6$ cm^3 mol^{-1} for the reaction

$$Co(NH_3)\ OH_2^{3+} + OH^- \rightarrow Co(NH_3)_5OH^{2+} + H_2O \qquad 5.14$$

combined with the known[37] molal volume for the autoprotolysis of water ($\Delta V = -21.3$ cm^3 mol^{-1}) under comparable conditions and yields $\Delta V_a = -0.7$ cm^3 mol^{-1}.

In the present studies K_1 has been redetermined at 25°C and total ionic strength 1.0 M and a pressure dependence study conducted up to 2 kbar.

5.9 Experimental

5.9.1 Materials

$[Co(NH_3)_5CO_3]ClO_4$ was prepared by the method of Basolo and Murmann[38].

$[Co(NH_3)_5H_2O](ClO_4)_3$

Carbonatopentaamminecobalt III perchlorate (10 g) was suspended in water (25 ml) and perchloric acid (5 M, 20 ml) was added slowly with stirring. When the evolution of carbon dioxide had subsided, methanol (100 ml) was added, and the aquopentaamminecobalt III perchlorate that formed was collected at the pump and washed with ethanol and ether. Recrystallisation was achieved by dissolving the crude product in a minimum amount of water, at room temperature, and making the solution 2 M in $HClO_4$. The resultant solution was heated to 90°C on a water bath and allowed to cool slowly overnight. The overall yield was 60%.

Standard Sodium Hydroxide solution

1 litre of standard 0.1 M sodium hydroxide solution was prepared from the phial of "Volucon" pre-standardised sodium hydroxide concentrate, supplied by May and Baker Ltd.

All other materials used have been described previously.

5.9.2 Apparatus

Pressure Vessel

The optical reactor used in this study is described in Appendix I.

5.9.3 Spectrophotometric Measurements

Absorbance data were obtained at 20.0 ± 0.1°C using a Shimadzu spectrophotometer equipped with a thermostatted cell compartment. The solutions were matched against blanks containing 1.0 M $NaClO_4$ in deionised distilled water, and 1 cm quartz cells were used throughout. The absorbance values were varied as a function of pH by mixing a solution of $[Co(NH_3)_5OH_2](ClO_4)$ with standard $HClO_4$ or NaOH and adjusting $[ClO_4^-]$ to 1.0 M. Molar absorptivities of $[Co(NH_3)_5OH_2](ClO_4)_3$ and $[Co(NH_3)_5OH](ClO_4)_2$ were obtained from measurements on solutions at pH 3 and pH 11 respectively. Experiments at pH 12.5 revealed that the absorbance, particularly in the ultra-violet region, increased appreciably in the time needed for the measurements probably because of base hydrolysis of the complex. No such drift was observed at pH 11.

5.9.4 pK_a Determination

Solutions of the aquo complex (0.01 M in complex with ionic strength made up to unity with sodium perchlorate) were titrated against 0.01 M sodium hydroxide at 20°C using an Automatic Titrator, Type TTT1 in combination with a Scale Expander Model PH A 630 T. The pK_a values were calculated via standard methods.

5.9.5 Procedure for Equilibrium Measurements at High Pressures.

Solutions of 0.01 M $Co(NH_3)_5OH_2^{3+}$ were made up with sodium hydroxide to give one half neutralisation and the ionic strength adjusted to unity with sodium perchlorate. The pH was measured after the solution was made up to its total volume. The sample solution

was transferred to the pressure cell and treated in an identical manner to that described in Section 3.2.4. Apparent absorbance changes were measured at 370 nm and 500 nm, and 20°C using a scale expansion factor of 10. Solutions were left at a particular pressure for at least five minutes (to allow re-equilibrium of the solution) before absorbance readings were taken. The uncertainty in the absorbance measurements was ± 0.001 absorbance units.

5.10 Results

5.10.1 Acidity Constant and Solution Spectra

The potentiometrically determined pK_a value at ionic strength 1.0 M ($NaClO_4$) and 20°C is 6.35. No pK_a value has been reported at these conditions for comparison. However this value is in reasonable agreement with pK_a = 6.55, 1 M $NaNO_3$, 25°C[35] and pK_a = 6.40, 1 M NH_4NO_3, 30°C[39] determined at similar conditions.

The visible spectra of $[Co(NH_3)_5OH_2](ClO_4)_3$ and $[Co(NH_3)_5OH](ClO_4)_2$ are shown in Figure 5.5. The aquo species was found to exhibit two absorption maxima at 491 nm and 345 nm. In basic solution at pH 11, the hydroxy species also has two absorption bands, the maxima of which occur at 504 nm and 370 nm. The molar absorptivities of the two species are listed in Table 5.6 for the different wavelengths studied and are the average of five independent measurements. A comparison with data obtained by other workers using the same cation (though not necessarily the same anion) is also given in Table 5.6. The agreement is generally good.

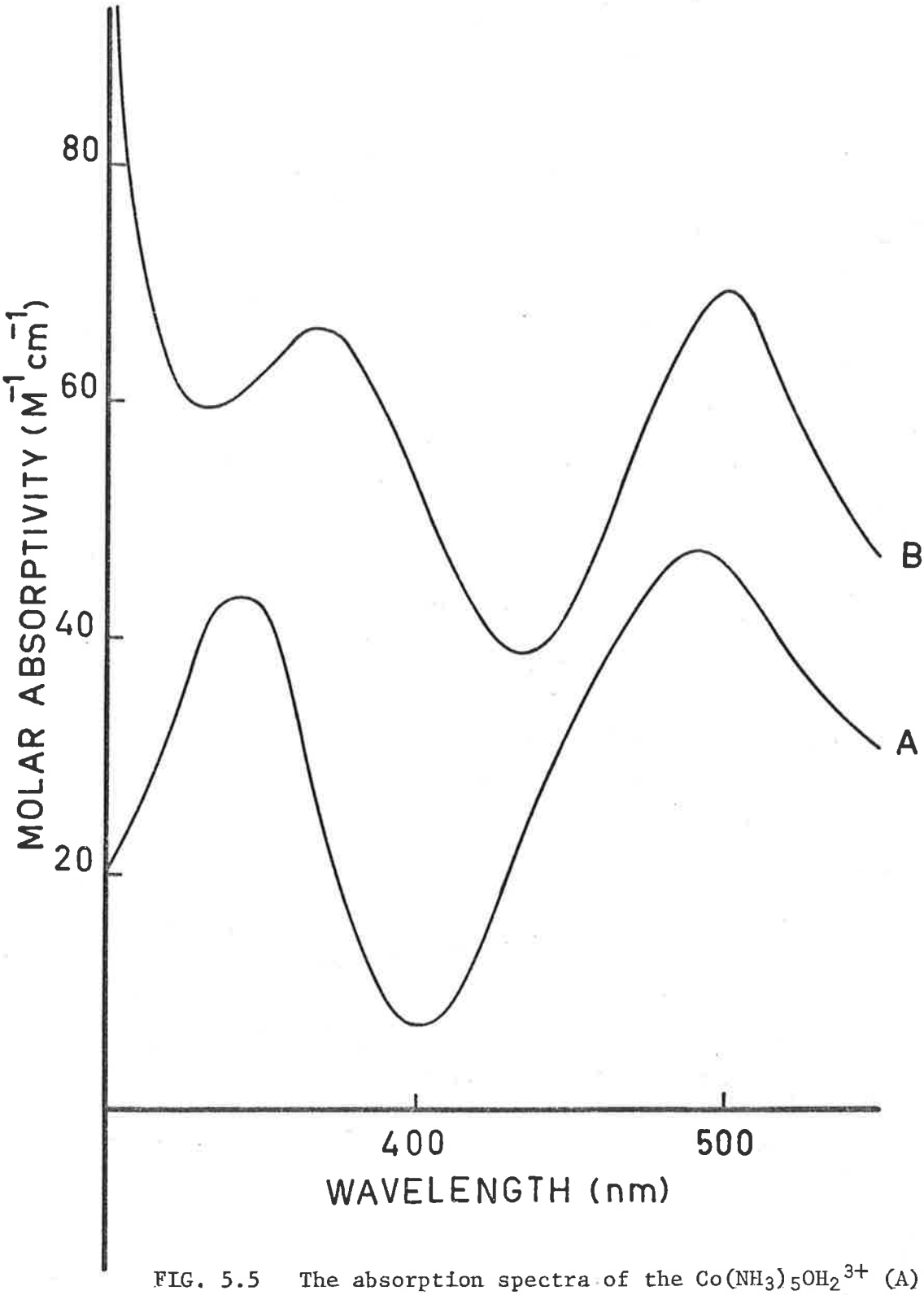

FIG. 5.5 The absorption spectra of the $Co(NH_3)_5OH_2^{3+}$ (A) and $Co(NH_3)_5OH^{2+}$ (B) ions.

Table 5.6

Molar Absorptivities (cm^{-1} M^{-1}) at selected wavelengths

λ (nm)	$Co(NH_3)_5OH_2^{3+}$	$Co(NH_3)_5OH.^{2+}$
550	20.3,[34] 21.0,[40] 20.6[a]	
500	46.5,[34] 47.0,[40] 46.9[a]	67.0,[34] 66.8,[40] 67.1[a]
504[b]		67.2,[34] 67.4[a]
491[b]	47.3,[34] 47.5,[41] 48.2[a]	
370[b]	28.4[a]	63.4,[34] 63.8[a]
345[b]	44.3,[34] 44.8,[41] 44.8[a]	

[a] This work

[b] Band maxima

5.10.2 Evaluation of equilibrium data

For equilibrium 5.13, the optical absorbance, OD, for a 1 cm light path expressed in terms of the molar absorptivity of the aquo acid ε_{H_2O}, and its conjugate base ε_{OH}, and the total cobalt ammine concentration C_T, is given by the relationship:

$$OD = \varepsilon_{OH} C_{OH} + \varepsilon_{H_2O} (C_T - C_{OH})$$

where C_{OH} represents the concentration of the hydroxy species. Therefore, the effect of pressure on K_a may be evaluated by measuring, at any wavelength, the change in optical absorbance of the cobalt ammine solution at half neutralisation as a function of pressure. The assumptions are made that ε_{H_2O} and ε_{OH} do not vary significantly with

pressure and the change in acid concentration equals the change in concentration of the hydroxy species at any pressure.

5.10.3 The Effect of Pressure on K_a

The pressure dependence of K_a was studied at 370 nm and 500 nm, 20°C and total ionic strength of 1.0 M. The results at two different wavelengths are summarised in Table 5.7; the K_a values are the average of four determinations, the standard deviation in K_a being about 6% in all cases. Good agreement in optical absorbance were obtained both within an individual measurement when ascending and

Table 5.7

Effect of pressure on K_a

Temp. 20.0 ± 0.1°C; μ= 1.0 M

	370 nm	500 nm
Pressure (bar)	10^7. K (M)	10^7. K (M)
1	4.47 ± 0.10	4.47 ± 0.10
689	4.81 ± 0.14	4.75 ± 0.14
1724	5.10 ± 0.10	5.35 ± 0.10

descending the pressure and between different determinations.

The partial molal volume change, ΔV, at both wavelengths was calculated using equation 5.10. The data are shown in

figure 5.6 and a least squares analysis yielded $\Delta V_a = -2.2 \pm 0.6$ cm^3 mol^{-1} and $\Delta V_a = -2.3 \pm 0.6$ cm^3 mol^{-1} at 370 nm and 500 nm respectively.

FIG. 5.6 Variation of K_a with Pressure.

The solid line represents the data at 500 nm.

The dotted line represents the data at 370 nm.

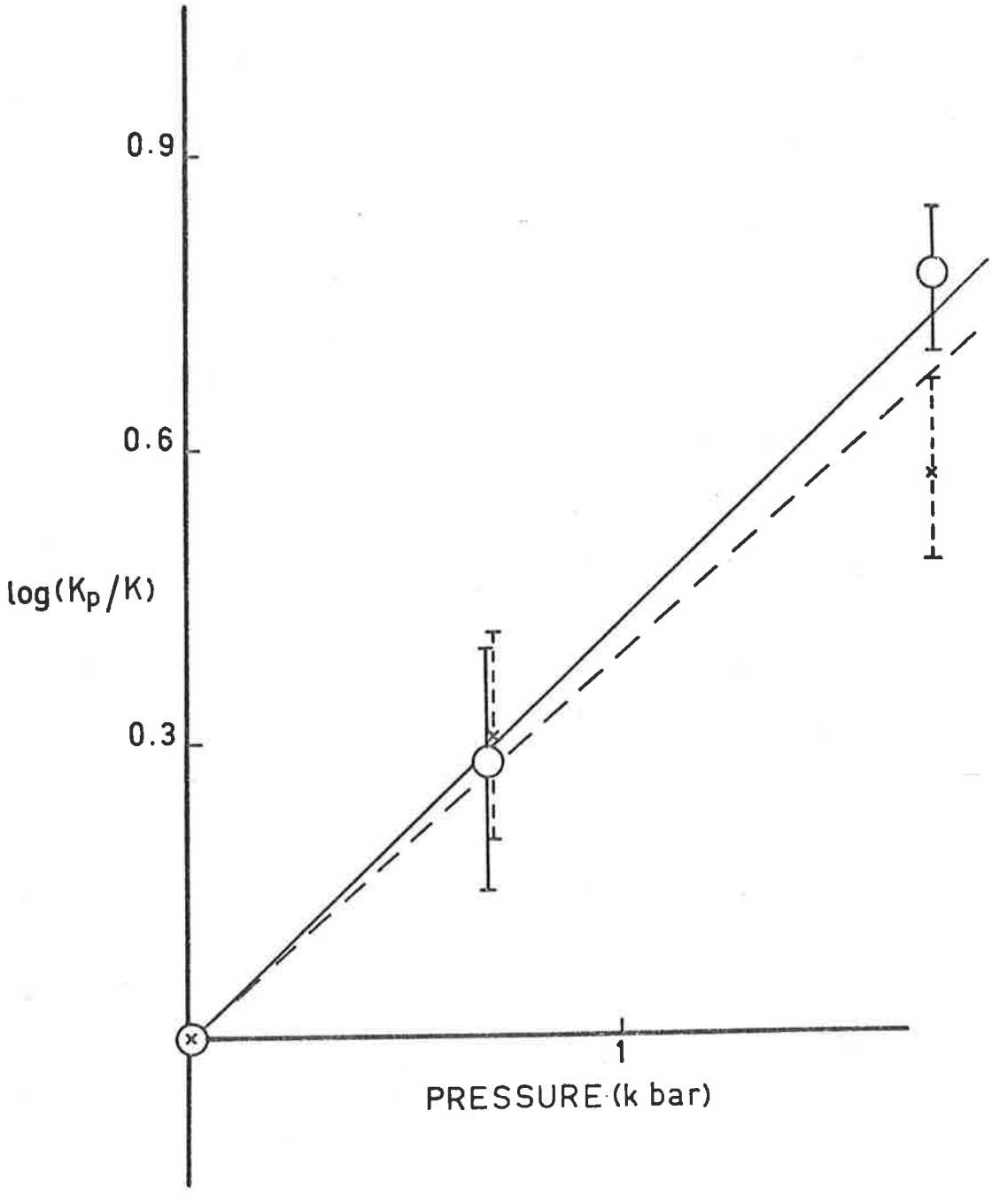
0.9
0.6
0.3
log(Kp/K)
1
PRESSURE (k bar)

5.11 *Discussion*

5.11.1 *The Effect of Pressure on Metal-Ion Hydrolysis*

The partial molal volume change for metal ion hydrolysis

$$M^{3+}_{aq} + H_2O \overset{K_a}{\rightleftharpoons} MOH^{2+} + H^+ \qquad 5.15$$

may be expressed as

$$\Delta V_a = \bar{V}_{H^+} + \bar{V}_{MOH^{2+}} - \bar{V}_{M^{3+}_{aq}} \qquad 5.16$$

in which, by convention, $\bar{V}_{H^+} = 0$. The MOH^{2+} and M^{3+}_{aq} cations are best described as six-coordinate metal III cations with the respective formulations $M(OH_2)_5OH^{2+}$ and $M(OH_2)_6{}^{3+}$. The radii of both these aquated species should approximate to the same value, this value being the sum of the M^{3+} ionic radius and the crystallographic diameter of a coordinate water molecule. Similarly, when M^{3+}_{aq} and MOH^{2+} represents the cations $M(NH_3)_5OH_2{}^{3+}$ and $M(NH_3)_5OH^{2+}$, the radii of these two species should again approximate to the same value. The expected value of ΔV_a will then be determined primarily by the difference in electrostriction of solvent water by these two equal-sized cations of different formal charge.

The electrostrictive contraction, ΔV_{el}, of a medium of dielectric constant D about a sphere of radius r and charge Ze is given by the Drude-Nernst equation

$$\Delta V_{el} = \frac{-Z^2e^2}{2\ Dr}\left(\frac{\partial\ \ln\ D}{\partial P}\right) \qquad 5.17$$

The metal ion hydrolysis reaction (equation 5.4) involves a charge difference $\Delta Z^2 = +4$ and the calculated electrostrictive contribution

to ΔV_a is then + 8.4 $cm^3\ mol^{-1}$. This is in marked contrast to the sign and magnitude of the experimental values $\Delta V_a(M^{3+}_{aq} = Fe^{3+}_{aq})$ = - 1.2 ± 0.5 $cm^3\ mol^{-1}$, $\Delta V_a(M^{3+}_{aq} = Tl^{3+}_{aq})$ = - 3.2 ± 0.9 $cm^3\ mol^{-1}$ and $\Delta V_a(M^{3+}_{aq} = Co(NH_3)_5OH_2{}^{3+})$ = - 2.3 ± 0.6 $cm^3\ mol^{-1}$. The inadequacy of equation 5.17 in predicting ΔV_a is unlikely to be the assumption of the bulk solvent value $(\partial \ln D/\partial P)$ = 47.1 x 10^{-6} bar^{-1} since this value is likely to be attained outside the first hydration spheres of the M (III) species. The more likely deficiency in applying equation 5.17 is the gross assumption for ML_5OH^{2+}(where L = H_2O or NH_3) of a symmetrical spherical cation of net charge +2.

The inadequacy of the symmetrical charge assumption is also suggested by analogy with ΔV_a values for hydrolytic reactions of the type $HX^- \rightarrow H^+ + X^{2-}$. These reactions involve a charge difference ΔZ^2 = -4 whereas for the metal hydrolysis reaction 5.15 ΔZ^2 = +4. For HX^- = $HPO_4{}^-$, ΔV_a^0 = - 24 $cm^3\ mol^{-1}$; for $HSO_4{}^-$, ΔV_a^0 = - 22 $cm^3\ mol^{-1}$; and $HCO_3{}^-$, ΔV_a^0 = - 26 $cm^3\ mol^{-1}$. The radii of these species are somewhat larger (2.46 - 2.23 Å) than those for the metal III cations (2.02 Å for the aquo iron III species,[42] 2.22 Å for the aquo thallic III ion[42], and about 2.05 Å for the aquopentaamminecobalt III cation[43].) In the last example it is assumed that the radius of the aquo ligand approximates closely the radius of a coordinated ammine group. By comparison with these HX^- systems, the metal ion hydrolysis might have been expected to exhibit a value $\Delta V_a \sim 28$ $cm^3\ mol^{-1}$ which differs greatly from the small negative experimental values.

The anomaly between simple electrostrictive predictions and measured values of ΔV_a is also suggested by empirical treatments and correlations of partial molal volumes of ions which are considered to be spherical ions with no charge asymmetry. Couture and Laidler[44] have proposed the following empirical relation for the partial molal volume, $\bar{V}_+$ of a cation of radius r and charge Z_+:

$$\bar{V}_+ = 16 + 4.9\ r^3 - 20\ Z_+ \qquad 5.18$$

Since MOH^{2+} and M^{3+}_{aq} should have equal radii (see above), then it follows from equation 5.18 that

$$\bar{V}_{MOH^{2+}} - \bar{V}_{M^{3+}_{aq}} = \bar{V}_a = +\ 20\ cm^3\ mol^{-1}$$

The Noyes treatment suggests[45] that $\bar{V}_+$ may be estimated from

$$\bar{V}_+ = \bar{V}_{+(conv)} + Z_+\bar{V}_{H+} \qquad 5.19$$

where $\bar{V}_{+(conv)}$ is the conventional partial molal volume of an ion. The semiempirical equation 5.20 was used by Noyes to estimate $\bar{V}_{H^+}$ as follows:

$$\bar{V}_{+(int)} - \bar{V}_{+(conv)} = \bar{V}_{H^+} + \frac{4.175}{r} + \frac{C_2}{r^2} \qquad 5.20$$

where $\bar{V}_{+(int)}$ represents the intrinsic partial molal volume for the ion and C_2 is an empirical constant. This approach yielded $\bar{V}_{H^+} = -\ 1.5\ cm^3\ mol^{-1}$. Substitution into equation 5.19 for ions of formal charge +2 and +3 yields $\bar{V}_{MOH^{2+}} = -\ 20\ cm^3\ mol^{-1}$, $\bar{V}_{M^{3+}_{aq}} = -\ 40\ cm^3\ mol^{-1}$ and $\Delta V_a = +\ 20\ cm^3\ mol^{-1}$.

All predictions based on electrostrictive effects by symmetrical cations yield positive values for ΔV_a. The small negative value for MOH_2^{3+} hydrolysis is however comparable to the

measured value[46] of $\Delta V_a = -3.8 \pm 0.7$ cm^3 mol^{-1} for the analogous hydrolysis of the $Cr(OH_2)_6^{3+}$ cation. Similarly, the estimated ΔV_a value for reaction 5.13 based on the independent dilatometric data of Spiro et al[36] is - 0.7 cm^3 mol^{-1} which is again small and negative.

In all these four systems, the hydroxo-complex ion of formal charge +2 is better represented as an ion-pair M^{3+} ^-OH in which the two charge centres are separated by about 2Å. The Couture-Laidler and Noyes treatments both suggest that the symmetrical cation $M(OH_2)_6^{3+}$ should exhibit $\bar{V}_{M^{3+}_{aq}} = -40$ cm^3 mol^{-1}. This is likely to be a reliable estimate. Since $\Delta V_a \simeq -2 \pm 1$ cm^3 mol^{-1} then it follows from equation 5.16 that $\bar{V}_{MOH} \simeq -42$ cm^3 mol^{-1}. It appears that the two charge centres exert individual electrostrictive effects which do not cancel to a value which would be characteristic of a 2+ cation (estimated as $\bar{V} = -20$ cm^3 mol^{-1}). This phenomenon probably arises form the unusually large electrostrictive effect[44] of the HO^- ion in water (- 21.8 cm^3 mol^{-1}) combined with the extended charge separation in the ion-pair structure.

5.11.2 Conclusion

The effect of pressure on the first hydrolysis stage of trivalent metal cations is relatively minor. The first hydrolysis constant for hexa-aquo iron III ion is increased from a value $K_a = 2.89 \times 10^{-3}$ at 1 bar pressure to $K_a = 3.16$ at 1.72 kbar; for hexa-aquo thallic III ion from $K_a = 8.2 \times 10^{-2}$ at 1 bar pressure to $K_a = 10.3 \times 10^{-2}$ at 1.72 kbar; and for aquopentaamminecobalt III from

$K_a = 4.47 \times 10^{-7}$ at 1 bar pressure to $K_a = 5.23 \times 10^{-7}$ at 1.72 kbar. The partial molal volume change is $\Delta V_a(Fe^{3+}_{aq}) = -1.2 \pm 0.5$ cm^3 mol^{-1}, $\Delta V_a(Tl^{3+}_{aq}) = -3.2 \pm 0.9$ cm^3 mol^{-1}, and $\Delta V_a(Co(NH_3)_5H_2O^{3+}) = -2.3 \pm 0.6$ cm^3 mol^{-1}. The sign and magnitude of ΔV_a cannot be accounted for by predictions based on the electrostrictive effect of a symmetrical ion ML_5OH^{2+} of net formal charge +2. An ion-pair model is suggested to explain the anomaly.

References to Chapter 5.

1. S.D. Hamann, *"Volume Changes for the ~~Isomerisation~~ Ionisation of Weak Electrolytes and the Effects of Pressure on Ionisation", A Critical Compilation, Chemistry Technical Paper,* No. 3, *C.S.I.R.O. Australia,* 1972.
2. W. Jolley, *Ph.D. Thesis, University of Adelaide,* 1970.
3. F.A. Cotton and G. Wilkinson, *"Advanced Inorganic Chemistry",* 2nd. edition, *Interscience, New York,* 1966, p. 858.
4. W.C. Bray and A.V. Hershley, *J. Amer. Chem. Soc.,* 1934, 56, 1889.
5. C. Brosset, *Svensk. kem. Tidskv,* 1941, 53, 434.
6. F. Linstrand, *Svensk. kem. Tidskv.,* 1944, 56, 251.
7. T.V. Arden, *J. Chem. Soc.,* 1951, 350.
8. B.O.A. Hedstrom, *Arkiv. Kemi.,* 1953, 6, 1.
9. I. Ito and N. Yui, *Sci, Rpts. Tohoku Univ.,* 1953, 37, 19.
10. R.E. Connick and M.S. Tsao, *J. Amer. Chem. Soc.,* 1954, 76, 5311.
11. A.B. Lamb and A.G. Jacques, *J. Amer. Chem. Soc.,* 1938, 60, 1215.
12. E. Rabinowitch and W.H. Stockmayer, *J. Amer. Chem. Soc.,* 1942, 64, 335.
13. A.R. Olson and T.R. Simonson, *J. Phys. Chem.,* 1949, 17, 1322.
14. T.H. Siddall and W.C. Vosburgh, *J. Amer. Chem. Soc.,* 1951, 73, 4270.
15. J. Sutton, *Nature,* 1952, 169, 71.
16. A.R. Wilson and H. Taube, *J. Amer. Chem. Soc.,* 1952, 74, 3509.
17. R.M. Milburn and W.C. Vosburgh, *J. Amer. Chem. Soc.,* 1955, 77, 1352.
18. J. Hudis and R.W. Dodson, *J. Amer. Chem. Soc.,* 1956, 78, 911.
19. R.E. Connick, L.G. ~~Hel~~per, Z.Z. Hugus, K.W. Kury, W.M. Latimer,

and M.S. Tsao, *J. Amer. Chem. Soc.*, 1956, 78, 1827.

20. R.C. Turner and K.E. Miles, *Canad. J. Chem.*, 1957, 35, 1002.
21. B. Behar and G. Stein, *Israel J. Chem.*, 1969, 7, 831.
22. N. Bjerrum, *Z. Phys. Chem.*, 1907, 59, 336.
23. J.N. Bronsted and K. Velquartz, *Z. Phys. Chem.*, 1928, 134, 97.
24. L.N. Mulay and P.W. Selwood, *J. Amer. Chem. Soc.*, 1955, 77, 2693.
25. A.I. Vogel, *"Quantitative Inorganic Analysis"*, 3rd edition, *Longmans*, 1961, p. 787.
26. S.D. Hamann, *"Physico-Chemical Effects of Pressure"*, *Butterworths Scientific Publications, London*, 1957, p. 146.
27. G. Biederman, *Rec. Trav. Chim.*, 1956, 75, 716.
28. F. Ya Kul'la, Yu. B. Yakovlev and V.E. Mironov, *Zhur. Neorg. Khim*, 1964, 9, 2573.
29. T.E. Rogers and G.M. Waind, *Trans. Faraday Soc.*, 1961, 57, 1360.
30. E.A. Biryuk, V.A. Nazarenko and L.N. Thu, *Zhur. Neorg. Khim.*, 1969, 14, 714.
31. G. Biedermann, *Arkiv Kemi*, 1953, 5, 441.
32. T. Moeller and S. Cohen, *Anal.Chem.*, 1950, 22, 686.
33. E.A. Burns and R.A. Whitaker, *J. Amer. Chem. Soc.*, 1957, 79, 866.
34. R.C. Splinter, S.J. Harris, and R.S. Tobias, *Inorg. Chem.*, 1968, 7, 897.
35. L.G. Sillén and A.E. Martell, *"Stability Constants of Metal-Ion Complexes"*, *Special Publication No. 17, The Chemical Society, London*, 1964.

36. T.G. Spiro, A. Rävesz, and J. Lee, *J. Amer. Chem. Soc.*, 1968, 90, 4000.

37. A. Bodanszky, and W. Kauzmann, *J. Phys. Chem.*, 1962, 69, 965.

38. F. Basolo and R.K. Murmann, *Inorg. Synthesis IV*, pg. 171.

39. J. Bjerrum, *"Metal Ammine Formation in Aqueous Solution"*, *P. Haase and Son, Copenhagen*, 1941.

40. A.W. Adamson and F. Basolo, *Acta. Chem. Scand.*, 1955, 9, 1261.

41. A. Taube, *J. Amer. Chem. Soc.*, 1960, 82, 524.

42. *International Tables for X-ray Crystallography*, Vol. 3, *Kynoch Press (Birmingham) Eng.* 1962.

43. M.T. Barnet, B.M. Craven and H.C. Freeman, *Chem. Comm.*, 1966, 307.

44. A.M. Couture and K.J. Laidler, *Canad. J. Chem.*, 1956, 34, 1209.

45. R.M. Noyes, *J. Amer. Chem. Soc.*, 1964, 86, 971.

46. T.W. Swaddle and P.C. Kong., *Canad. J. Chem.*, 1970, 48, 3223.

Appendix I

High Pressure Apparatus and Techniques

Two types of pressure vessels were used during the course of these studies. The optical vessel allowed the reactions to be monitored directly while continuously pressurized. With the sampling vessel, aliquots of sample solution were withdrawn and then analysed. Both vessels are based on the original design of Jolley*.

The basic requirements are that the vessels withstand pressures up to 3 kbar without bursting; that the vessel components be readily demounted and assembled for cleaning, that the reaction solution does not come in contact with the pressure vessel material and that the temperature of the samples be maintained to ± 0.05°C.

A: High Pressure Sampling Vessel

The main body, sealing plug and screw plug were constructed from Type 431 stainless steel with Type 316 stainless steel used for the other parts. The pressure seal for the main body of the vessel was effected by a Viton-A O-ring and an annealed copper or aluminium gasket of 1.6 mm thickness seated immediately below the sealing plug. It was later found possible to achieve a satisfactory seal with a gasket along. Each gasket could be used for some six to eight runs before replacement.

---

* W.H. Jolley, *Ph.D. Thesis, University of Adelaide*, 1970.

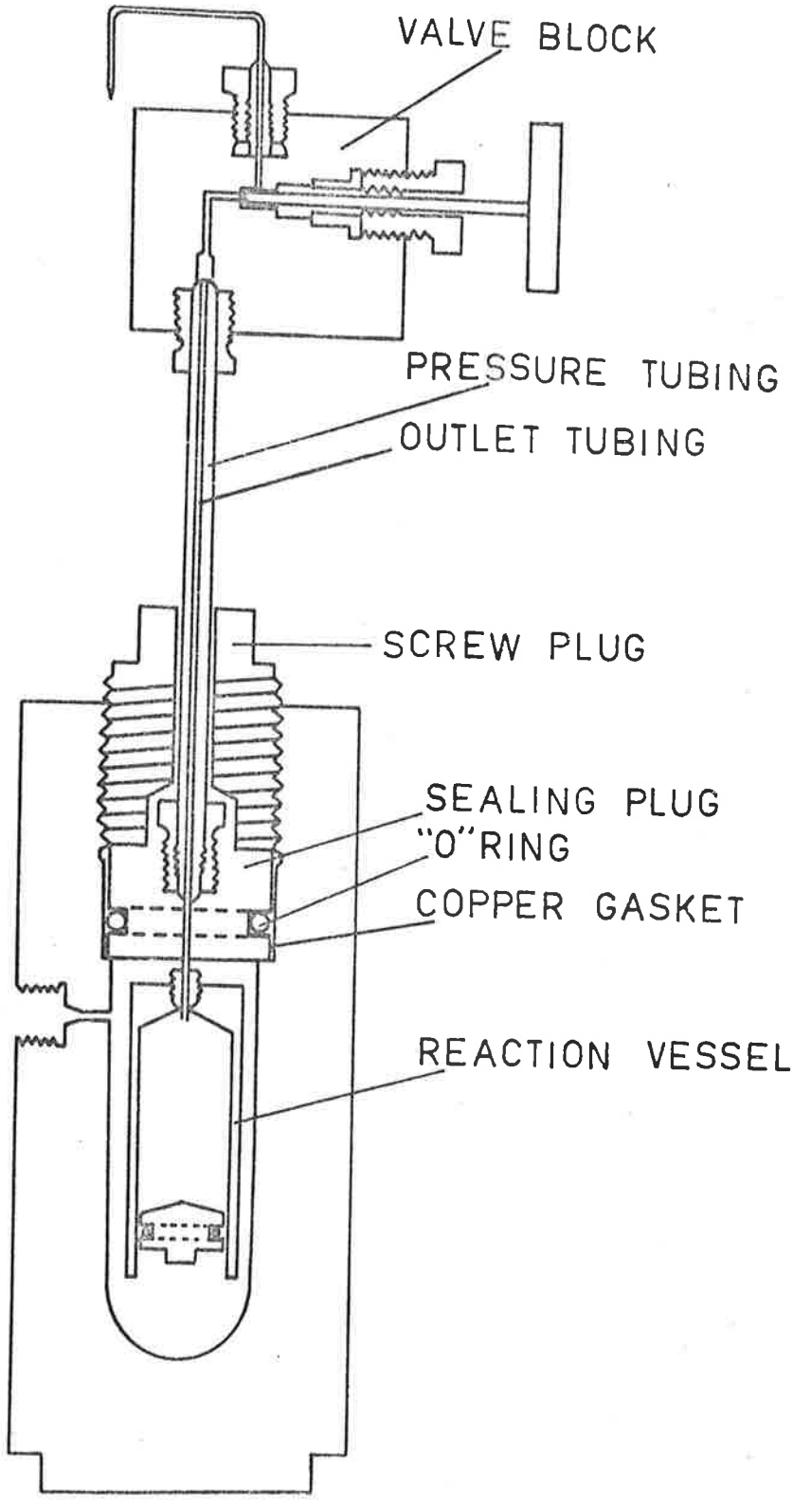

FIG. 1 High Pressure Sampling Vessel

The reaction vessel itself was made of Perspex with a tight fitting Teflon plunger. The reaction vessel was threaded to the sealing plug, the pressure seal being achieved by a circular Neoprene disc of 7.0 mm diameter and 3.2 mm thickness. There were several interchangeable vessels ranging in capacities from 30 ml to 110 ml.

The reaction vessel was connected to the sample valve block by a length of high pressure tubing. A stainless steel capillary tube within this pressure tubing and silver-soldered to it at one end served to connect the reaction solution to the valve block. The needle valve of the valve block consisted of brass handle and a stainless steel needle stem. When the gland nut of the needle valve was tightened it sealed against a teflon packing piece and the needle stem covered the outlet bore. To remove an aliquot of sample solution, the needle valve was opened and pressure forced the solution out through the outlet tubing as the plunger moved up the reaction vessel. The pressure was then quickly readjusted with the pump.

Details of the high pressure sampling vessel is shown in Figure 1.

B: Optical Reactor

Details of the optical pressure vessel are shown in Figures 2 and 3. The main body was constructed from Type 431 stainless steel in the form of a cylinder through which water channels were drilled for the passage of thermostatted water. The sample cuvette was constructed from 1 cm x 1 cm square-sectioned optical quartz terminating in a cylindrical neck. The sample solution under

FIG. 2 Optical Reactor (Vertical Section)

A: main body

B: water jackets

C: sample cell

D: teflon plunger with O-ring

E: brass holder

F: cell compartment

G: sapphire windows

H: screw plugs

I: threaded supporting cap

J: external seal

K: oil inlet

L: inlet and outlet water channel

M: top screw plug

N: copper gasket

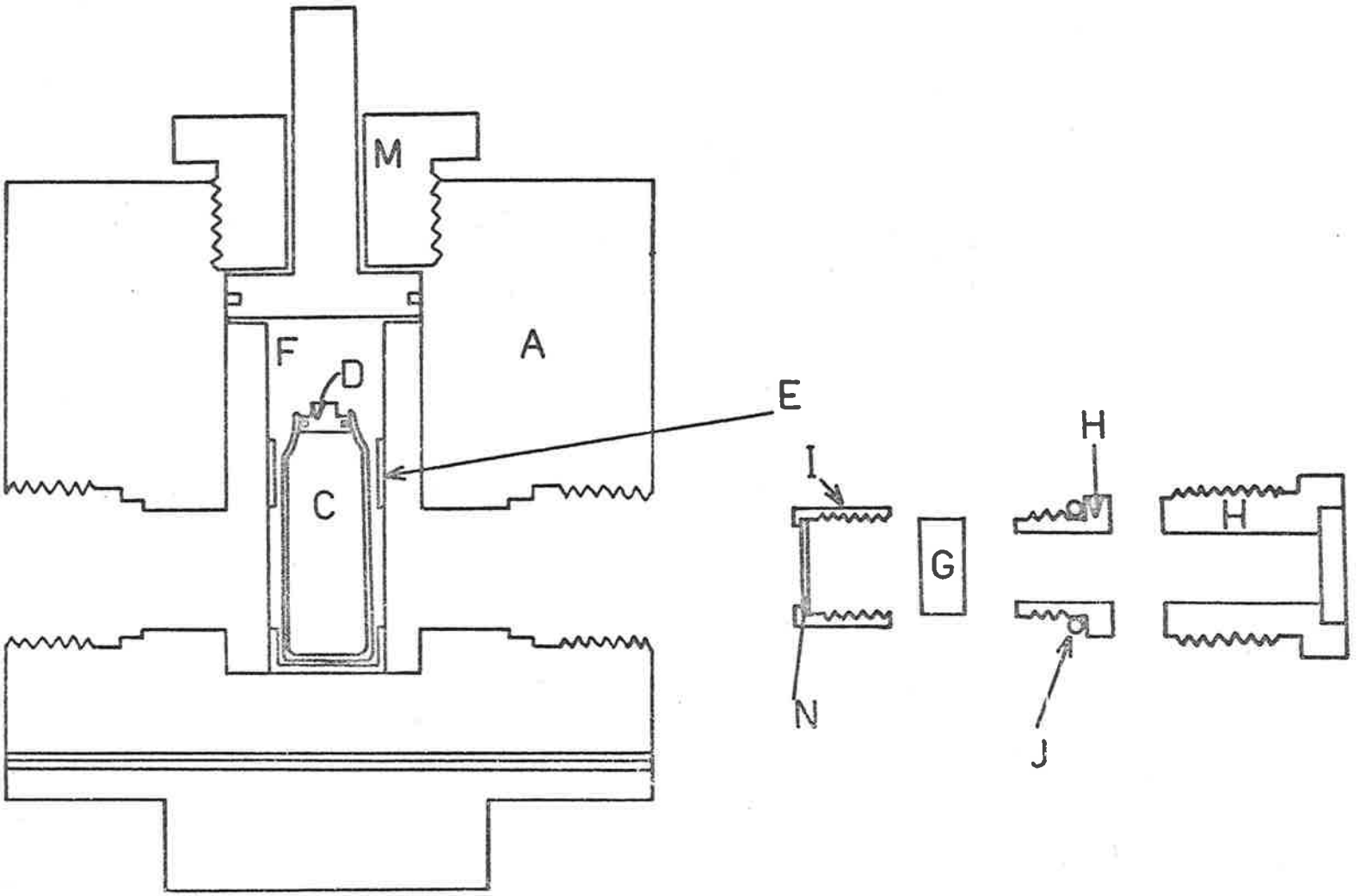
M
A
F
D
E
C
I
H
G
H
N
J

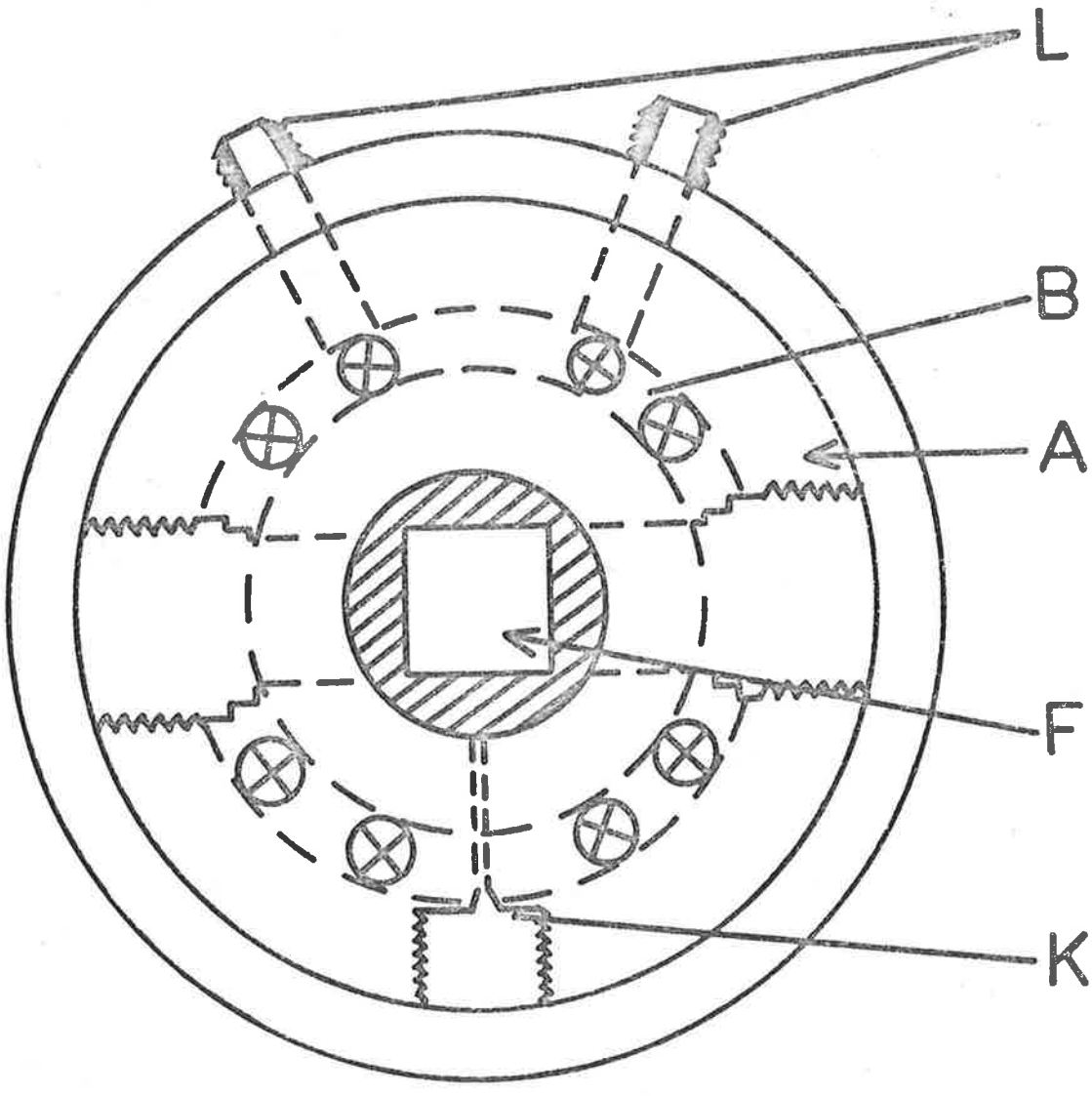

FIG. 3 Optical Reactor (Transverse Section)

study was placed within the cuvette and located within a brass former which in turn was positioned in the central recess in the pressure vessel. The optical path is at right angles to two parallel sides of the cuvette. The pressure vessel was sealed along the optical path by a pair of sapphire windows held with special screw plugs made of 316 stainless steel. The sapphire windows were 12.5 mm diameter, 6.5 mm thickness, with their C axis at 90° to the optically flat surfaces. These crystals transmitted down to 140 nm and so were suitable for studies in the visible - U.V. spectral regions.

Each sapphire window was forced by a threaded steel cap, with a soft annealed copper gasket of 0.6 mm thickness, against the polished surface of a stainless steel supporting plug. For this purpose the steel cap was tightened with a torque-wrench to a torque of 100 in - lb. The steel plug and window were retained in the body of the main cell by an outer screw plug, the pressure seal being made by a Neoprene O-ring.

When the cell was initially pressurised, the soft copper gasket at first yielded, and after depressurisation further tightening was necessary. A reliable seal was established after this one further tightening and thereafter could be used for at least fifty pressure cycles without further attention.

C: General Pressure Equipment

C.1 Pressure Gauges

Experimental pressures were measured with Budenburg Pressure

Gauges, which are Bourdon-type gauges. The gauge was situated about mid-way along the pressure line between the pump and pressure vessel. Three interchangeable gauges with ranges 0 - 0.26 kbar, 0 - 1.7 kbar and 0 - 4.8 kbar were used depending on the pressure required. The gauges were guaranteed by the manufacturers to have an error of not more than 1% of the maximum scale value when operated within 10% and 90% of full deflection.

C.2 Hydraulic Pumps

With the high pressure sampling vessel the pressure was generated by a manual hydraulic pump, Blackhawk Enerpac Model P-228, rated as 2.75 kbar. A reservoir containing Ondina 17 oil, supplied by the Shell Company, was fed into the pump and forced directly through the pressure line into the pressure vessel by the pump.

When the optical reactor was used the pressure was achieved by an oil injector, SKF Model 226400 A also rated at 2.75 kbar. In this case an oil feeder was filled with Ondina 17 oil and the oil pumped through the pressure line by a hand operated lever.

C.3 High Pressure Tubing and Valves

The high pressure tubing used was of 316 stainless steel and the size utilised most frequently was 6.25 mm O.D. tubing. This tubing, rated at 6.9 kbar, was supplied by the American Instrument Company. For the inlet to the spectrophotometer, 3.125 mm O.D. tubing rated at 6.2 kbar and supplied by the Harwood Engineering

Company, U.S.A., was used since this tubing formed more easily to the shape required to enter the spectrophotometer.

The T-piece connectors and valves were standard AMINCO fittings, all rated at 4.1 kbar and supplied by the American Instrument Company. All connections with high pressure tubing were made using the standard line-seal method, created by a 59° cone-ending and a 60° cone-insert.

C.4 Oil Reservoir

After an aliquot of reaction solution was withdrawn from the high pressure sampling vessel, the pressure was readjusted by pumping more oil into the pressure vessel. To maintain a constant temperature inside the vessel, therefore, it was necessary to have a reservoir of oil situated immediately before the inlet to the pressure vessel and thermostatted to the same temperature as the pressure vessel.

The oil reservoir was constructed of Type 431 stainless steel and was connected directly to the pressure vessel by a length of 6.25 mm O.D. high pressure tubing.

C.5 Phase Separator

For spectral studies below 330 nm Ondina 17 oil was not suitable as the pressure medium since it absorbs strongly in this region. Instead n-hexane was used with a phase separator between the pump and the optical pressure vessel.

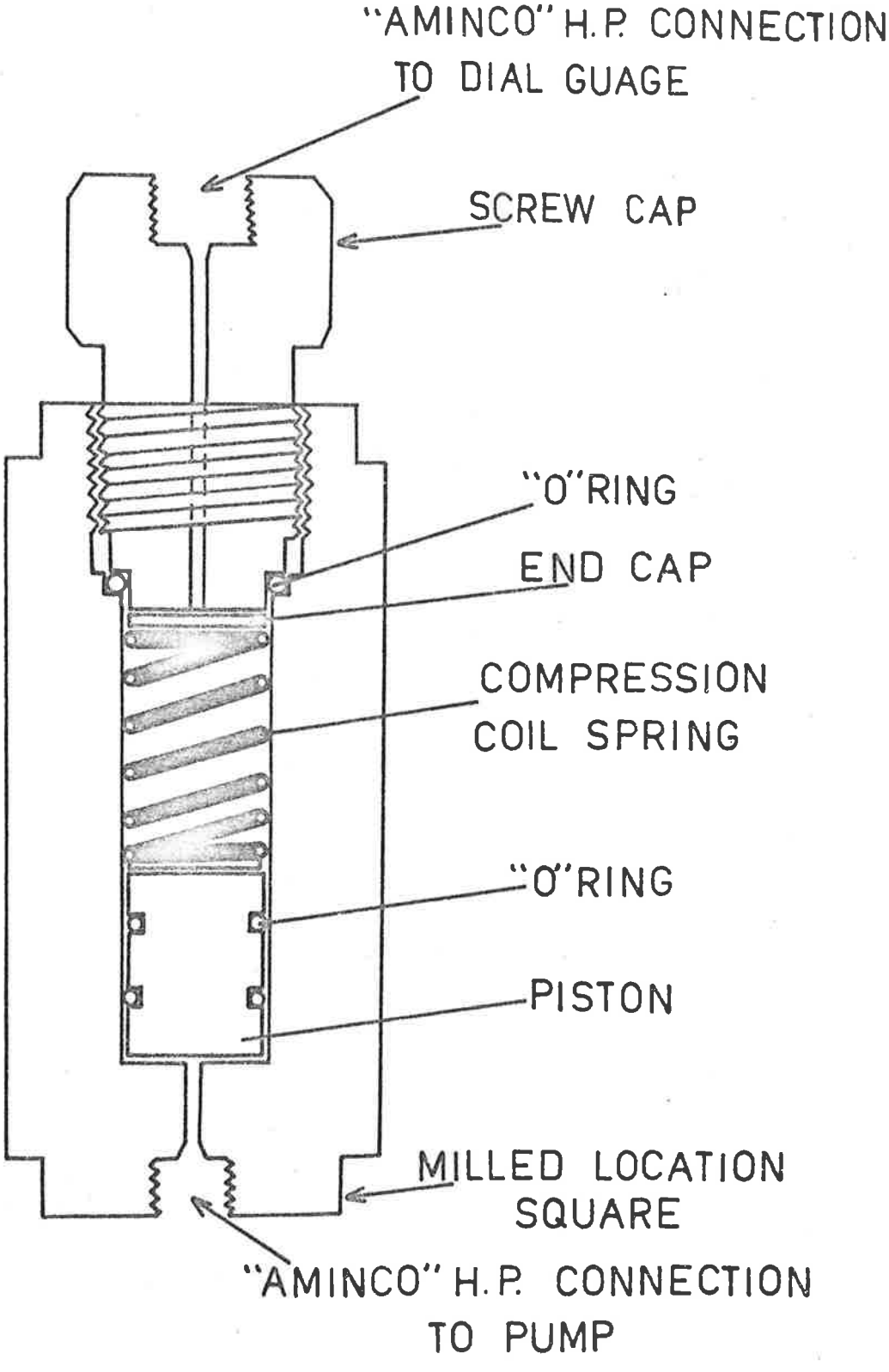

FIG. 4 Phase Separator

Details of the phase separator are shown in Figure 4. All parts were constructed from Type 316 stainless steel. The pressure seal between the main body and the hexagon screw cap was effected by a size 0 - 15 Viton O-ring. Within the central base of the main body and positioned at the lower end was a cylindrical piston with a pair of size 0 - 11 Viton O-rings. This served to separate the two pressure media and transmitted the applied pressure to the reaction solution. A coiled spring placed above the piston served to return the piston to its original position upon depressurisation.

C.6 Displacement unit

The high pressure sampling vessel could only be immersed in an oil bath to the top of the main body. At temperatures above 45°C, heat loss from the exposed top of the vessel caused a temperature difference up to 0.5°C between the reaction solution inside the pressure vessel and the oil surrounding the vessel. To overcome this difficulty a sealed hollow cylinder was attached to the side of the bath. This unit could be raised or lowered and provided sufficient displacement of oil to submerge the reservoir and sampling vessels to above the screw plug. In this way the temperature differential was reduced by some 50%.

The schematic diagrams (Figure 5) show the complete arrangement of the high pressure equipment when using the two reactors.

FIG. 5 Schematic representation of the high pressure systems.

Top diagram: the arrangement of the apparatus with the sampling vessel.

Bottom diagram: the arrangement of the apparatus with the optical reactor.

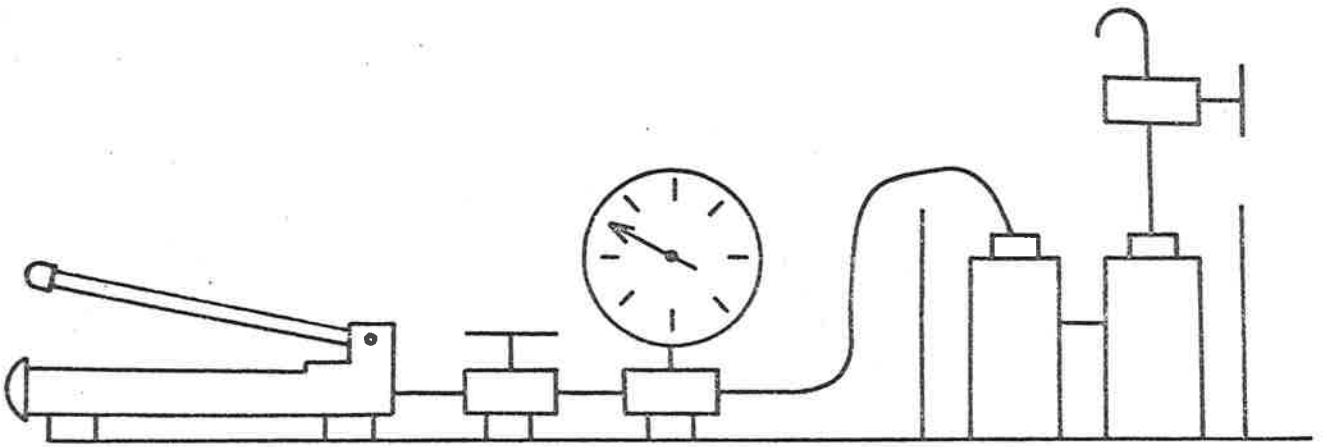

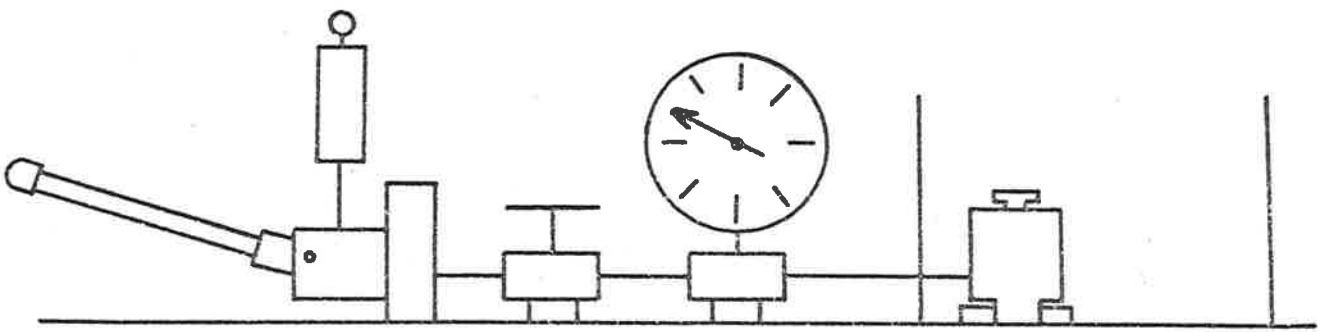

Appendix II

Computer Programs

a: Evaluation of kinetic data

Four main programs were used for the evaluation of the kinetic data

1) PRØGRAM FOPW : calculates the observed rate coefficient from conventional first order plots.

2) PRØGRAM GUGGEN : evaluates the observed rate coefficient by the Guggenheim method.

3) PRØGRAM OXAN : this program determines the anation rate and ion-pair equilibrium value from previously evaluated observed rate coefficients (Chapter 4).

4) PRØGRAM FEHYD : this program evaluates the first hydrolysis constant and absorption coefficient for hydrolysis of Fe^{3+}_{aq} and Tl^{3+}_{aq} (Chapter 5).

To these main programs were fitted a linear least-squares subroutine (SUBRØUTINE LIREG) and a plotting subroutine (SUBRØUTINE PLØTIT). Given below are the listing of these main programs and subroutines.

```
PROGRAM FOPW (INPUT.OUTPUT)
DIMENSION TIME(100).OD(L00),X(200),Y(200)
DIMENSION W(200),CON(200)
DATA(W(I),I=1,200)/50.,199*1./
DATAX(1)/0./
DATAY(1)/0./
COMMON/GRAPH/IPLOT,IRUN
REAL J,K
CALL PLOTS(5HSCSNV,5)
```

```
    IPLOT=10HQIKPLT
  1 READ100,M,N
100 FORMAT(A1,10X,12)
    READ10,IPRES,IRUN
 10 FORMAT(I5,10X,I3)
    PRINT 16
 16 FORMAT(1H1,35X,*LINEAR REGRESSION OF Y =LN(OD)/(OD) VS TIME * ,
   $ /,40X,*SLOPE = OBSERVED ANATION RATE CONSTANT *     ,///)
    PRINT150 ,IPRES,IRUN
150 FORMAT(35X,*PRESSURE =*,15,* POUNDS/SQ.INCH*,///,35X,
   $*RUN NUMBER =*,13,///)
    READ102,J,K
102 FORMAT(2F10.5)
    READ 101,(TIME(I),OD(I),I=1,N)
101 FORMAT(8F10.0)
     1J=N+1
    P=K-J
    DO2I=1,N
    JK=I+1
    Q=K-OD(I)
    Y(JK)=ALOG(P/Q) $ X(JK)=TIME(I)
  2 CONTINUE
    CALL LIREG (X,Y,N+1,KOBS,SEB,+1,N+21,CON)
    IF(M.EQ.1H ) GO TO 1
    END FOPW


    PROGRAM GUGGEN(INPUT,OUTPUT)
    DIMENSION TIME(100),ODONE(100),ODTWO(100),X(100),Y(100)
    DIMENSION W(200),CON(200)
    COMMON/GRAPH/IPLOT,IRUN
    COMMON/REGRESS/A,C,TO25,SEA2,SEB2,XBAR
    CALL PLOTS(5HSCSNV,5)
    IPLOT=10HQIKPLT
  1 READ100,M,N
100 FORMAT(A1,10X,I2)
    READ 10,IPRES,IRUN,ITEMP
 10 FORMAT(I5,10X,I3,2X,I3)
    PRINT 16
 16 FORMAT(1H1,35X,*LINEAR REGRESSION OF Y = LN(ODONE - ODTWO)   VS
   *   TIME*,/,40X,*GUGGENHEIM PLOT*,/,40X,*SLOPE = OBSERVED RATE CONS
   *TANT*,///)
    PRINT150 ,IPRES,IRUN,ITEMP
150 FORMAT(35X,*PRESSURE =*,15,* POUNDS/SQ.INCH*,///,35X,
   $*RUN NUMBER =*,13,///,35X,*RUN TEMPERATURE =*,13,///)
    READ 102,(TIME(I),ODONE(I),ODTWO(I),I = 1,N)
102 FORMAT(16F5.0)
    DO 2 I = 1,N
    Y(I) = ALOG(ODONE(I) - ODTWO(I))
    X(I) = TIME(I)
  2 CONTINUE
```

```
      CALL LIREG(X,Y,N,KOBS,SEB,+1,N+21,CON)
      IF(M.EQ.1H ) GO TO 1
      STOP
      END GUGGEN


      PROGRAM OXAN (INPUT.OUTPUT)
C     THIS PROGRAM ONLY EVALUATES THE REAL K ANATION RATE CONSTANT
C     FROM THE PREVIOUSLY EVALUATED OBSERVED K ANATION RATE CONSTANT
      REAL KOBS(100),OX(100),INKOBS(100),INOX(100),X(100),Y(100)
      REAL CON(100)
      COMMON/GRAPH/IPLOT,IRUN
      COMMON/REGRESS/A,C,TO25,SEA2,SEB2,XBAR
      IPLOT = 10HQIKPLT
    4 READ1,M,N
    1 FORMAT(A1,10X,I2)
      READ 5,IPRES,IRUN,ITEMP
    5 FORMAT(I5,I5,I5)
      PRINT 7
    7 FORMAT(1H1,30X,*EVALUATION OF ANATION RATE AND ION PAIR EQUILIBRIU
     $M CONSTANT*,///)
      PRINT 8,IPRES,ITEMP,IRUN
    8 FORMAT(30X,* PRESSURE =*,I5,* POUNDS/SQ. INCH*,///,30X,* RUN TEMPE
     $RATURE =*,I3,* CENT. *,///,30X,* RUN NUMBER *,I3,///)
      READ 10,(OX(I),KOBS(I),I=1,N)
   10 FORMAT (4(F10,E10))
      DO 12I=1,N
      X(I) = 1./OX(I)
      Y(I) = I./KOBS(I)
   12 CONTINUE
      CALL LIREG (X,Y,N,SLOPE,SESLOPE,+1,N+20,CON)
      ANRAT = 1./A
      EQUIP = 1./(SLOPE*ANRAT)
      SEANRAT = (SQRT(SEA2)/A)*ANRAT
      SEAQUIP = (A+SQRT(SEA2))/(C+SQRT(SEB2))-EQUIP
      PRINT 20,ANRAT, SEANRAT,EQUIP,SEEQUIP
   20 FORMAT (////,20X,* TRUE ANATION RATE *,5X,G13.6,5X,* ERROR *,
     $5X,G13.6,////,20X,* ION PAIR EQUILIBRIUM VALUE *,5X,G13.6,5X
     $* ERROR *,5X,G13.6)
      IF (M.EQ.1H ) GO TO 4
      END OXAN


      PROGRAM FEHYD (INPUT,OUTPUT)
C     THIS PROGRAM EVALUATES THE FIRST HYDROLYSIS CONSTANT OF IRON
C     TOGETHER WITH ABSORPTION COEFFICIENT OF FEOH
      DIMENSION OF(100),HCONC(100),X(100),Y(100)
      DIMENSION CON(100)
      COMMON/GRAPH/IPLOT,IRUN
```

```
      COMMON/REGRESS/A.C.TO25,SEA2,SEB2,XBAR
      REALJ,K,KOBS
      CALL PLOTS(5HSC5NV,5)
      IPLOT=10HQIKPLT
    1 READ 5,M,N
    5 FORMAT(A1,9X,I3)
      READ 10,PRES,IRUN
   10 FORMAT (I5,10X,I3)
      PRINT 16
   16 FORMAT(1H1,35X,*LINEAR REGRESSION OF H+ VS 1/(OD) *)
      PRINT 20,IPRES,IRUN
   20 FORMAT(///,35X,*PRESSURE =*,I5,* POUNDS/SQ.INCH*,///,35X,
     $*RUN NUMBER =*,I3,///)
      READ 25,(HCONC(I),OD(I),I=1,N)
   25 FORMAT(8F10.5)
      DO 30 I=1,N
      X(I) = HCONC(I)
      Y(I) = 1./OD(I)
   30 CONTINUE
      CALL LIREG (X,Y,N,B,SEB,+1,N+21,CON)
      READ 35,FE
   35 FORMAT(F10.0)
      EXT =1/(FE*A)
      KOBS =A/B
      SEEXT = (SQRT(SEA2)/A)*EXT
      SEKOBS = ((SQRT(SEA2)/A)+(SQRT(SEB2)/B))*KOBS
      PRINT 4,EXT,SEEXT,KOBS,SEKOBS
   40 FORMAT (*    EXTINCTION COEFFICIENT = *,E11.4,//,
     $*     S.E. EXTINCTION COEFFICIENT =*,F6,2,//,*     KOBS =*,F11.4,
     $//,*     S.E. KOBS =*,F6.2)
      IF (M.EQ.1H ) GO TO 1
      END FEHYD


      SUBROUTINE LIREG(X,Y,N,B,SEB,IFLAG,M,Z)
      DIMENSION X(1),Y(1),T(100),Z(M,3)
      COMMON/GRAPH/IPLOT,IRUN
      COMMON/REGRESS/A.C.TO25,SEA2,SEB2,XBAR
      DATA(T(I),I= 1, 6)/12.705,4.303,3.182,2.776,2.571,2.447/
      DATA(T(I),I= 7,12)/2.365,2.306.2.262,2.228,2.201.2.179/
      DATA(T(I),I-13,18)/2.160,2.145.2.131.2120.2.110,2.101/
      DATA(T(I),I-19,24)/2.093,2.086.2.080,2.074,2.069,2.064/
      DATA(T(I),I=25,30)/2,060,2.056,2.052,2.048,2.045,2.042/
      DATA(T(I),I=31,40)/10*2.03/
      DATA(T(I),I=41,50)/10*2.01/
      TO25=T(N-2)
      IF(N.GT.50)TO25=2.0
      XBAR=YBAR=XYBAR=XXBAR=YYBAR=0.
```

```
      XN=N
      DO1I=1,N
      XI=X(I)
      YI=Y(I)
      XBAR=XBAR+XI
      YBAR=YBAR+YI
      XXBAR=XXBAR+XI*XI
      YYBAR=YYBAR+YI*YI
    1 XYBAR=XYBAR+XI*YI
      XBAR=XBAR/XN
      YBAR=YBAR/XN
      XXBAR=XXBAR=XN*XBAR*XBAR
      YYBAR=YYBAR-XN*YBAR*YBAR
      XYBAR=XYBAR-XN*XBAR*YBAR
      B=XYBAR/XXBAR
       C=B
      A=YBAR-B*XBAR
      XAB=(YYBAR-B*XYBAR)/(N-2.)
      SEA2=SAB/XN
      SEA=SQRT(SEA2)
      SEB2=SAB/XXBAR
      SEB=SQRT(SEB2)
      IF(IFLAG.LT.0) RETURN
      SAB=SQRT(SAB)
      CONA=T025*SAB/SQRT(XN)
      COMB=T025*SAB/SQRT(XXBAR)
      PRINT 2,A,B
    2 FORMAT(///40X*Y=*G13.6*+*G13.6*X*)
      CONA1=A+CONA
      CONA2=A-CONA
      CONB1=B+CONB
      CONB2=B-CONB
      PRINT3,A,SEA,CONA2,CONA1,B,SEB,CONB2,CONB1
    3 FORMAT(////31X63(1H-)/31X*;     VALUE      :*
     $*STANDARD ERROR : CONFIDENCE LIMITS*11X*:*/
     $20X*:INTERCEPT: *G13.6* : *G13.6* ; (*G13.6*,*G13.6*):*/
     $20X*: SLOPE    : *G13.6* : *G13.6* ; (*G13.6*,*G13.6*):*/
     $20X74(1H-))
      PRINT 7
    7 FORMAT(///30X*95 PERCENT CONFIDENCE LIMITS FOR REGRESSION*
     $* EQUATION*)
      PRINT4,A,B,T025,SEA2,SEB2,XBAR,XBAR
    4 FORMAT(////10X*Y=*G13.6*+*G13.6*X+*F6.4*SQRT(*
     $G13.6*+*G13.6*(X-*G13.6*)(X-*G13.6*))*)
      PRINT5,A,B,T025,SEA2,SEB2,XBAR,XBAR
    5 FORMAT(////10X*Y=*G13.6*+*G13.6*X-*F6.4*SQRT(*
     $G13.6*+*G13.6*(X-*G13.6*)(X-*G13.6*))*)
      DO6I=1,N
      Z(I)=Y(I)
      XI=X(I)
```

```
      YBAR=XI-XBAR
      XXBAR=A+B*XI
      YYBAR=TO25*SQRT(SEA2+SEB2*YBAR*YBAR)
      Z(I,2)=XXBAR+YYBAR
    6 Z(I,3)=XXBAR-YYBAR
      PRINT 9
    9 FORMAT(////10X*   HCONC       L/OD      ESTIMATED FROM EQUATION*
     $*       CONFIDENCE LIMITS PERCENTAGE ERROR*)
      DO11I=1,N
      XI=X(I)
      YBAR=A+B*XI
      PERC=100.*ABS(YBAR-Y(I))/YBAR
   11 PRINT12,XI,Y(I),YBAR,Z(I,3),Z(I,2),PERC
   12 FORMAT(BX2G13.6.4XG13.6,9XG13.6,2XG13.6,2XG13.6)
      IF(IPLOT.EQ.10HQIKPLT    ) GO TO 17
      IF(IPLOT.EQ.10HAUTPLT    ) GO TO 16
      CALL PAUPLOT (27HBLNK PPR,.3M PN,BLK INK PLS,27)
   16 CALL PLOTIT(X,Y.N)
      RETURN
   17 XJUMP=(X(N)-X)/20.
      XMIN=(X(2)+XJUMP
      I=N+1
      DO15J=I,M
      XMIN=XMIN+XJUMP
      YBAR=XMIN-XBAR
      XXBAR=A+B*XMIN
      YYBAR=TO25*SQRT(SEA2,SEB2*YBAR*YBAR)
      X(J)=XMIN
      Z(J)=Z(J,2)=XXBAR+YYBAR
   15 Z(J,3)=XXBAR-YYBAR
      CALL QIKPLT(X,Z,J,-3,15H*TIME (SECS) →*,
     $22H*↑ CONFIDENCE  PLOT  *)
      RETURN
      END


      SUBROUTINE PLOTIT(X,Y,N)
      DIMENSION X(1),Y(1)
      DIMENSION AUTO(1500)
      COMMON/GRAPH/IPLOT,IRUN
      COMMON/REGRESS/A,B,TO25,SEA2,SEB2,XBAR
      CALL PLOT (0.,1.,-1)
      XSCALE=5
      YXCALE=7
      HEIGHT=.7/6
      XJUMP=(X(N)-X)/240.
      XMIN=XJUMP
      N1=758+N
      DO16I=1,250
```

```
      AUTO(N1+I)=XMIN=XMIN+XJUMP
      XXBAR=AUTO(I)=A+B*XMIN
      YBAR=XMIN-XBAR
      YYBAR=TO25*SQRT(SEA2,SEB2*YBAR*YBAR)
      AUTO(252+I)=XXBAR+YYBAR
   16 AUTO(504+I)=XXBAR-YYBAR
      N1=1010+N
      DO17I=1,N
      AUTH(756+I)=Y(I)
   17 AUTO(N1+I)=X(I)
      AUTO(251)=AUTO(252)=AUTO(253)
      AUTO(503)=AUTO(504)=AUTO(505)
      AUTO(755)=AUTO(756)=AUTO(757)
      AUTO(1009+N)=AUTO(1010+N)=AUTO(1011+N)
      CALL SCALE(AUTO(759+N),XSCALE,252+N,1)
      CALL SCALE(AUTO,YSCALE,756+N,1)
      AUTO(251)=AUTO(503)=AUTO(755)=AUTO(757+N)
      AUTO(252)=AUTO(504)=AUTO(756)=AUTO(758+N)
      AUTO(1009+N)=AUTO(1011+N+N)
      AUTO(1010+N)=AUTO(1012+N+N)
      CALL AXIS(0.,0.,12H1./[OXALATE],-12,XSCALE,0.,AUTO(1009+N)
     $,AUTO(1010+N),0)
      CALL AXIS(0.,YSCALE,12H         ,12,XSCALE,0.,AUTO(1009+N)
     $,AUTO(1010+N),0)
      CALL AXIS(0.,0..15H             ,15,YSCALE,90,,AUTO(251)
     $,AUTO(252),-1)
      CALL AXIS(XSCALE,0.,15HCONFIDENCE PLOT,-15,YSCALE,90.,AUTO(251)
     $,AUTO(252),-1)
      CALL LINE(AUTO(759+N),AUTO,250,1,0,0)
      CALL LINE(AUTO(1011+N),AUTO(757),N,1,-1.4)
      YCOORD=YSCALE-.3
      CALL SYMBOL(.2,YCOORD,HEIGHT,29HLOG (OD1 - OD2) VS TIME(SECS),0.,29)
     *9)
      YCOORD=YCOORD-.2
      CALL SYMBOL(,2,YCOORD,HEIGHT,19HRUN NUMBER = R(  ),0.,19)
      CALL NUMBER (1.5,YCOORD,HEIGHT,IRUN,0., 2H13)
      YCOORD=YCOORD-.2
      CALL SYMBOL(.2,YCOORD,HEIGHT,19HX EXPERIMENTAL DATA,0.,19)
      YCOORD=YCOORD-.2
      CALL SYMBOL(.2,YCOORD,HEIGHT,27H- ESTIMATED REGRESSION LINE,0.,27)
      YCOORD=YCOORD-.2
      CALL SYMBOL(.2,YCOORD,HEIGHT,29H  NINETY FIVE PERCENT CONFIDENCE L
     $ITS,0.,39)
      CALL PAUPLOT(22H.3M PEN,RED INK PLEASE,22)

      CALL SYMBOL(2,4.3,HEIGHT,1H-,0.,1)
      CALL LINE(AUTO(759+N),AUTO(253),250,1,0,0)
      CALL LINE(AUTO(759+N),AUTO(505),250,1,0,0)
      CALL PLOT(8.0,0.0,-3)
      RETURN
      END
```

b: Determination of Arrhenius Parameters

This program consists of a main program (PRØGRAM ACTAR) and a least-squares subroutine (SUBRØUTINE LSQU). The function of the main program is to arrange the data in the form of the Arrhenius equation. The full listing is given below.

```
    PROGRAM ACTPAR (INPUT,OUTPUT)
    DIMENSION VT(100),RC(100),X(100),Y(100)
  2 READ1,M,N
  1 FORMAT(A1,9X,I2)
    READ 101,PC,BC,GC,T,RCC
101 FORMAT(2E10.3.3F10.0)
    READ 100,(VT(I),RC(I),I=1,N)
100 FORMAT(BF10.0)
    DO 3 I=1,N
    X(I)=1/VT(I)     $     Y(I)=ALOG(RC(I))
  3 CONTINUE
    CALL LSQU(X,Y,N,S,R,YI,SERINT,PEI,SERS,PES)
    E=-GC*S
    SEE=PES*E/100.
    H=E-GC*T
    SEH=PES*H/100.
    RK=EXP(S/T+YI)
    EN=GC*ALOG((RK*PC*EXP(H/(GC*T)))/(BC*T))
    EN2=GC*ALOG((RCC*PC*EXP(H/(GC*T)))/(BC*T)
    ENT=GC*(YI-ALOG(BC*T/PC))
    SEENT=PEI*ENT/100.
    PRINT 200
200 FORMAT(1H1,30X,*ACTIVATION     PARAMETERS*,///)
    PRINT 201
201 FORMAT(25X,*X*,30X,*Y*,//)
    PRINT 202,(X(I),Y(I),I=1,N)
202 FORMAT(20X,E10.3,20X,E10.3)
    PRINT 203,S,YI,SERS,PES,SERINT,PEI,R,SEE,SEH
203 FORMAT(///.*     SLOPE = *,E10.3,/,*     Y INT = *,E10.3,/,*     S.E.
   * SLOPE = *,E10.3,/,*     P.E. SLOPE =*,F6.2,/,*     S.E. INTERCEPT =
   **,E10.3,/,*     P.E. INTERCEPT = *,F6.2./,*     CORRELATION COEFF =
   **,F8.5,/,*     S.E. ACT. ENERGY= *,E10.3,/,*     S.E. ENTHALPY= *,
    1E10.3)
    PRINT 204,T
204 FORMAT(///,*     TEMP.= *,F7.2)
    PRINT 207
207 FORMAT(//,    * ENTROPY CALCULATED BY DIRECT SUBSTITUTION INTO T. S
   1. EQUATION*)
```

```
      PRINT 205,E,H,EN
  205 FORMAT(//,*    ACT.ENERGY= *,F7,/,*    ENTHALPY= *,F7,/,
     1*    ENTROPY= *,F6.2)
      PRINT 208
  208 FORMAT(//,   * ENTROPY CALCULATED FROM INTERCEPT*)
      PRINT 206,E,H,ENT,SEE,SEH,SEENT
  206 FORMAT(//,*    ACT. ENERGY= *,F7,/,*    ENTHALPY= *,F7,/,*    ENTR
     1OPY= *,F6.2,/,*    S.E. ACT. ENERGY= *,E10.3,/,*    S.E. ENTHALPY=
     1 *,E10.3,/,*    S.E. ENTROPY= *,E10.3)
      PRINT 205,E,H,EN2
      IF(M.EQ.1H ) GOTO 2
      END ACTPAR


      SUBROUTINE LSQU(X,Y,N,S,R,YI,SERINT,PEI,SERS,PES)
      DIMENSION X(100),Y(100)
C     SUBROUTINE LSQU APPLIES LEAST SQUARES METHOD TO Y VS X
      XY=X2=Y2=CX=CY=0.
      DO 2 I=1,N
      CX=CX+X(I)
      CY=CY+Y(I)
      XY=XY+X(I)*Y(I)
      X2=X2+X(I)*X(I)
    2 Y2=Y2+Y(I)*Y(I)
      XB=CX/N
      YB=CY/N
      SX=(X2/N-XB*XB)**0.5
      SY=(Y2/N-YB*YB)**0.5
      R=(XY/N-XB*YB)/(SX*SY)
C     CALCULATE SLOPE OF LINE OF BEST FIT
      S=(R*SY)/SX
      YI=YB-S*XB
      SYY=Y2-CY*CY/N
      SXX=X2-CX*CX/N
      SERY=SQRT((SYY-S*S*SXX)/(N-2.0))
C     CALCULATE STANDARD ERROR IN SLOPE AND INTERCEPT
      SERS=SERY/SQRT(SXX)
      SERINT=SERY*SQRT(1.0/N+XB*XB/SXX)
      PCSE=(SERS/S)*100.0
      PES=ABS(PCSE)
      PEI=(SERINT*100.0)/YI
      PEI=ABS(PEI)
      RETURN
      END  LSQU
```

c: Evaluation of Activation Parameters

The program reads in the log of the rate coefficient, Y(I), and pressure XD(I). The data may then be fed into polynomials usually up to degree four. A linear regression analysis follows by calling REGAL which is a library subroutine. Below is the listing of the full program.

```
      PROGRAM SOLVE(INPUT,OUTPUT)
      DIMENSION Y(100),XD(100),X(100,10)
      DIMENSION X(BAR(10)
      COMMON/REG/SSQ(10),B(31),SE(31)
      MM = 1
2000  CONTINUE
      M-1
      READ 1,N
    1 FORMAT(I2)
      READ B,(Y(I),XD(I),I=1,N)
    8 FORMAT(8F10)
      PRINT 20,(Y(I),XD(I),I=1,N)
   20 FORMAT(X2F10.4/)
      CALL QIKPLT(XD,Y,-N,+1,10H*X-VALUES*,10H*Y-VALUES*)
      YBAR=0.
      DO 21 I=1,N
   21 YBAR=YBAR+Y(I)
      YBAR=YBAR/N
      DO 22 I=1,N
   22 Y(I)=Y(I)-YBAR
1000  CONTINUE
      DO 6 J=1,M
    6 XBAR(J)=0.
      DO 5 I=1,N
      DO 60 J=1,M
      X(I,J)=XD(I)**J
   60 XBAR(J)=XBAR(J)+X(I,J)
    5 CONTINUE
      DO 32 I=1,N
      DO 31 J=1,M
   31 X(I,J)=X(I,J)-XBAR(J)/N
   32 CONTINUE
      CALL REGAL(N,M,X,100,Y,0,0,1)
      S=0.
      DO 33 J=1,M
   33 S=S+B(J)*XBAR(J)/N
      YINT=YBAR-S
```

```
      PRINT 34,YINT
   34 FORMAT(//10X*THE VALUE OF THE Y-INTERCEPT IS=*E20.10)
      IF(M.EQ.3) GO TO 30
      M=M+1
      GO TO 1000
   30 CONTINUE
      MM = MM+1
      IF(MM.EQ.7) GO TO 2001
      GO TO 2000
 2001 CONTINUE
      END
```